TIME-WINDOWED MULTIUSER DECORRELATING RECEIVERS FOR
ASYNCHRONOUS CODE DIVISION MULTIPLE ACCESS COMMUNICATION
CHANNELS

By

MICHAEL STEPHEN FEENEY

A DISSERTATION PRESENTED TO THE GRADUATE SCHOOL
OF THE UNIVERSITY OF FLORIDA IN PARTIAL FULFILLMENT
OF THE REQUIREMENTS FOR THE DEGREE OF
DOCTOR OF PHILOSOPHY

UNIVERSITY OF FLORIDA

1994

This work is dedicated to my wife, Su San, my parents, Glen and Nancy, and my sister, Lori.

TABLE OF CONTENTS

Abstract of Dissertation Presented to the Graduate School
of the University of Florida in Partial Fulfillment of the
Requirements for the Degree of Doctor of Philosophy

TIME-WINDOWED MULTIUSER DECORRELATING RECEIVERS FOR
ASYNCHRONOUS CODE DIVISION MULTIPLE ACCESS COMMUNICATION
CHANNELS

By

Michael Stephen Feeney

December, 1994

Chairman: Dr. Scott L. Miller
Major Department: Electrical Engineering

The focus of this dissertation is on the design and
performance analysis of multiuser receivers for asynchronous
code division multiple access communication channels. In
many applications, such as mobile radio networks, the power
levels of the received signals at the central base station
receiver are unequal, resulting in stronger users
interfering with weaker users. Historically, adaptive power
control has been suggested as a solution; more recently,
however, multiuser detectors have been demonstrated to
operate independently of the received power levels and offer
better system performance than could be obtained through the
use of power control alone. One particular multiuser
detection method, the decorrelating strategy, has the
advantage over other methods of not requiring the side

information of the received power levels. The decorrelating strategy suffers, however, from long decoding delays, huge memory requirements, and the burden of computing the inverse of an enormous matrix, all of which render it impractical. In this work, a method of implementing a decorrelating receiver which does not suffer from long decoding delays, huge memory requirements, or the inversion of an enormous matrix is proposed for both additive white Gaussian noise channels and frequency-nonselective Rayleigh fading channels.

A new performance measure, the near-far spread of the receiver, is introduced. The performance of the proposed receiver is analyzed for both the additive white Gaussian noise and frequency-nonselective Rayleigh fading channels. Numerical examples successfully demonstrate the receiver's immunity to unequal received energies. The sensitivity of the proposed receiver to errors in the timing information it requires is examined, as well as the computational complexity associated with its operation.

CHAPTER 1
INTRODUCTION

Wireless Multiple Access Communication Systems

Wireless multiple access communication systems are among the fastest growing technologies in the field of communications. Cellular telephones, cordless telephones, and pagers have become commonplace items, seen almost everywhere. Indoor wireless communication networks and personal communication networks are becoming more popular in the business and public arenas. A typical wireless multiple access communication system is illustrated in Figure 1.1. The system is characterized by multiple, possibly mobile, users sharing a common channel. Each user has a wireless link to a common, centralized base station. The base station is typically connected to the existing telephone infrastructure.

One of the first decisions which must be made when designing any multiple access communication system is how the users will be allowed to share the channel. Currently there are three competing technologies for this task: frequency division multiple access (FDMA), time division multiple access (TDMA), and code division multiple access (CDMA). In FDMA, the available bandwidth is divided into
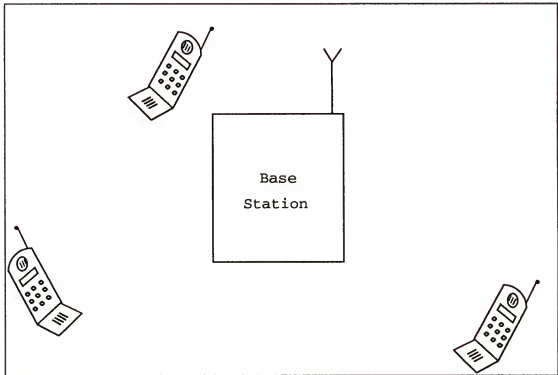
Figure 1.1 - Wireless Multiple Access Communication System

narrow, nonoverlapping channels. Multiplexing is achieved by
assigning each user to a different channel. In TDMA, time
is divided into nonoverlapping slots, and multiplexing is
achieved by assigning each user to a different time slot.
For the duration of each time slot, the corresponding user
has access to the entire available bandwidth. In CDMA, all
users share the entire available spectrum at all times. The
focus of this work will be on direct sequence code division
multiple access (DS-CDMA), in which multiplexing is achieved
by assigning a unique signature waveform to each user.
Knowledge of a particular user's signature waveform is
normally required in order to decode that user's data from
the resulting multitude of signals.

Recently, CDMA has received much attention as an attractive alternative to FDMA and TDMA for urban digital mobile radio networks [1]-[16]. Several papers suggest that a CDMA system could support more simultaneous users than an FDMA or a TDMA system [1], [2], [7], [8]. One reason for the increased capacity in voice networks is that users are speaking only roughly 35% of the time; the rest of the time they are listening [1]. This voice activity cycle thus serves to reduce the overall mutual interference. It has also been suggested that a CDMA system could overlay across the same frequency bands currently being used for other purposes without the performance of either system being affected, thus saving valuable spectrum [3], [17]-[24]. An important parameter in cellular networks is the frequency reuse factor, which dictates how often the same carrier frequency can be used across adjacent cells. Typically, FDMA and TDMA cellular systems repeat the same frequency in only one of every seven cells [2]. For cellular applications, CDMA allows for a frequency reuse factor of one since every cell can use the same frequencies. In multipath fading channels, multiple reflections of the transmitted signal can arrive at the receiver, resulting in destructive interference. Since DS-CDMA signals are wideband, they have the capability of resolving multipath signal components which can then be recombined to provide improved performance in multipath fading channels [25]-[28].

Review of DS-CDMA Systems

Before proceeding, it will be helpful to review the
architecture of a direct sequence code division multiple
access communication system.   Figure 1.2 illustrates the
system model.   There are K users sharing an additive white
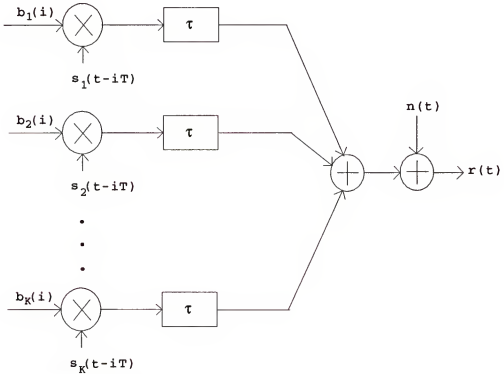

Figure 1.2 - Synchronous DS-CDMA System Model

Gaussian noise (AWGN) channel.   Here the users are assumed
to employ binary phase shift keying (BPSK) modulation.   Each
user transmits on the same carrier frequency denoted by ω_c;
multiplexing is achieved by assigning a unique signature
waveform to each user.   The signature waveform of the kth
user can be written as

$$s_k(t) = \begin{cases} \sqrt{\dfrac{2}{T}} \displaystyle\sum_{j=1}^{N} a_j^k p_{T_c}\left(t-(j-1)T_c\right)\cos\left(\omega_c t + \theta_k\right), & 0 \le t < T \\[2em] 0, & \text{otherwise} \end{cases} \quad (1.1)$$

where

$$a_j^k \in \{\pm 1\}, \qquad j = 1,2,\cdots,N \qquad (1.2)$$

is the signature sequence of the kth user, p_{T_c} is the pulse shape of the signature chip waveform whose duration is $T_c = T/N$ seconds where T is the common bit duration, and θ_k is the carrier phase of the kth user. Note that in this model the signature waveforms are normalized to unit energy and are nonzero only during the time interval $[0,T)$. Each user is assumed to transmit a message of length M bits, and for simplicity the system is assumed to be synchronous; that is, the ith bits of all users arrive simultaneously at the base station. The more general asynchronous system, in which each user may experience a different propagation delay, will be considered in the remaining chapters. The received signal at the base station can be written as

$$r(t) = \sum_{i=1}^{M} \sum_{k=1}^{K} w_k(i) b_k(i) s_k(t - iT - \tau) + n(t) \qquad (1.3)$$

where $w_k(i)$ is the received energy of the ith bit of the kth user, $b_k(i) \in \{\pm 1\}$ is the ith transmitted bit polarity of the kth user, τ is the common propagation delay from each user to the base station, and $n(t)$ is additive white Gaussian noise with power spectral density σ^2.

The job of the base station receiver is to simultaneously demodulate the data for each of the K users.

It was shown by Verdu [29] that a sufficient statistic for determining the maximum likelihood transmitted sequences $b_k(i)$ for $k = 1,2,\cdots,K$ and $i = 1,2,\cdots,M$ can be obtained by passing the received signal $r(t)$ through a bank of filters matched to the allowed signature waveforms. The matched filter bank is shown in detail in Figure 1.3. The received signal is correlated with appropriately delayed replicas of
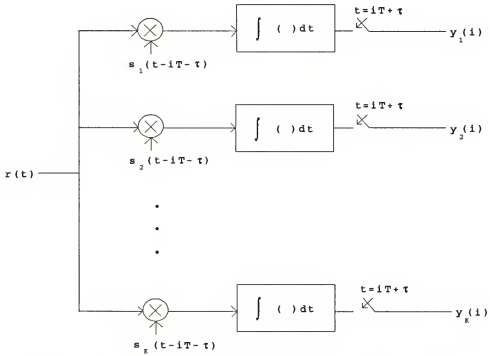

Figure 1.3 - Matched Filter Bank for Synchronous System

each of the allowed signature waveforms and the results are then sampled at the end of each bit interval. Define the K by K element system cross-correlation matrix R such that its $(m,n)^{th}$ element is

$$R_{mn} = \int_{-\infty}^{\infty} s_m(t)s_n(t)\,dt \qquad (1.4)$$

The output of the kth matched filter sampled at the end of the ith bit interval is then

$$y_k(i) = \int_{iT+\tau}^{(i+1)T+\tau} r(t)s_k(t-iT-\tau)dt$$
$$= \sqrt{w_k(i)}\,b_k(i) + \sum_{\substack{j=1 \\ j \neq k}}^{K} R_{kj}\sqrt{w_j(i)}\,b_j(i) + n_k(i) \quad (1.5)$$

where

$$n_k(i) = \int_{-\infty}^{\infty} n(t)s_k(t-iT-\tau)dt \quad (1.6)$$

is the noise component out of the matched filter. Finally, the vector of matched filter outputs sampled at the end of the ith bit interval may be written as

$$\overline{Y} = RW\overline{b} + \overline{n} \quad (1.7)$$

where $\overline{Y} = \left[y_1(i), y_2(i), \cdots, y_k(i)\right]^T$, $\overline{b} = \left[b_1(i), b_2(i), \cdots, b_k(i)\right]^T$, $W = \mathrm{diag}\left[\sqrt{w_1(i)}, \sqrt{w_2(i)}, \cdots \sqrt{w_k(i)}\right]$, and $\overline{n} = \left[n_1(i), n_2(i), \cdots, n_k(i)\right]^T$.

To understand the nature of the near-far problem, it is necessary to first understand the conventional method of demodulating the received signal. The conventional DS-CDMA receiver consists of the matched filter bank followed by a symbol-rate sampler and threshold device as shown in Figure 1.4. The ith input to the kth user's threshold device will thus be given by equation (1.5). The performance of the conventional DS-CDMA receiver has been extensively analyzed and many different bounds and approximations for its probability of error have been found [30]-[33]. Note that the decision statistic $y_k(i)$ is the sum of three distinct components: a desired signal component, a multiple-access-
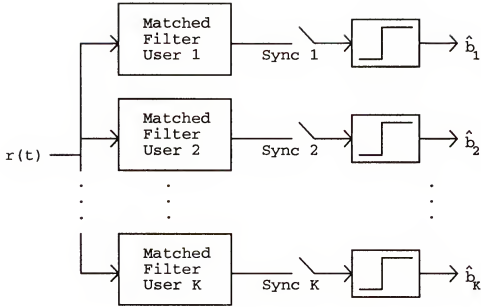
Figure 1.4 - The Conventional DS-CDMA Detector

interference (MAI) component, and a noise component. It is
the presence of the MAI component which accounts for the so-
called near-far problem. Since in practice the chosen
signature waveforms will not have zero cross-correlations
(particularly in the more general asynchronous case), the
magnitude of the MAI component will increase as the received
energies of the K-1 other users increase. As a result, even
for low signature waveform cross-correlations, the MAI
component can dominate the desired user's decision statistic
when the received energy of any other user becomes much
greater than that of the desired user. Thus, weaker users
will not be able to communicate in the presence of stronger
users. Since unequal received energies could occur at the
base station if some users were farther away than others,
this problem has been named the near-far problem.

Until recently, the most popular strategy for combating the near-far problem has been the user of transmitter power control, in which the base station continually monitors the received power levels of all users and instructs them to either increase or decrease their transmitter powers so that all received signals are of approximately equal strength at the base station [1], [34]-[36]. There are two major disadvantages to using a power control scheme, however. First, the rate at which power control updates could be performed is an open issue. While it may be feasible to counteract differences in received energies due to radial distances from the base station, a much greater update rate would be required to combat the effects of fading. Secondly, and more importantly, the use of power control will not eliminate the near-far problem but will only reduce it. That is, even if perfect power control was possible, there would still be an MAI component present in each user's decision statistic. The presence of the MAI component results in an irreducible error floor; consequently, the conventional detector can never obtain the same level of performance that a single user would have in the same channel.

Previous Work

As an alternative to using power control schemes, recent work has focused on using information known about the

signature waveforms, time delays, received energies, received carrier phases, and channel parameters to completely eliminate the MAI component from each user's decision statistic. The resulting structures are called multiuser detectors, and they are immune to the near-far problem. All multiuser detectors have a front-end consisting of the matched filter bank; the difference between the various proposed multiuser receivers is the algorithm chosen to follow the filter bank.

The optimum multiuser detector was derived by Verdu [29]; it consists of the matched filter bank followed by a dynamic programming algorithm which searches for the set of maximum likelihood transmitted sequences, for which the Viterbi algorithm may be used. Although this receiver is able to find the maximum-likelihood transmitted sequences, there are several practical limitations associated with its implementation. First, the number of computations required per demodulated data bit is exponential in the number of active users. For instance, for BPSK transmission the complexity is $O(2^K)$, where K is the number of active users. Furthermore, the optimum multiuser detector requires the perfect knowledge of the received energies and carrier phases of all bits. Perfect knowledge of each user's propagation delay is also required. The acquisition of this side information in the hostile urban digital mobile radio environment may be extremely difficult.

Motivated by the need to reduce the complexity of the optimum multiuser detector, Lupas and Verdu considered restricting the receiver to have a complexity which is linear in the number of users and arrived at the so-called decorrelating detector [37], [38]. A linear detector will form its decisions as

$$\hat{\overline{b}} = \text{sign}[L\overline{Y}] \tag{1.8}$$

where L is a linear transformation. It is interesting to note that the conventional detector is a linear detector which simply chooses $L = I$ (the identity matrix) as its transform. The decorrelator chooses $L = R^{-1}$ as its transformation and therefore forms its decisions as

$$\begin{aligned}
\hat{\overline{b}} &= \text{sign}[R^{-1}\overline{Y}] \\
&= \text{sign}[W\overline{b} + R^{-1}\overline{n}]
\end{aligned} \tag{1.9}$$

It is clear from equation (1.9) that the decorrelator would make no errors in the absence of noise since $\text{sign}[W\overline{b}] = \overline{b}$. Furthermore, note that there is no longer an MAI component present in equation (1.9); consequently, the decorrelator's decision is independent of the received energies of the other users and hence the decorrelator is immune to the near-far effect. It should be mentioned that the inverse of the matrix R is guaranteed to exist provided that the signature waveforms are linearly independent of one another, a rather mild restriction compared to that of the conventional DS-CDMA detector which would require the signature waveforms to be orthogonal in order to achieve

roughly the same level of performance. One advantage offered by the decorrelator is that it does not require knowledge of the received energies; however, for an asynchronous system it does require knowledge of the propagation delays and received carrier phases of all received bits. Furthermore, in an asynchronous system the decorrelator must observe the entire transmitted sequences of all users before it can begin decoding. Thus, the decorrelator will suffer from long decoding delays and large memory requirements. Also, the inverse of an MK by MK matrix must be computed, where M is the message length in symbols and K is the number of active users. Thus, the decorrelator is rendered impractical for most asynchronous systems. As an alternative implementation, a linear time-invariant transfer function was also found for the decorrelator [38], but this approach cannot accommodate changes in the timing configuration or the number of active users. Finally, it is interesting to note that when demodulation of only one user's data is required, as in the mobile receivers, for example, then the matched filter bank may be replaced with only one matched filter. Instead of correlating the received signal with a replica of the desired user's signature waveform, the received signal is correlated with the projection of the desired user's signature waveform onto the subspace which is orthogonal to the space spanned by the signature waveforms of the other active users.

Nonlinear multiuser detection techniques have also been proposed. These receivers generate tentative decisions for each user and later use them for cancellation of the MAI [39]-[41]. The multistage multiuser detector [39] utilizes the conventional DS-CDMA detector to form the initial polarity decisions in the first stage. These decisions are then used to reconstruct the MAI contributed from each user. The MAI contributions are summed together and subtracted from the desired user's initial decision statistic in the second stage. At this point, final decisions could be made, or additional stages of MAI re-creation and subtraction could be performed. The decorrelator has also been suggested as a replacement for the conventional detector in the first stage. The main disadvantage associated with these nonlinear detectors is that in order to correctly reconstruct the MAI, they require knowledge of all the received energies, carrier phases, and propagation delays of all bits from all users.

Another nonlinear technique proposed for multiuser decoding is to first decode the strongest user, then use that decision to help decode the next strongest user, and so on [42]-[44]. The idea is that the strongest user will have the least amount of MAI corruption present in the decision statistic, and so a conventional decision may be made. Then the MAI from the strongest user may be re-created and subtracted from the initial decision statistic of the next strongest user. This process then repeats itself until the

weakest user has been demodulated. Such a strategy also requires knowledge of the received energies, carrier phases, and propagation delays. Interestingly, the receiver presented by Dent [44] performs the MAI cancellation by nulling a component in a spectral domain and hence avoids the need to reconstruct the MAI in the time domain.

Others have suggested an adaptive filter based receiver structure for multiuser detection [45]-[47]. Both a minimum mean squared error criterion and a weighted least squares criterion have been investigated [45]. Although not a multiuser detector, the receiver structure presented by Miller [46] is able to obtain timing information on a single user and thus can be used for joint estimation/detection. Interestingly, this receiver does not require knowledge of the desired user's signature waveform.

The extension of multiuser receivers to noncoherent communication systems was presented by Varanasi [48], [49]. Unlike their coherent counterparts, these receivers do not require knowledge of received carrier phases.

The extension of multiuser detectors to fading channels includes [50]-[55]. The linear time-invariant transfer function version of the decorrelator was presented and analyzed for both flat Rayleigh fading and frequency selective fading channels by Zvonar [55]; as with their AWGN counterpart, these receivers cannot accommodate changes in the number of active users or their relative delays.

Outline of the Dissertation

Motivated by the promising features offered by the decorrelator, this work proposes a method by which a decorrelating detector may be implemented in an asynchronous communication system while avoiding the inversion of the MK by MK matrix and the need to observe and store the entire transmitted sequences of all users. One strategy to accomplish this goal is to apply the decorrelating procedure to a very small portion of the received sequences at a time, thus in effect windowing the received sequences. Such a strategy has been suggested [45], and a sliding window version of the decorrelator was proposed [56]. Neither work presented analytical results on the performance of such a receiver, however. Furthermore, the sliding window decorrelator [56] is dependent upon the system employing a rate 1/2 convolutional code for error correction purposes, thereby restricting the overall applicability of such a receiver. The main contributions of this work are to provide an analytical treatment of system performance when a windowed decorrelating strategy is used and to propose a method for implementing such a receiver independently of any error correction schemes, for both AWGN and frequency nonselective Rayleigh fading channels.

Chapter two presents a windowed decorrelating receiver suitable for use in additive white Gaussian noise (AWGN) channels. The performance of the receiver is analyzed and

compared to that of the conventional detector with power control and the full length decorrelator.

Chapter three presents a windowed decorrelating receiver suitable for use in frequency nonselective Rayleigh fading channels. The performance of the receiver is analyzed and compared to that of the conventional detector with power control and the full length decorrelator.

Chapter four discusses some of the practical issues associated with the implementation of the windowed decorrelator. Computational complexity and sensitivity to errors in the timing information are investigated.

Chapter five summarizes the windowed decorrelator in both AWGN and flat fading channels. Areas for further work related to the windowed decorrelator are suggested.

CHAPTER 2
WINDOWED DECORRELATING MULTIUSER RECEIVER FOR ADDITIVE WHITE
GAUSSIAN NOISE CHANNELS

System Description

The link from the users to the base station is assumed
to be asynchronous; that is, no effort is made by the users
to coordinate their transmitted sequences in time. The link
from the base station to the users is assumed to be
synchronous; that is, the base station would transmit the
i^{th} bit of each user simultaneously. The asynchronous
transmission makes the design for the base station receiver
much more challenging than the receiver for each of the
mobile units. To indicate why this is so, Figure 2.1
displays a three bit wide window in both a synchronous
system and an asynchronous system. The window spans bits i
through i+2. In the synchronous system, there is no
interference from bits outside the window; consequently, the
standard decorrelating strategy may be applied to each
consecutive window independently. In the asynchronous
system, however, bits outside the window overlap with bits
within the window thus introducing MAI from outside the
window. For instance, in Figure 2.1 the $(i+3)^{rd}$ bits of
users 1 through K-1 will interfere with the $(i+2)^{nd}$ bit of
user K. Furthermore, since the receiver will be attempting
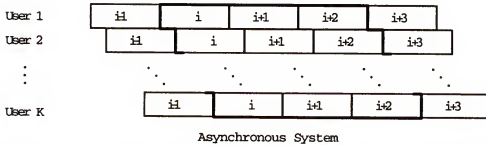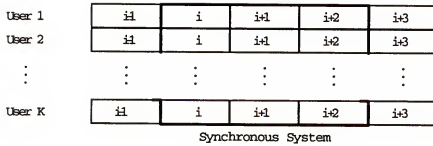
Figure 2.1 - Comparison of a Window in Synchronous and Asynchronous Systems

to determine the polarity of the bits contained within the current window, the polarities of the $(i+3)^{rd}$ bits of users 1 through K-1 are unknown. Consequently, the standard decorrelating procedure cannot be applied independently to each window and a more complex demodulation strategy must be chosen. The focus of this work will therefore be to propose a receiver for the base station and to analyze its performance.

The communication system of interest is one in which K users employ BPSK transmission through a common AWGN channel through use of direct sequence code division multiple access, as illustrated in Figure 2.2. For purposes of comparison, the notation used by Lupas [38] will be adopted.
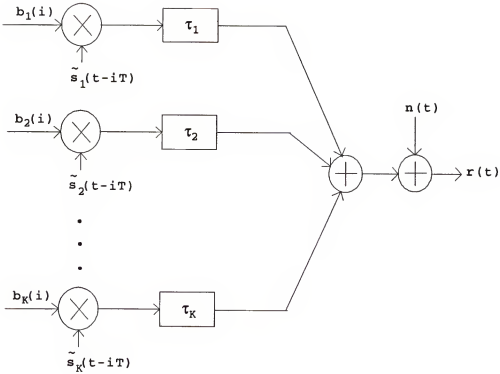
Figure 2.2 - Asynchronous DS-CDMA System Model

Each user transmits a sequence of length M bits, and without loss of generality the users are ordered according to their relative time delays $0 < \tau_1 < \tau_2 < \cdots < \tau_K < T$, where T is the common bit duration. The received signal at the base station is written as

$$r(t) = S(t, \overline{b}) + n(t) \qquad (2.1)$$

where n(t) is white Gaussian noise with power spectral density σ^2 and

$$S(t, \overline{b}) = \sum_{i=1}^{M} \sum_{k=1}^{K} b_k(i) \sqrt{w_k(i)} \tilde{s}_k(t - iT - \tau_k) \qquad (2.2)$$

where $b_k(i) \in \{\pm 1\}$ is the kth user's i^{th} data bit, $w_k(i)$ is the kth user's received power in the ith bit interval, and

$\tilde{s}_k(t)$ is the kth user's signature waveform which is zero outside the time interval $[0,T]$ and normalized to unit energy. The K by K signature waveform cross-correlation matrices are defined by their $(j,k)^{\text{th}}$ component

$$R_{j,k}(i) = \int_{-\infty}^{\infty} \tilde{s}_j(t - \tau_j)\tilde{s}_k(t + iT - \tau_k)dt \qquad (2.3)$$

From equation (2.3) it can be seen that $R(i) = 0$ for $|i| > 1$ and that $R(-1) = R^{\tau}(1)$.

It is important to note that the signature waveforms are RF waveforms and thus each user's RF carrier waveform is contained within each user's signature waveform. The base station is assumed to have knowledge of each user's signature waveform; thus, it is implied in this model that the received carrier phase of each user is known by the base station. This assumption will be justified for BPSK modulation since knowledge of the received carrier phases is required for coherent demodulation.

Another important observation from equation (2.3) is that baseband transmissions will maximize the signature waveform cross-correlations. To see why this is so, equation (2.3) can be re-written with baseband signature waveforms modulating RF carrier waveforms as

$$R_{j,k}(i) = \int_{-\infty}^{\infty} \tilde{s}_j(t - \tau_j)\cos(w_c t + \theta_j)\tilde{s}_k(t + iT - \tau_k)\cos(w_c t + \theta_k)dt \quad (2.4)$$

where $\tilde{s}_k(t)$ now represents the baseband signature sequence of the kth user. Using an appropriate trigonometric identity, equation (2.4) becomes

$$R_{j,k}(i) = \frac{1}{2} \int_{-\infty}^{\infty} \tilde{s}_j(t - \tau_j) \tilde{s}_k(t + iT - \tau_k) \cos(\theta_j - \theta_k) dt$$

$$+ \frac{1}{2} \int_{-\infty}^{\infty} \tilde{s}_j(t - \tau_j) \tilde{s}_k(t + iT - \tau_k) \cos(2w_c t + \theta_j + \theta_k) dt \qquad (2.5)$$

For $w_c t \gg 1$, the second integral in equation (2.5) is zero and the signature waveform cross-correlations become

$$R_{j,k}(i) = \frac{1}{2} \cos(\theta_j - \theta_k) \int_{-\infty}^{\infty} \tilde{s}_j(t - \tau_j) \tilde{s}_k(t + iT - \tau_k) dt \qquad (2.6)$$

Clearly, equation (2.6) will be maximized for baseband transmissions. Since the performance of an asynchronous DS-CDMA communication system will in general become better as the signature waveform cross-correlations become smaller in magnitude, baseband transmissions will therefore represent a worst case performance with respect to carrier phases. For the remainder of this chapter, baseband polar signaling will be the assumed modulation format.

It was shown by Verdu [29] that a sufficient statistic for determining the maximum-likelihood transmitted sequences through an AWGN channel can be obtained by passing the entire received signal r(t) through a bank of filters matched to the K signature waveforms. Therefore, the proposed multiuser receiver will consist of a matched filter bank followed by an appropriate decision algorithm, as shown in Figure 2.3. The matched filter bank is shown in more detail in Figure 2.4, from which it is apparent that both bit synchronization and code synchronization are required in order to operate the matched filter bank properly. Bit synchronization is necessary in order to sample the

Figure 2.3 - Structure of Multiuser Detector

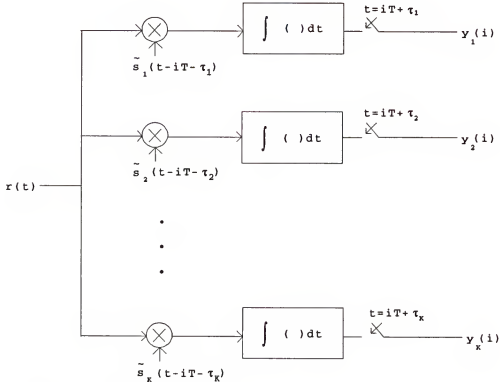Figure 2.4 - Matched Filter Bank for Asynchronous System

integrators at the proper intervals, and code synchronization is necessary in order to align the replica of each user's signature waveform with the corresponding arriving waveform. Acquisition of each user's time delay is thus necessary to achieve code synchronization. The output of the kth user's matched filter sampled at the end of the ith bit interval is

$$y_k(i) = \int_{iT+\tau_k}^{iT+T+\tau_k} r(t)\tilde{s}_k(t-iT-\tau_k)dt$$

$$= \sum_{j=k+1}^{K} R_{k,j}(1)\sqrt{w_j(i-1)}b_j(i-1) + \sum_{j=1}^{K} R_{k,j}(0)\sqrt{w_j(i)}b_j(i) \qquad (2.7)$$

$$+ \sum_{j=1}^{k-1} R_{k,j}(-1)\sqrt{w_j(i+1)}b_j(i+1) + n_k(i)$$

Defining $\overline{y}(i) = \left[y_1(i), y_2(i), \cdots, y_K(i)\right]^T$ to be the vector of matched filter outputs sampled at the end of the ith bit interval, $\overline{b}(i) = \left[b_1(i), b_2(i), \cdots, b_K(i)\right]^T$ to be the vector of ith transmitted bit polarities, $W(i) = \mathrm{diag}\left[\sqrt{w_1(i)}, \sqrt{w_2(i)}, \cdots, \sqrt{w_K(i)}\right]$ to be the matrix of received energies during the ith bit interval, and $\overline{n}(i) = \left[n_1(i), n_2(i), \cdots n_K(i)\right]^T$ to be the vector of matched filter noise outputs sampled at the end of the ith bit interval, equation (2.7) may be written more compactly as

$$\overline{y}(i) = R(-1)W(i+1)\overline{b}(i+1) + R(0)W(i)\overline{b}(i) + R(1)W(i-1)\overline{b}(i-1) + \overline{n}(i) \quad (2.8)$$

For a multiuser receiver operating on a data window spanning bits i through i+L-1, the entire vector of matched filter sampled outputs for the window can be written as

$$\overline{y}_L = R_{LK}W_L\overline{b}_L + \overline{n}_L + PW_e\overline{b}_e \qquad (2.9)$$

where $\overline{y}_L = \left[\overline{y}(i)^T, \overline{y}(i+1)^T, \overline{y}(i+2)^T, \cdots, \overline{y}(i+L-1)^T\right]^T$,
$\overline{b}_L = \left[\overline{b}(i)^T, \overline{b}(i+1)^T, \cdots, \overline{b}(i+L-1)^T\right]^T$, $W_L = \mathrm{diag}\left[W(i), W(i+1), \cdots, W(i+L-1)\right]$,
$\overline{n}_L = \left[\overline{n}(i)^T, \overline{n}(i+1)^T, \cdots, \overline{n}(i+L-1)^T\right]^T$, $W_e = \mathrm{diag}\left[W(i-1), W(i+L)\right]$,
$\overline{b}_e = \left[\overline{b}(i-1)^T, \overline{b}(i+L)^T\right]^T$, and the LK by LK and LK by 2K matrices

$$R_{LK} = \begin{pmatrix} R(0) & R(-1) & 0 & \cdots & 0 \\ R(1) & R(0) & R(-1) & \ddots & \vdots \\ 0 & \ddots & \ddots & \ddots & 0 \\ \vdots & \ddots & R(1) & R(0) & R(-1) \\ 0 & \cdots & 0 & R(1) & R(0) \end{pmatrix} \text{ and } P = \begin{pmatrix} R(1) & 0 \\ 0 & 0 \\ \vdots & \vdots \\ 0 & 0 \\ 0 & R(-1) \end{pmatrix}.$$

It is important to note that if the last term in equation (2.9) was missing, then equation (2.9) would be the same equation as for the vector of matched filter outputs for the full length decorrelator [38]. The additional term $PW_e\overline{b}_e$ is needed in equation (2.9) to take into account the edge effects of the windowing operation. Referring back to Figure 2.1, the matrix W_e contains the received powers of the bits immediately preceding and immediately following the current window; likewise, the vector $\overline{b}_e$ contains the polarities of these bits. The matrix P accounts for the cross-correlations between the signature waveforms modulated by these out-of-window interfering bits and those modulated by the bits within the window. For the full length decorrelator, the decorrelating operation is performed on all M bits of all users at once, and thus the full length decorrelator may be thought of as a windowed decorrelator which uses only one window of length M bits. Since the K users are not transmitting prior to the first bit nor after the Mth bit, there is no source of out-of-window MAI and hence the term $PW_e\overline{b}_e$ is not needed.

Performance Measures

The performance measures of interest are the probability of error and the multiuser asymptotic efficiency of each user, originally defined by Verdu [29]. For the kth

user operating at a probability of error P_e with a received energy w_k, the asymptotic efficiency is defined as

$$\eta_k(i) = \lim_{\sigma \to 0} \frac{w_{eff}}{w_k} \qquad (2.10)$$

where w_{eff} is the received energy required by a single user to achieve the same probability of error.

From equation (2.10) it is evident that an asymptotic efficiency equal to one would allow the kth user to communicate with the same probability of error as a single user while expending no additional transmitter power. For non-zero asymptotic efficiencies, the kth user can attain the same probability of error as a single user, but will require additional transmitter power. Of course, an asymptotic efficiency of zero would mean that the kth user could never achieve the same probability of error as a single user, regardless of how much additional transmitter power was available. These observations lead to the conclusion that if the kth user is operating at a non-zero asymptotic efficiency, then in the absence of noise the probability of error would be zero. In other words, the kth user's performance is not interference limited. On the other hand, if the kth user is operating at an asymptotic efficiency of zero, then in the absence of background noise there will still be an irreducible error floor due to the presence of the other users. Thus, the kth user's performance will be interference limited and hence the receiver will not be immune to the near-far effect.

Finally, just as probability of error is in general a function of signal-to-noise ratio, asymptotic efficiency is in general a function of the differences between received energies. A useful performance measure therefore is the kth user's near-far resistance, defined as the minimum value of the kth user's asymptotic efficiency over all possible energies of the other bits, both interfering and noninterfering.

Proposed Multiuser Receiver Structure

The standard decorrelating strategy of multiplying the vector of matched filter outputs by the inverse of the signature sequence cross-correlation matrix will no longer yield a decision statistic vector entirely free from MAI due to the presence of the out-of-window MAI, namely the term $PW_e\overline{b}_e$ in equation (2.9). The strategy chosen here is to first subtract off an estimate of the out-of-window MAI, call it $P\hat{W}_e\hat{\overline{b}}_e$, from $\overline{y}_L$ before multiplying by R_{LR}^{-1}. Since the matrix P is known, this strategy amounts to obtaining reliable estimates of the received energies contained in W_e and the bit polarities contained in $\overline{b}_e$. The final decision statistic vector for the current window will then become

$$\overline{z}_L = R_{LR}^{-1}\left(\overline{y}_L - P\hat{W}_e\hat{\overline{b}}_e\right)$$
$$= W_L\overline{b}_L + R_{LR}^{-1}\overline{n}_L + R_{LR}^{-1}P\left(W_e\overline{b}_e - \hat{W}_e\hat{\overline{b}}_e\right) \tag{2.11}$$

If the receiver was able to produce perfect estimates or had

knowledge of the true received energies and bit polarities, then the last term in equation (2.11) would equal zero and equation (2.11) would be the same as given by Lupas [38] for a full length decorrelator for which all users transmit L bits. In practice, of course, the receiver will not be able to produce perfect estimates; however, from equation (2.11) it is reasonable to expect that the windowed decorrelator's performance will improve as the estimates $\hat{W}_e$ and $\hat{\overline{b}}_e$ become closer to the true quantities W_e and $\overline{b}_e$. A block diagram depicting the general structure of the windowed decorrelator is presented in Figure 2.5. The delay block inserted before the matched filter bank is included since knowledge of the timing information will be necessary in order to operate the matched filter bank. The problem of extracting this timing information from the received signal is currently an area of active research [57]-[59]. In this work it will be assumed that perfect timing information is available to the receiver and that the matched filter bank is ideal and operating according to equation (2.9).

The requirement of producing an estimate of the out-of-window MAI affecting the current window can be divided into two separate tasks: estimating the received energies of the interfering bits and estimating the polarities of the interfering bits. For an RF system, the received carrier phase of the interfering bits will be required as well; however, since it is assumed that the multiuser receiver is
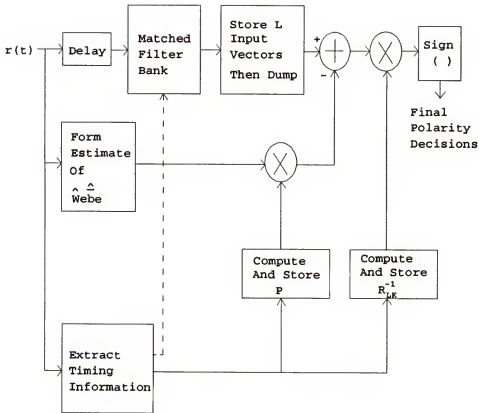
Figure 2.5 - Generalized Block Diagram of Windowed
Decorrelator

tracking the carrier phases for the purpose of coherent
demodulation, these quantities would not need to be
estimated. An interesting point to note is that if a
noncoherent modulation/demodulation technique were employed
by the system, such as DPSK, the carrier phases of the out-
of-window MAI bits would need to be known and hence would
require estimating. Thus the windowed decorrelator would in
a sense be self-defeating, since the advantage of using a
noncoherent scheme is that knowledge of carrier phases is
not required. Nonetheless, for situations in which tracking
the received carrier phases is either not possible or not
desirable, a noncoherent technique could be used with a

windowed decorrelator provided that estimates of the carrier phases before and after each window could be obtained.

To eliminate the need for estimating the polarities of the out-of-window MAI bits, pilot-symbol-assisted-modulation (PSAM) can be used. In PSAM, known symbols (pilot symbols) are periodically inserted into the transmitted sequence. PSAM is commonly used to obtain information on the channel characteristics in a dynamically evolving environment [28]. For the multiuser scenario considered here, the $(L+1)$th bit of each user would be a pilot bit as illustrated in Figure 2.6. The pilot bits thus serve to separate the data windows from one another and the multiuser receiver will simply discard them at the output of the matched filter bank.

| L data bits | pilot bit | L data bits | pilot bit | . . . |
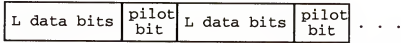
Figure 2.6 - Data Block Structure of Each User

Incorporating PSAM into the system offers two important advantages over other polarity estimation techniques. First, since the polarities of the pilot bits are known apriori by the multiuser receiver, PSAM will result in computational savings compared to any method which actually computes out-of-window MAI polarity estimates. The second advantage derived from using PSAM is that $\hat{\overline{b}}_e = \overline{b}_e$ for all windows, whereas any algorithm which attempts to compute $\hat{\overline{b}}_e$ will always be subject to errors introduced by a combination

of the background noise and MAI. That is, just as in
decision-directed feedback, it is possible that a polarity
estimate would be in error and could therefore cause errors
in the final polarity decisions of the data bits within the
current window. If these data bits are then used by the
algorithm to estimate the out-of-window MAI polarities
affecting the next window, the end result could be a
"snowball effect" in which one estimation error leads to
many final bit decision errors. Of course, using PSAM
eliminates this potential threat.

There are, however, two disadvantages in using PSAM.
First, each user will have a $\frac{1}{L+1}$% overhead due to the
presence of the pilot bits. The overhead results in a
reduction of each user's data rate by $\frac{1}{L+1}$% and an increase
in total required transmitter power by $\frac{1}{L+1}$%. The reduction
in data rate and increase in transmitter power occur since
each pilot bit has no message content; the same information
previously transmitted in L bits will now require L+1 bits.
Since the mobile units will most likely be battery powered,
any increase in the total amount of transmitter power
required can be costly. For this reason, care should be
used when incorporating PSAM to keep the overhead as low as
possible. The second disadvantage in using PSAM is that the
multiuser receiver must now acquire and maintain pilot
synchronization. In other words, the link from the mobile
units to the base station is no longer asynchronous in the
strictest sense since the receiver must align the mth pilot

bit of each user at the output of the matched filter bank to within T seconds. From the viewpoint of each user, though, the system is still completely asynchronous since the K users do not need to coordinate their transmitted sequences in time; this task is relegated to the base station. Recall that both code synchronization and bit synchronization are required to properly operate the matched filter bank (Figure 2.4). Assuming that the receiver has already obtained these levels of synchronization, obtaining pilot synchronization would then seem quite feasible. For the remainder of this analysis it will be assumed that pilot synchronization has been accomplished.

All that remains is for the multiuser receiver to form the matrix of required energy estimates, $\hat{W}_e$. For a full length decorrelator, the magnitudes obtained from the decorrelating solution are maximum-likelihood estimates of the corresponding received energies [29]. That is, the decorrelator bases its final polarity decisions upon the sign of the appropriate element in the decision statistic vector, but the magnitude of that element yields a maximum-likelihood received energy estimate. Of course, a full length decorrelating receiver does not require any knowledge of received energies; however, this available side information can be used to provide the required energy estimates for the windowed decorrelator. For slowly varying received energies, the multiuser receiver can use the energy

estimates derived from the previous window's decorrelating solution as its out-of-window MAI energy estimates for the current window. The energy estimates used for the very first window will be zero, since no past decorrelating solutions are available. Due to the presence of the out-of-window MAI, this estimation scheme will no longer be maximum-likelihood but its savings in computational complexity make it a very attractive choice.

The proposed receiver structure is now complete. A detailed block diagram of the receiver is shown in Figure 2.7. It is important to note that the cross-correlation matrix R_{LK} is a function of only the active signature sequences and the relative time delays between the active users. As these quantities may remain static for many consecutive windows, the computation of R_{LK}^{-1} will only need to be performed when the receiver senses a change in either the number of active users or their timing configuration.

Performance Analysis

The probability that the ith bit of the kth user is in error will be

$$P_k(i) = \Pr\left\{ \text{sign}\left[\overline{z}_L\right]_v^u = 1 \mid b_k(i) = -1 \right\} \tag{2.12}$$

where the notation $\left[\overline{x}\right]_v^u$ represents the vth element in the uth window of the vector $\overline{x}$. The window index u is given by

$$u = \text{int}\left[\tfrac{i-1}{L}\right] + 1 \tag{2.13}$$

and the vector element v is given by
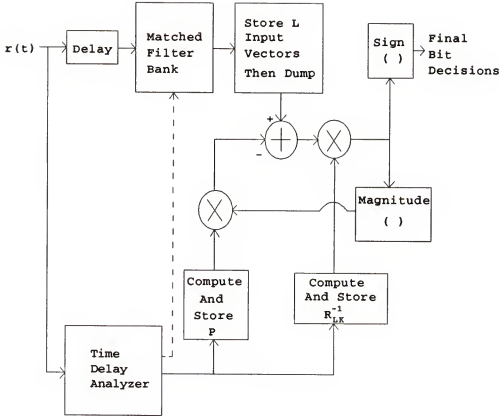
Figure 2.7 - Detailed Block Diagram of Windowed Decorrelator

$$v = (i-1)K + k - \text{int}\left[\frac{i-1}{L}\right]LK \qquad (2.14)$$

where the notation int[x] represents the integer part of x. Now,

$$\Pr\left\{\left[\overline{z}_L\right]_v^u > 0 \,\middle|\, b_k(i) = -1\right\} = \Pr\left\{\left[W_L \overline{b}_L\right]_v^u + \left[R_{LK}^{-1} \overline{n}_L\right]_v^u + \left[R_{LK}^{-1} P\left(W_e \overline{b}_e - \hat{W}_e \hat{\overline{b}}_e\right)\right]_v^u > 0 \,\middle|\, b_k(i) = -1\right\} \qquad (2.15)$$

which reduces to

$$P_k(i) = \Pr\left\{\left[R_{LK}^{-1} \overline{n}_L\right]_v^u > \sqrt{w_k(i)} - \left[R_{LK}^{-1} P\left(W_e \overline{b}_e - \hat{W}_e \hat{\overline{b}}_e\right)\right]_v^u\right\} \qquad (2.16)$$

Let $c_{m,n}$ denote the element in the mth row and n^{th} column of the matrix R_{LK}^{-1}. Then

$$R_{LK}^{-1} = C = \begin{bmatrix} c_{1,1} & c_{1,2} & \cdots & c_{1,LK} \\ c_{2,1} & c_{2,2} & \cdots & c_{2,LK} \\ \vdots & \vdots & \ddots & \vdots \\ c_{LK,1} & c_{LK,2} & \cdots & c_{LK,LK} \end{bmatrix} \qquad (2.17)$$

The noise component in equation (2.16) will be Gaussian with zero mean and a variance which is the vth diagonal element of

$$E\left\{\left[R_{LK}^{-1}\overline{n}_L\right]^u \left(\left[R_{LK}^{-1}\overline{n}_L\right]^u\right)^T\right\} = R_{LK}^{-1}\left(\sigma^2 R_{LK}\right)R_{LK}^{-1} \qquad (2.18)$$
$$= \sigma^2 R_{LK}^{-1}$$

Thus

$$\mathrm{var}\left\{\left[R_{LK}^{-1}\overline{n}_L\right]_v^u\right\} = \sigma^2 c_{v,v} \qquad (2.19)$$

From equation (2.16), the probability of error will be

$$P_k(i) = Q\left(\frac{\sqrt{w_k(i)} - \left[R_{LK}^{-1}P\left(W_e \overline{b}_e - \hat{W}_e \hat{\overline{b}}_e\right)\right]_v^u}{\sigma\sqrt{c_{v,v}}}\right) \qquad (2.20)$$

where the Q-function is defined as

$$Q(x) = \frac{1}{\sqrt{2}}\int_x^\infty e^{-\frac{t^2}{2}}dt \qquad (2.21)$$

Note that if PSAM was not used, then the probability of error given by equation (2.20) would need to be averaged over the 2^{2K} possible MAI polarity vectors $\overline{b}_e$ and would thus be a sum of Q-functions.

Before proceeding further, it is of interest to consider the ideal case in which the receiver has perfect knowledge (or perfect estimates) of the out-of-window MAI. This special case will indicate the best performance possible from a windowed decorrelating receiver. In this

scenario $\hat{W}_e \hat{\overline{b}}_e = W_e \overline{b}_e$ and equation (2.20) reduces to

$$P_k(i) = Q\left(\frac{\sqrt{w_k(i)}}{\sigma\sqrt{c_{v,v}}}\right) \qquad (2.22)$$

which is a function of only the kth user's received energy
and not of the other users' energies. Since the probability
of error for a single user employing BPSK in an AWGN channel
is

$$P_k(i) = Q\left(\frac{\sqrt{w_{eff}}}{\sigma}\right) \qquad (2.23)$$

then clearly $w_{eff} = w_k(i)/c_{v,v}$ and from equation (2.10) the
asymptotic efficiency for the ith bit of the kth user will
be

$$\eta_k(i) = \frac{1}{c_{v,v}} \qquad (2.24)$$

Since the asymptotic efficiency is a nonzero constant, the
near-far resistance will be equal to this constant as well
and the receiver is indeed immune to the near-far effect.
The actual value of the near-far resistance will depend upon
the cross-correlations between the signature sequences
through the term $c_{v,v}$. It should be noted that equation
(2.24) is the same result which would be obtained for a full
length decorrelator operating on a transmission of L bits.
Another interesting observation is that both the probability
of error and the asymptotic efficiency of the windowed
decorrelator are a function of the transmitted bit index;
more specifically, they are a function of the bit position
within each window through the term $c_{v,v}$. Thus the kth

user's probability of error and asymptotic efficiency will differ from bit to bit within each window, a property which is different from that of an infinite length decorrelator whose performance measures are independent of the bit index.

To evaluate the probability of error given by equation (2.20) further, the last term in the numerator must be investigated. For convenience it will be assumed that all pilot bits have a polarity of +1, although in practice this is not a necessary condition. The uth window of the vector $\left[W_e \overline{b}_e - \hat{W}_e \hat{\overline{b}}_e\right]$ will then become

$$\left[W_e \overline{b}_e - \hat{W}_e \hat{\overline{b}}_e\right]^u = \begin{bmatrix} \sqrt{w_1\big((u-1)(L+1)\big)} - \sqrt{\hat{w}_1\big((u-1)(L+1)\big)} \\ \sqrt{w_2\big((u-1)(L+1)\big)} - \sqrt{\hat{w}_2\big((u-1)(L+1)\big)} \\ \vdots \\ \sqrt{w_K\big((u-1)(L+1)\big)} - \sqrt{\hat{w}_K\big((u-1)(L+1)\big)} \\ \sqrt{w_1\big(u(L+1)\big)} - \sqrt{\hat{w}_1\big(u(L+1)\big)} \\ \sqrt{w_2\big(u(L+1)\big)} - \sqrt{\hat{w}_2\big(u(L+1)\big)} \\ \vdots \\ \sqrt{w_K\big(u(L+1)\big)} - \sqrt{\hat{w}_K\big(u(L+1)\big)} \end{bmatrix} \qquad (2.25)$$

Define the error in the energy estimate for the jth bit of the kth user as

$$\Delta w_k(j) = \sqrt{w_k(j)} - \sqrt{\hat{w}_k(j)} \qquad (2.26)$$

Actually, equation (2.26) represents an error in an amplitude estimate; indeed, the receiver actually needs to form amplitude estimates rather than energy estimates. For consistency, however, equation (2.26) will be referred to as an energy estimation error. Expanding out the term $\left[R_{LK}^{-1}P\Big(W_e\overline{b}_e - \hat{W}_e\hat{\overline{b}}_e\Big)\right]_v^u$ yields

$$\left[R_{LK}^{-1} P \left(W_e \overline{b}_e - \hat{W}_e \overline{b}_e \right) \right]_v^u = \sum_{l=2}^{K} \sum_{j=1}^{l-1} c_{v,j} R_{j,l}(1) \Delta w_l \big((u-1)(L+1) \big)$$
$$+ \sum_{l=1}^{K-1} \sum_{j=(L-1)K+1}^{LK} c_{v,j} R_{1,j-(L-1)K}(-1) \Delta w_l \big(u(L+1) \big) \tag{2.27}$$

Recall that the subscript v denotes the vth element in the corresponding vector, and thus in equation (2.27) v will range from 1 to LK. Substituting equation (2.27) into the equation for probability of error given by equation (2.20) produces

$$P_k(i) = Q \Bigg\{ \Big\{ \sqrt{w_k(i)} - \sum_{l=2}^{K} \sum_{j=1}^{l-1} c_{v,j} R_{j,l}(1) \Delta w_l \big((u-1)(L+1) \big) $$
$$- \sum_{l=1}^{K-1} \sum_{j=(L-1)K+1}^{LK} c_{v,j} R_{j-(L-1)K,l}(-1) \Delta w_l \big(u(L+1) \big) \Big\} \frac{1}{\sigma \sqrt{c_{v,v}}} \Bigg\} \tag{2.28}$$

Note that $\Delta w_k(i)$ may be either positive or negative, depending upon whether the corresponding received energy was underestimated or overestimated, respectively. It is therefore necessary to consider the worst-case probability of error which corresponds to the following least favorable event

$$\text{sign}\big\{ \Delta w_l \big((u-1)(L+1) \big) \big\} = \text{sign} \big\{ c_{v,l} R_{j,l}(1) \big\}, \quad l=2,3,\cdots,K$$
and
$$\text{sign}\big\{ \Delta w_l \big(u(L+1) \big) \big\} = \text{sign} \big\{ c_{v,l} R_{j-(L-1)K,l}(-1) \big\}, \quad l=1,2,\cdots,K-1 \tag{2.29}$$

The worse-case probability of error will therefore be

$$P_k(i)_{max} = Q \Bigg\{ \Big\{ \sqrt{w_k(i)} - \sum_{l=2}^{K} \sum_{j=1}^{l-1} \big| c_{v,j} R_{j,l}(1) \big\| \Delta w_l \big((u-1)(L+1) \big) \big| $$
$$- \sum_{l=1}^{K-1} \sum_{j=(L-1)K+1}^{LK} \big| c_{v,j} R_{j-(L-1)K,l}(-1) \big\| \Delta w_l \big(u(L+1) \big) \big| \Big\} \frac{1}{\sigma \sqrt{c_{v,v}}} \Bigg\} \tag{2.30}$$

The actual value of $P_k(i)_{max}$ will depend upon how large in magnitude the out-of-window MAI energy estimation errors are. Of course, for perfect energy estimates equation

(2.30) reduces to equation (2.22). The worst-case asymptotic efficiency can be found from equation (2.30); applying equation (2.10) gives

$$\eta_k(i)_{min} = \max^2\Bigg\{\ 0, \Bigg[\ 1 - \sum_{i=2}^{K}\sum_{j=1}^{i-1}|c_{v,j}R_{j1}(1)|\frac{\left|\Delta w_j((u-1)(L+1))\right|}{\sqrt{w_k(i)}}$$
$$- \sum_{l=1}^{K-1}\sum_{j=(L-1)K+1}^{LK}|c_{v,j}R_{j-(L-1)K,1}(-1)|\frac{\left|\Delta w_j(u(L+1))\right|}{\sqrt{w_k(i)}}\ \Bigg]\frac{1}{\sqrt{c_{v,v}}}\ \Bigg\}$$

$$(2.31)$$

The form of equation (2.31) provides some valuable insight into the behavior of the windowed decorrelator's asymptotic efficiency. First, as the magnitudes of the out-of-window MAI energy estimation errors approach zero, the asymptotic efficiency approaches the constant value found in equation (2.22). As the energy estimation errors become larger in magnitude, the asymptotic efficiency will decrease until the two summation terms yield a combined value of one, after which the asymptotic efficiency will remain zero. Thus the near-far resistance of the windowed decorrelator is zero. It is important to observe from equation (2.31), however, that the errors in the estimates of the interfering amplitudes are divided by the amplitude of the desired user in determining the desired user's asymptotic efficiency. Thus, the estimation errors are in effect normalized by the desired user's amplitude. The stronger the desired user's received signal is, the less effect the energy estimation errors will have upon the desired user's performance. Thus, even though the near-far resistance is zero, the differences between received energies at which the asymptotic efficiency

becomes zero may be sufficiently large to cover any reasonable near-far scenario which might be encountered in practice.

All that remains to complete the performance analysis of the windowed decorrelator is to substitute appropriate expressions for $\left|\Delta w_j\big((u-1)(L+1)\big)\right|$ and $\left|\Delta w_j\big(u(L+1)\big)\right|$ into the expression for worst-case asymptotic efficiency given by equation (2.31). Decorrelating the first window will yield energy estimates of the K users for the bit intervals 1 through L. The second window will use the estimates corresponding to the most recent bit interval, the Lth interval, to modify its matched filter output vector. Decorrelating the second window will produce energy estimates of the K users for the bit intervals L+2 through 2L+2. The third window will then use the estimates corresponding to the $(2L+2)^{nd}$ interval to modify its matched filter output vector, and so on.

Consider the very first window (u=1) spanning bits 1 through L. No past estimates are available and so

$$\hat{w}_j(L+1) = 0, \qquad j = 1,2,\cdots,K \tag{2.32}$$

The receiver forms the decision statistic vector

$$\begin{aligned}\overline{z}_L &= R_{Lk}^{-1}\overline{y} \\ &= W_L\overline{b}_L + \overline{\gamma}_L + R_{LK}^{-1}PW_e\overline{b}_e\end{aligned} \tag{2.33}$$

where the noise component vector $\overline{\gamma}_L$ has been defined as

$$\overline{\gamma}_L = R_{LK}^{-1}\overline{n}_L \tag{2.34}$$

The last term in equation (2.33) represents the out-of-

window MAI corrupting the first window's decision statistic vector. Expanding out this term and denoting it by $\overline{I(1)}$ yields its vth element to be

$$\left[\overline{I(1)}\right]_v = \sum_{l=1}^{K-1} \sum_{j=(l-1)K+l+1}^{lK} c_{v,j} R_{j-(l-1)K,1}(-1)\sqrt{w_j(L+1)} \qquad (2.35)$$

The estimate of the kth user's received energy will be formed as

$$\sqrt{\widehat{w_k(L)}} = \left| \sqrt{w_k(L)} b_k(L) + \gamma_k(L) + I_k(1) \right| \qquad (2.36)$$

Since the expression for asymptotic efficiency given by equation (2.31) was derived in the limit as $\sigma \to 0$, the noise component in equation (2.36) may be neglected. Thus

$$\sqrt{\widehat{w_k(L)}} = \left| \sqrt{w_k(L)} b_k(L) + I_k(1) \right| \qquad (2.37)$$

The error in this estimate is then

$$\Delta w_k(L) = \sqrt{w_k(L)} - \left| \sqrt{w_k(L)} b_k(L) + I_k(1) \right| \qquad (2.38)$$

Equation (2.37) is of the general form

$$\sqrt{w} - \left| \pm \sqrt{w} \pm I \right| \qquad (2.39)$$

which is shown in Appendix A to be bounded by

$$-|I| \le \sqrt{w} - \left| \pm \sqrt{w} \pm I \right| \le |I| \qquad (2.40)$$

Therefore the estimation error will be bounded by

$$\left| \Delta w_k(L) \right| \le \left| I_k(1) \right| \qquad (2.41)$$

The worst-case estimation error will occur when each term inside the summations in equation (2.35) has the same sign, resulting in

$$\left| \Delta w_k(L) \right|_{max} = \sum_{l=1}^{K-1} \sum_{j=(l-1)K+l+1}^{lK} \left| c_{(l-1)K+1,j} R_{j-(l-1)K,1}(-1) \right| \sqrt{w_1(L+1)} \qquad (2.42)$$

To proceed, the vector of maximum possible energy estimation

errors obtained from decorrelating the uth window is defined as

$$\overline{\Delta w(u)} = \begin{bmatrix} \left| \Delta w_1 \big(u(L+1)-1 \big) \right|_{max} \\ \left| \Delta w_2 \big(u(L+1)-1 \big) \right|_{max} \\ \vdots \\ \left| \Delta w_K \big(u(L+1)-1 \big) \right|_{max} \end{bmatrix} \qquad (2.43)$$

Note that the kth element of $\overline{\Delta w(1)}$ will be given by equation (2.42).

Now consider the second window (u=2), spanning bits L+2 through 2L+2. Recall that the $(L+1)^{th}$ bit of each user is a pilot bit and is discarded by the multiuser receiver. The decision statistic vector for the second window will be

$$\overline{z}_L = W_L \overline{b}_L + \overline{\gamma}_L + R_{LK}^{-1} P \big(W_e \overline{b}_e - \hat{W}_e \overline{b}_e \big) \qquad (2.44)$$

In an AWGN channel, the received energies will be changing slowly relative to a bit duration. For small window lengths, it will be assumed that the received energies are constant over a span of L+2 bits; in other words

$$\sqrt{w_j(i+m)} = \sqrt{w_j(i)}, \qquad |m| \le L+2 \qquad (2.45)$$

With the above simplifying assumption, equation (2.25) becomes

$$\left[W_e \overline{b}_e - \hat{W}_e \overline{b}_e \right]^{u=2} = \begin{bmatrix} \Delta w_1(L) \\ \Delta w_2(L) \\ \vdots \\ \Delta w_K(L) \\ \Delta w_1(L) \\ \Delta w_2(L) \\ \vdots \\ \Delta w_K(L) \end{bmatrix} \qquad (2.46)$$

Pre-multiplying equation (2.46) by $R_{Lk}^{-1}P$ and using the worst case estimation errors given by equation (2.42) results in an expression for the vth element of the out-of-window MAI term affecting the second window's decision statistic

$$\left[\overline{I(2)}\right]_v = \left[R_{Lk}^{-1}P\left(w_e\overline{b}_e - \hat{w}_e\overline{b}_e\right)\right]_v^2$$
$$= \sum_{l=2}^{K}\sum_{j=1}^{l-1}c_{v,j}R_{j,l}(1)\left[\Delta w_1(L)\right]_{max} + \sum_{l=1}^{K-1}\sum_{j=(l-1)K+1}^{LK}c_{v,j}R_{j-(l-1)K,l}(-1)\left[\Delta w_1(L)\right]_{max} \quad (2.47)$$

By re-grouping terms, equation (2.47) can be written as

$$\left[\overline{I(2)}\right]_v = \sum_{l=2}^{K}\left[\Delta w_1(L)\right]_{max}\sum_{j=1}^{l-1}c_{v,j}R_{j,l}(1) + \sum_{l=1}^{K-1}\left[\Delta w_1(L)\right]_{max}\sum_{j=(l-1)K+1}^{LK}c_{v,j}R_{j-(l-1)K,l}(-1)$$

$$(2.48)$$

Finally, the energy estimates will be based upon the last bit of each user within the window so that the kth element in the vector of worst case energy estimation errors obtained from decorrelating the second window becomes

$$\left[\left[\overline{\Delta w(2)}\right]_{max}\right]_k = \sum_{l=2}^{K}\left[\left[\overline{\Delta w(1)}\right]_{max}\right]_l\sum_{j=1}^{l-1}c_{(l-1)K+k,j}R_{j,l}(1)$$
$$+ \sum_{l=1}^{K-1}\left[\left[\overline{\Delta w(1)}\right]_{max}\right]_l\sum_{j=(l-1)K+1}^{LK}c_{(l-1)K+k,j}R_{j-(l-1)K,l}(-1) \quad (2.49)$$

A relationship between the vector of worst case energy estimation errors obtained from consecutive windows is now evident from equation (2.49). The initial out-of-window MAI term corrupting the first window's decision statistic vector has been reduced after the second window has been decorrelated. This process will repeat itself for each additional window which is processed by the receiver; in other words, the initial out-of-window MAI term will decrease as the number of windows processed by the receiver

increases. The generic form of this relationship will be

$$\overline{\Delta w(u)} = A\overline{\Delta w(u-1)}, \quad u \geq 2 \tag{2.50}$$

where A is the appropriate recursion matrix. To determine
an expression for the contents of the K by K matrix A,
equation (2.50) can be expanded out to obtain

$$\begin{bmatrix} \Delta w_1\big(u(L+1)-1\big) \\ \Delta w_2\big(u(L+1)-1\big) \\ \vdots \\ \Delta w_K\big(u(L+1)-1\big) \end{bmatrix} = \begin{bmatrix} a_{1,1} & a_{1,2} & \cdots & a_{1,K} \\ a_{2,1} & a_{2,2} & \cdots & a_{2,K} \\ \vdots & \vdots & \ddots & \vdots \\ a_{K,1} & a_{K,2} & \cdots & a_{K,K} \end{bmatrix} \begin{bmatrix} \Delta w_1\big((u-1)(L+1)-1\big) \\ \Delta w_2\big((u-1)(L+1)-1\big) \\ \vdots \\ \Delta w_K\big((u-1)(L+1)-1\big) \end{bmatrix} \tag{2.51}$$

It is clear from equation (2.51) that the pth row of the
matrix A must correspond to the pth user, so the subscript k
in equation (2.49) can be replaced with p. Also, the qth
column of the matrix A must correspond to the lth element in
the previous error vector, so the subscript l in equation
(2.49) can be replaced with q. Finally, since the ranges of
l in the summations in equation (2.49) overlap, each
summation will contribute a component to each $a_{p,q}$ term and
thus their contributions must be summed. The resulting
coefficient of $\big[\Delta w(u-1)\big]_l$ in equation (2.49) (for which u=2)
must then be $a_{p,q}$. Therefore, the element in the pth row
and q^{th} column of the matrix A is given by

$$a_{p,q} = \sum_{j=(L-1)K+1+q}^{LK} \Big| c_{(L-1)K+p,j} R_{j-(L-1)K,q}(-1) \Big| + \sum_{j=1}^{q-1} \Big| c_{(L-1)K+p,j} R_{j,q}(1) \Big| \tag{2.52}$$

From equation (2.50) the vector of worst case energy
estimation errors obtained from decorrelating the uth window
can be related to those obtained from decorrelating the
first window by

$$\overline{\Delta w(u)} = A^{u-1} \overline{\Delta w(1)}, \qquad u \geq 1 \tag{2.53}$$

Under the assumption of equation (2.45), equation (2.46) can be substituted into the expression for asymptotic efficiency given in equation (2.31) to obtain

$$\eta_k(i)_{min} = \max^2 \Bigg\{ 0, \Bigg[1 - \sum_{l=2}^{K} \sum_{j=1}^{l-1} |c_{v,j} R_{j1}(1)| \frac{\left|\Delta w_j((u-1)L)\right|}{\sqrt{w_k(i)}} \\ - \sum_{l=1}^{K-1} \sum_{j=(L-1)K+1}^{LK} |c_{v,j} R_{j-(L-1)K,1}(-1)| \frac{\left|\Delta w_j((u-1)L)\right|}{\sqrt{w_k(i)}} \Bigg] \frac{1}{\sqrt{c_{v,j}}} \Bigg\} \tag{2.54}$$

Finally, using the relationship between the uth window and the first window given by equation (2.53), the windowed decorrelator's worst case asymptotic efficiency for the ith bit of the kth user is

$$\left[\eta_k(i)\right]_{min} = \max^2 \Bigg\{ 0, \frac{1}{\sqrt{c_{v,v}}} \Bigg[1 - \sum_{l=2}^{K} \sum_{j=1}^{l-1} |c_{v,j} R_{j,1}(1)| \frac{\left[A^{u-2}\overline{\Delta w(1)}\right]_j}{\sqrt{w_k(i)}} \\ - \sum_{l=1}^{K-1} \sum_{j=(L-1)K+1}^{LK} |c_{v,j} R_{j-(L-1)K,1}(-1)| \frac{\left[A^{u-2}\overline{\Delta w(1)}\right]_j}{\sqrt{w_k(i)}} \Bigg] \Bigg\} \tag{2.55}$$

where as before the notation $[\overline{x}]_l$ represents the lth element in the vector x and the window index u is related to the bit index i through equation (2.13).

A very important observation from equation (2.55) is that if

$$\lim_{u \to \infty} A^u = 0 \tag{2.56}$$

then

$$\lim_{i \to \infty} \eta_k(i) = \frac{1}{c_{v,v}} \tag{2.57}$$

Thus, if equation (2.56) is satisfied, then the asymptotic efficiency of the windowed decorrelating receiver will converge to the same value as for the full length

decorrelating receiver. In other words, after a sufficient number of windows has been processed, the windowed decorrelator will for all practical applications be near-far resistant and hence immune to the near-far effect. It is therefore important to determine under what conditions equation (2.56) will hold; however, it is easier to first consider the conditions under which equation (2.56) will not hold.

It was shown by Lupas [38] that a stable realization of the decorrelating receiver will exist as the message length approaches infinity if and only if the signature waveform cross-correlations satisfy

$$\det\left[R^{\tau}(1)e^{j\omega} + R(0) + R(1)e^{-j\omega}\right] \neq 0, \qquad \forall \omega \in [0, 2\pi) \qquad (2.58)$$

One way to arrive at this result is by considering equation (2.9), without the term due to the edge effects of the windowing operation, in the limit as the message length approaches infinity and taking Z-transforms. Defining

$$S(z) = R^{\tau}(1)z + R(0) + R(1)z^{-1} \qquad (2.59)$$

it is clear that the transfer function of the infinite length decorrelating receiver must be

$$G(z) = [S(z)]^{-1} \qquad (2.60)$$

A stable transfer function will therefore not exist unless equation (2.58) is satisfied. Clearly, if equation (2.58) is not satisfied then equation (2.56) cannot be satisfied; that is, if a stable infinite length decorrelator does not exist, then there will be no receiver for the windowed

decorrelator to converge to as the window index increases. For a K user system, the appropriate cross-correlations will need to be checked according to equation (2.58) to determine if an infinite length decorrelator exists; however, for a two user system equation (2.58) reduces to a rather simple condition. For this special case the cross-correlation matrices may be defined as

$$R(0) = \begin{bmatrix} 1 & \rho_{12} \\ \rho_{12} & 1 \end{bmatrix} \quad \text{and} \quad R(1) = \begin{bmatrix} 0 & \rho_{21} \\ 0 & 0 \end{bmatrix} \qquad (2.61)$$

so that equation (2.58) becomes

$$\det \begin{bmatrix} 1 & \rho_{12} + \rho_{21} e^{-j\omega} \\ \rho_{12} + \rho_{21} e^{+j\omega} & 1 \end{bmatrix} \neq 0 \qquad (2.62)$$

which upon taking the determinant yields

$$\rho_{12}^2 + \rho_{21}^2 + 2\rho_{12}\rho_{21} \cos(\omega) \neq 1 \qquad (2.63)$$

Now,

$$\rho_{12}^2 + \rho_{21}^2 + 2\rho_{12}\rho_{21} \cos(\omega) \leq \left(|\rho_{12}| + |\rho_{21}| \right)^2 \qquad (2.64)$$

so that if

$$|\rho_{12}| + |\rho_{21}| < 1 \qquad (2.65)$$

then

$$\rho_{12}^2 + \rho_{21}^2 + 2\rho_{12}\rho_{21} \cos(\omega) < 1 \qquad (2.66)$$

and equation (2.58) is always satisfied and a stable infinite length decorrelator will exist. Note that equation (2.65) is a rather loose constraint upon the signature sequence cross-correlations; in practice it is not difficult to find a pair of signature sequences satisfying this condition.

Unfortunately, the existence of an infinite length decorrelator would not seem to guarantee that the windowed decorrelator will converge to the same performance. It therefore remains to determine under what conditions equation (2.56) will be valid. To do this, some well known theorems from linear algebra will be used.

If the matrix A is diagonalizable then it can be written as [60]

$$A = B \Lambda B^{-1} \qquad (2.67)$$

where Λ is the diagonal matrix whose diagonal elements $\lambda_1, \lambda_2, \cdots, \lambda_k$ are the eigenvalues of A, and B is a matrix of corresponding eigenvectors. It can be shown [60] that

$$A^u = B \Lambda^u B^{-1} \qquad (2.68)$$

so that equations (2.56) and (2.57) become

$$\lim_{i \to \infty} \eta_k(i) = \frac{1}{c_{v,v}} \quad \text{if} \quad \lim_{u \to \infty} \Lambda^u = 0 \qquad (2.69)$$

Since Λ is a diagonal matrix, the above condition simplifies to

$$\lim_{i \to \infty} \eta_k(i) = \frac{1}{c_{v,v}} \quad \text{if} \quad \left| \lambda_j \right| < 1, \quad j = 1, 2, \cdots, K \qquad (2.70)$$

Thus, if the matrix A defined by equation (2.52) is diagonalizable and its eigenvalues all have magnitudes less than one, then the asymptotic efficiency of the windowed decorrelator will approach a nonzero constant as the window index increases. Due to the analytical intractability of determining the eigenvalues of a K by K matrix, the focus here will be on a two user system. In addition to being

mathematically convenient, the two user case may provide valuable insight into the general K user scenario.

It is shown in Appendix B that the matrix A will always be diagonalizable for the case of two users; it therefore only remains to compare the magnitudes of the eigenvalues of A with unity. For a window of length three bits, the eigenvalues of A are the solutions to the equation

$$\lambda^2 - \left(\left|c_{5,6}\rho_{21}\right| + \left|c_{6,1}\rho_{21}\right|\right)\lambda + \rho_{21}^2\left(\left|c_{5,6}c_{6,1}\right| - \left|c_{6,6}c_{5,1}\right|\right) = 0 \tag{2.71}$$

Upon substituting equations (B.13) and (B.17) into equation (2.71) and using the relationships given by equations (B.4) and (B.5), the eigenvalues of the matrix A are found from the quadratic formula to be

$$\lambda_{1,2} = \frac{1}{2}\left\{\left|\frac{\rho_{12}^3\rho_{21}^3}{D}\right| + \left|\frac{\rho_{21}N}{D}\right| \pm \left[\left(\left|\frac{\rho_{12}^3\rho_{21}^3}{D}\right| + \left|\frac{\rho_{21}N}{D}\right|\right)^2\right.\right.$$
$$\left.\left. - 4\left(\left|\frac{\rho_{12}^3\rho_{21}^3}{D}\right|\right)\left(\left|\frac{\rho_{21}N}{D}\right| - \left|\frac{\rho_{21}-\rho_{21}\rho_{12}N}{D}\right|\right)\right]^{\frac{1}{2}}\right\} \tag{2.72}$$

where

$$N = -\rho_{12}^5 + 2\rho_{12}^3 + \rho_{12}\rho_{21}^2 - \rho_{12} \tag{2.73}$$

and

$$D = \rho_{12}^6 - 3\rho_{12}^4 - \rho_{21}^4 + 3\rho_{12}^2 + 2\rho_{21}^2 - 2\rho_{12}^2\rho_{21}^2 - 1 \tag{2.74}$$

Unfortunately, equation (2.72) does not appear to lend itself to a more compact form. In an attempt to gain further insight into the behavior of equation (2.72) a numerical approach was taken. The values of the cross-correlations ρ_{12} and ρ_{21} were varied between -1 and +1 in increments of 0.1. For each combination of values, the

matrices R, C, and A were computed and the eigenvalue of A with the largest magnitude was then found. The results are summarized in Table 2.1, from which it is readily apparent that the condition for convergence of the windowed decorrelator given in equation (2.70) is equivalent to

$$\lim_{i \to \infty} \eta_k(i) = \frac{1}{c_{v,v}} \quad \text{if} \quad |\rho_{12}| + |\rho_{21}| < 1, \quad k=1,2 \qquad (2.75)$$

Interestingly, the condition given in equation (2.75) is equivalent to that given in equation (2.65) for the existence of an infinite length decorrelator. Thus, if a stable infinite length decorrelating receiver exists for a two user system, then the windowed decorrelating receiver will always become near-far resistant as the window index increases.

Repeating the previous analysis for the more general K user system is not feasible. One reason for the difficulty in such an analysis is that for a K user system, there will be K(K-1) cross-correlations to deal with; finding a

Table 2.1 - Dominant Eigenvalue of the Matrix A For a Two User System

$|\rho_{21}|$ \ $|\rho_{12}|$	0.1	0.2	0.3	0.4	0.5	0.6	0.7	0.8	0.9	1.0
0.1	.010	.021	.036	.055	.082	.123	.195	.349	1.00	1.18
0.2	.021	.045	.075	.116	.176	.272	.457	1.00	2.12	1.45
0.3	.033	.072	.122	.192	.301	.497	1.00	35.5	1.14	1.89
0.4	.049	.106	.183	.300	.505	1.00	9.01	1.25	1.41	2.74
0.5	.069	.153	.276	.489	1.00	8.00	1.26	1.33	2.05	5.03
0.6	.098	.228	.450	1.00	16.4	1.20	1.36	2.00	3.69	32.5
0.7	.148	.381	1.00	9.84	1.14	1.50	2.22	3.97	16.4	7.02
0.8	.261	1.00	2.07	1.28	1.88	3.00	6.09	130	6.69	3.05
0.9	1.00	1.13	1.95	3.43	7.56	975	8.44	4.20	2.70	1.84
1.0	19.9	9.89	6.51	4.79	3.73	3.00	2.44	2.00	1.59	1.00

constraint upon these cross-correlations similar to equation (2.75) will simply not be practical as K increases. Of course, equation (2.58) must be satisfied in order for a stable full length decorrelator to exist in the limit as the message length becomes infinite, and therefore any set of signature sequences not satisfying equation (2.58) should be discarded for use with the windowed decorrelator as well.

In an attempt to gain some insight into the K user scenario, a numerical approach was again taken. A system with ten active users was considered with signature sequences derived from Gold codes of length 31 chips. For convenience, a three bit wide window was used. Ten Gold codes were selected at random from the set of 33 possible codes, and nine relative delays were randomly chosen as integers between 0 and 30 chips. This selection process yielded one particular timing configuration for the ten user system, and the corresponding matrix A was computed along with its eigenvalues. This procedure was then repeated 10,000 times, thus yielding 10,000 different timing configurations. For each realization, the magnitude of the dominant eigenvalue of the matrix A , $|\lambda_{max}|$, was computed and compared with unity. If $|\lambda_{max}| < 1$, then that particular timing configuration was labeled as "good"; otherwise it received the label "bad." The results of the 10,000 trials are displayed in Table 2.2, where it is seen that approximately 23% of the tested timing configurations fell

Table 2.2 - Numerical Investigation of 10,000 Timing
Configurations For a Ten User Asynchronous System

No. of "good" timing scenarios	No. of "bad" timing scenarios	No. of "necessary not satisfied"	No. of "sufficient not satisfied"	$\left.\lambda_{max}\right|_{max}$	$\left.\lambda_{max}\right|_{min}$	$\left.\lambda_{max}\right|_{avg}$
7661 (76.61%)	2339 (23.39%)	0	2339	0.99998	0.27306	0.75981

into the "bad" category, meaning that under those timing
configurations the windowed decorrelator would not converge
to a near-far resistant receiver. Of course, there may not
always be a stable infinite length decorrelator for the
windowed decorrelator to converge to; therefore, for each
"bad" timing configuration found, equation (2.58) requires
checking. Due to the fact that the variable ω is defined
along a continuum of values, numerically evaluating equation
(2.58) is not possible and an alternative method must be
used. It has been shown by Lupas [61] that a necessary
condition for equation (2.58) is

$$\det\left[R(0) + R(1) + R^T(1)\right] \neq 0 \quad \text{and} \quad \det\left[R(0) - R(1) - R^T(1)\right] \neq 0 \quad (2.76)$$

and a sufficient condition for equation (2.58) is

$$\lambda_{min}^2\left(R(0)\right) > \max\left\{\lambda_{max}^2\left(R_+\right), \lambda_{min}^2\left(R_+\right)\right\} + \lambda_{max}^2\left(R_-\right) \quad (2.77)$$

where

$$R_+ = R^T(1) + R(1) \quad (2.78)$$

and

$$R_- = j\left[R^T(1) - R(1)\right] \quad (2.79)$$

For each "bad" timing configuration found in Table 2.2,
equations (2.76) and (2.77) were evaluated; those cases for
which the necessary condition of equation (2.76) was not

satisfied were labeled "necessary not satisfied", and those
for which the sufficient condition of equation (2.77) was
not satisfied were labeled "sufficient not satisfied." As
shown in Table 2.2, it was found that the necessary
condition for the existence of the infinite length
decorrelator was always satisfied for the "bad" timing
configurations, whereas the sufficient condition was never
satisfied. Thus, the results of the numerical investigation
listed in Table 2.2 cannot be interpreted as conclusive
proof that the infinite length decorrelator did not exist
whenever the windowed decorrelator failed to converge to a
near-far resistant receiver. The fact that the sufficient
condition was never satisfied when the windowed decorrelator
failed, however, together with the proof given for the case
of two users, strongly implies this relationship. It is
therefore conjectured that as long as a stable version of
the full length decorrelator exists in the limit as the
message length becomes infinite, then the windowed
decorrelator will always converge to a near-far resistant
receiver as the window index increases. This, of course,
means that equation (2.58) represents the conditions imposed
upon the signature sequences for the windowed decorrelator
as well as the full length decorrelator.

Also listed in Table 2.2 are the largest, smallest, and
average $|\lambda_{max}|$ values found from the 10,000 timing
configurations tested. This information is of interest

since the value of the dominant eigenvalue will control the rate at which the asymptotic efficiency of the windowed decorrelator will converge to a constant value. The smaller the value of $|\lambda_{max}|$, the faster the convergence of the windowed decorrelator will be.

Since the relative time delays between the users' received signals are defined along a continuum of values, an infinite number of possible timing configurations exists; fortunately, it was reasoned by Lupas [61] that the probability of error based upon integer chip delays will be worse than for continuous delays. Indeed, this claim was proven for the two user case and numerical results support the extension to more users [61]. Thus, restricting the delays in the previous numerical analysis to be integer multiples of a chip not only reduces the number of total timing configurations possible, but also represents a worst case scenario with respect to the time delays.

The results presented in Table 2.2 would suggest that the decorrelating solution will not be applicable approximately 23% of the time for a system with ten active users employing Gold codes of length 31 chips as their signature sequences. It is important to recall, however, that the analysis of this chapter has been based upon each user employing baseband polar signaling, since it was shown in section 2.1 that baseband transmission represents worst case performance compared to RF transmission due to the fact

that the signature waveform cross-correlations are maximized for baseband transmission. Therefore the results presented in Table 2.2 should be considered to be worst case results since they represent a combination of baseband transmission and integer chip delays. To obtain results more representative of a practical communication system, the previous numerical analysis was repeated for a system employing RF signature waveforms. For each of the 10,000 timing configurations tested, each user was also assigned a random received carrier phase uniformly distributed over the interval $[0, 2\pi)$. The results of the RF system investigation are presented in Table 2.3, where it is seen that no timing configurations were encountered for which the decorrelating strategy would not work. Furthermore, the values of $|\lambda_{max}|$ are now very small, indicating that the windowed decorrelator will converge to a near-far resistant receiver very rapidly in an RF system. Also, the results in Table 2.3 are still worst case with respect to the time delays, since integer chip delays were again used; thus, the preceding analysis would suggest that the windowed decorrelator would be very robust in a near-far RF scenario.

Table 2.3 - Numerical Investigation of 10,000 Timing Configurations For a Ten User Asynchronous RF System

No. of "good" timing scenarios	No. of "bad" timing scenarios	No. of "necessary not satisfied"	No. of "sufficient not satisfied"	$|\lambda_{max}|_{max}$	$|\lambda_{max}|_{min}$	$|\lambda_{max}|_{avg}$
10,000 (100 %)	0 (0 %)	0	0	0.1800	0.0286	0.0777

Numerical Examples

In this section several numerical examples are presented to highlight different features of the windowed decorrelator and to compare its performance to that of the conventional DS-CDMA detector and the full length decorrelator. All examples represent worst case performance with respect to carrier phases and time delays, as baseband waveforms and integer chip delays are used.

For the first example, the dependence of the asymptotic efficiency of the windowed decorrelator on bit position within the window was investigated for a system with two active users. A window of length five bits was used, and the cross-correlations were arbitrarily chosen to be $R_{12}(0) = 0.3$ and $R_{12}(1) = 0.35$. Equation (2.55) was used to plot the asymptotic efficiency of user 2 for the bits contained within the second window processed by the receiver. The results for all five bit positions $v = 2, 4, 6, 8,$ and 10 are shown in Figure 2.8, from which several interesting features of the windowed decorrelator are apparent. First, regardless of the bit position, all the asymptotic efficiency curves decay to a value of zero; consequently, the near-far resistance for all the bits processed in the second window is zero. Define the near-far spread, W_f, to be the largest difference in received energies for which the windowed decorrelator has a nonzero asymptotic efficiency. As long as the near-far spread is larger than the worst case
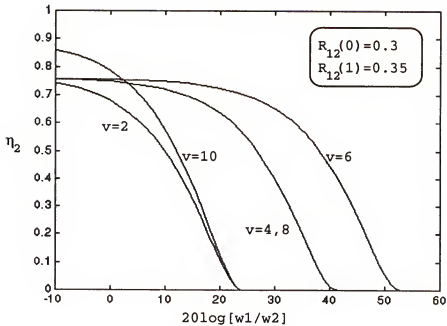
Figure 2.8 - Asymptotic Efficiency as a Function of Bit Position for Two Users with a Five Bit Wide Window

difference in received energies encountered in practice, then for all practical purposes the windowed decorrelator will be near-far resistant. Secondly, it is seen in Figure 2.8 that there can be a large difference in the value of near-far spread obtained for different bit positions within the same window. In this example, the value of near-far spread ranges from approximately 24 dB for positions $v=2$ and $v=10$ to approximately 53 dB for $v=6$. Note that the largest near-far spread occurs for the bit in the middle of the window, whereas the smallest near-far spread occurs for the first and last bits within the window (the edge bits). This phenomenon makes sense since the bits at either edge of the window are directly interfered with by the out-of-window MAI and therefore should feel the largest amount of out-of-

window MAI influence. Multiplying the window vector by the inverse of the cross-correlation matrix has the effect of distributing the out-of-window MAI across all the bits within the window; however, bits further away from the source of the out-of-window MAI will be affected less. The fact that there is out-of-window MAI both preceding and following each window, with the exceptions of the very first and last windows, accounts for why bits near the middle of the window will have the largest near-far spread and why there is a high degree of symmetry about the center of the window (positions $v=2$ and $v=10$ have the same near-far spread, as do positions $v=4$ and $v=8$). Thirdly, another interesting feature of the windowed decorrelator is that the maximum value of asymptotic efficiency varies with bit position as well. From equation (2.55), the maximum value of asymptotic efficiency will be $1/c_{v,v}$, and for this example $1/c_{2,2} = 0.7732$, $1/c_{4,4} = 0.7592$, $1/c_{6,6} = 0.7590$, $1/c_{8,8} = 0.7611$, and $1/c_{10,10} = 0.8957$. In summary, the performance of the windowed decorrelator will be limited by its performance for its worst case bit position, which will occur for either the first or the last bit in the window, with approximately even symmetry about the center of the window.

The second example illustrates the convergence of the windowed decorrelator to a full length decorrelator as the number of windows processed increases. A two user system is again investigated, and a window length of three bits is

used. The cross-correlations are $R_{12}(0) = 2/7$ and $R_{12}(1) = 1/7$, corresponding to signature sequences derived from Gold codes of length seven chips with a fixed relative delay of one chip. For this example, the initial amplitude estimation error vector is

$$\overline{\Delta w(1)} = \begin{bmatrix} |\Delta w_1(3)|_{max} \\ |\Delta w_2(3)|_{max} \end{bmatrix} = \begin{bmatrix} c_{5,6}R_{21}(-1)|\sqrt{w_1(4)} \\ c_{6,6}R_{12}(1)|\sqrt{w_1(4)} \end{bmatrix} = \begin{bmatrix} 0.0455\sqrt{w_1(4)} \\ 0.1559\sqrt{w_1(4)} \end{bmatrix}$$

and the matrix A is

$$A = \begin{bmatrix} |c_{5,6}R_{21}(-1)| & |c_{5,1}R_{12}(1)| \\ |c_{6,6}R_{21}(-1)| & |c_{6,1}R_{12}(1)| \end{bmatrix} = \begin{bmatrix} 0.0455 & 0.0003 \\ 0.1559 & 0.0001 \end{bmatrix}$$

The eigenvalues of A are easily found to be $\lambda_1 = 0.0466$ and $\lambda_2 = -0.0010$; since equation (2.70) is satisfied, the convergence of the windowed decorrelator to a full length decorrelator is guaranteed. Figure 2.9 displays the asymptotic efficiency of the windowed decorrelator for bits within the second, third, and fourth windows processed. These curves represent the worst case bit position, which was found to be v=2 for this example. The asymptotic efficiency of the conventional detector is also shown, as is the asymptotic efficiency for a window index of infinity. For this example the conventional detector has a near-far spread of only 7.3 dB, whereas the windowed decorrelator has near-far spreads of 43 dB, 70 dB, and 96 dB for the second, third, and fourth windows, respectively. Furthermore, note that even if perfect power control was used in conjunction with the conventional detector, the best asymptotic
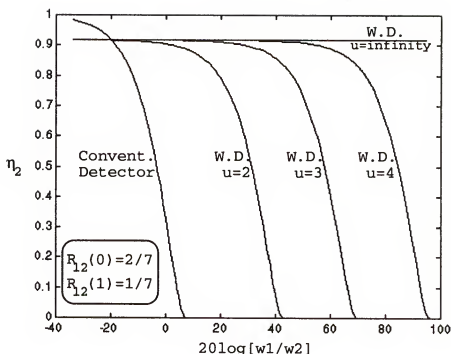
Figure 2.9 - Asymptotic Efficiency as a Function of Window Index for Two Users with a Three Bit Wide Window

efficiency it could achieve would be approximately 0.3. On the other hand, the convergence of the windowed decorrelator's asymptotic efficiency to a constant value of 0.91 is readily apparent, and thus the windowed decorrelator is capable of obtaining an asymptotic efficiency approximately three times larger than the conventional detector with perfect power control. This convergence is even more readily apparent from Figure 2.10, which displays the near-far spread versus window index. Indeed, after only the fourth window, corresponding to processing only 12 received data bits in this example, the windowed decorrelator is able to tolerate differences in received energy of up to 96 dB.

In Figure 2.11, the results of the second example are extended to include the effects of additional users. Here the near-far spread of user 2 is plotted as a function of the number of active users. The cross-correlations between all users were kept equal; that is, $R_{jk}(0)=2/7, j \neq k$ and $R_{jk}(1)=1/7, k>j$. Also, all users except for the desired user (user 2) were assumed to be at the same received power level, thus representing a worst case scenario. For instance, for the case of five active users, a near-far spread of 30 dB means that the four other users each had a received power level 30 dB greater than that of the desired user. As can be seen from Figure 2.11, the windowed decorrelator maintains its ability to achieve any desired level of near-far spread as the number of active users
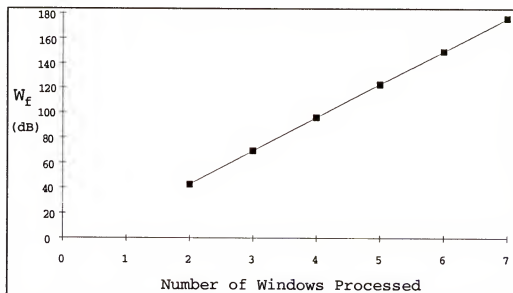
Figure 2.10 - Near-far Spread versus Window Index for the System of Example Two
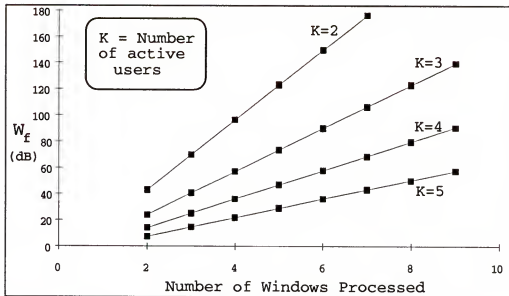
Figure 2.11 - Near-far Spread as a Function of the Number of Active Users for the System of Example Two

increases; however, the rate of obtaining this near-far spread decreases with each additional user. For example, a three user system can achieve a near-far spread of 90 dB after processing six windows (18 bits), whereas a four user system will require nine windows (27 bits). It should be noted that for this particular example in which the cross-correlations were derived from Gold codes of length seven chips, the case of five active users represents a very heavily congested system.

The third example is identical to the second example, but now the cross-correlations are given larger magnitudes. Now $R_{12}(0) = 0.3$ and $R_{12}(1) = 0.5$ are arbitrarily chosen and the matrix A becomes

$$A = \begin{bmatrix} 0.2402 & 0.0312 \\ 0.5720 & 0.0093 \end{bmatrix}$$

The eigenvalues of A are now found to be $\lambda_1 = 0.3012$ and

$\lambda_2 = -0.0517$, so that again equation (2.70) is satisfied and convergence is guaranteed. The asymptotic efficiencies for the second, third, and fourth windows are displayed in Figure 2.12. Note, however, that the rate of convergence is not as rapid as in the previous example, due to the higher cross-correlations. Also, the maximum value of asymptotic efficiency, 0.6246, is significantly lower than in the previous example. The conclusion is that even when a decorrelating strategy is used, it is still important to choose signature waveforms with low cross-correlations.
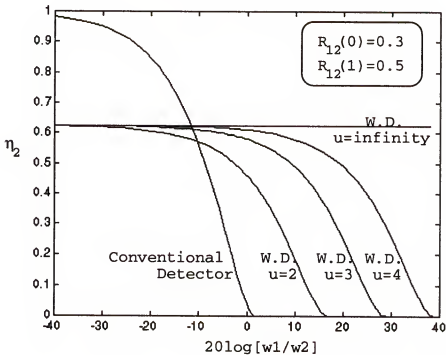
Figure 2.12 - Asymptotic Efficiency of System in Figure 2.9 with Larger Cross-correlations

Since all of the previous examples have been based upon the results for asymptotic efficiency derived in this work,

the fourth example is a computer simulation which serves to
verify the analytical results. A two user asynchronous
system was simulated with the same cross-correlations used
in the second example. Constant cross-correlations and
received energies were used. The simulation sent 100 bits
through a windowed decorrelator and found the magnitude of
the final decision statistic $\overline{z}_L$ given by equation (2.11).
This decision statistic is the sum of three terms: the
desired signal component, the remaining MAI component, and
the noise component. If the receiver is operating as
expected, the MAI component in the decision statistic will
become smaller as the window index increases, until it
eventually disappears. Thus, $\left|z_k(i)\right|$ should converge to
$\sqrt{w_k(i)}$ plus zero-mean noise. Figure 2.13 shows the results
of the simulation when no background noise was present and
$20\log(w1/w2) = 96$ dB. The solid line indicates the value of
$20\log\sqrt{w_2}$, chosen to be 8 here. Indeed, after approximately
13 received data bits the receiver has converged for user 2,
agreeing very strongly with the analytical results presented
in the second example.

Figure 2.14 shows the results of the simulation when
user 2 is operating at a signal-to-noise ratio of 8 dB and
the near-far effect is again 96 dB. Here the magnitude of
the decision statistic converges to a noisy value of $\sqrt{w_2}$.
Note that Figure 2.14 was plotted on a log scale due to the
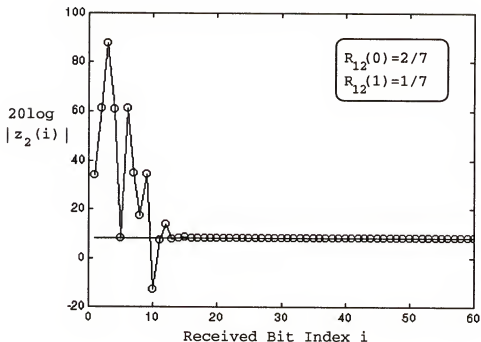enormous near-far effect of 96 dB; for this reason, Figure

Figure 2.13 - Simulation Results for the Magnitude of the Decision Statistic vs. Number of Received Bits for Two Users with a Near-far Effect of 96 dB, and no Background Noise
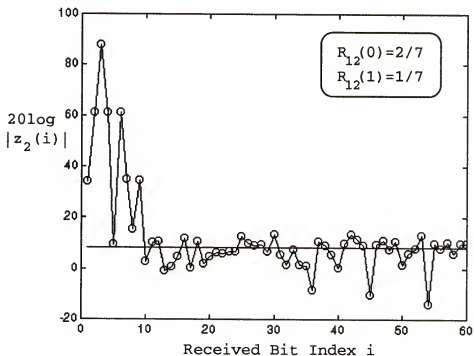

Figure 2.14 - Results for the Simulation of the Decision Statistic Magnitude vs. Number of Received Bits with User 2 Having a Signal-to-noise-ratio of 8 dB
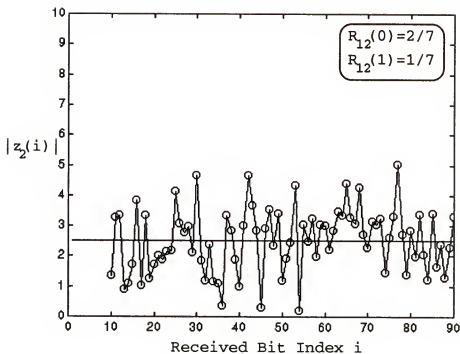
Figure 2.15 - Steady-State Portion of Figure 2.14 on a
linear scale

2.15 displays the steady-state portion of Figure 2.14 on a
linear scale so that it is more readily apparent that $|z_2(i)|$
has converged to $\sqrt{w_2}$ plus zero-mean noise.

CHAPTER 3
WINDOWED DECORRELATING MULTIUSER RECEIVER FOR FREQUENCY-
NONSELECTIVE RAYLEIGH FADING CHANNELS

System Description

In the presentation of the windowed decorrelator for
AWGN channels given in chapter 2, it was assumed that the
multiuser receiver had knowledge of the received carrier
phase of each user, thus allowing for coherent demodulation
of the BPSK modulated signals. In an AWGN channel, the
received phases will be changing slowly relative to a symbol
interval, and tracking of the phases may therefore be
possible. It should be noted, however, that the standard
single-user phase-lock-loop structure will not be adequate
to accomplish this task due to the presence of the MAI;
thus, some other method of obtaining knowledge of the phases
will be required. In fading channels the received phases
will be changing much more rapidly, in many cases precluding
the possibility of successfully tracking these quantities.
Therefore, DPSK will be the assumed modulation format of all
users in the fading channel. As mentioned in chapter 2, the
use of DPSK in conjunction with the windowed decorrelator is
somewhat self-defeating, since the received phases of all
users will need to be estimated between consecutive windows

in order to correct for the out-of-window MAI. DPSK does, however, allow for the data bits contained within each window to be demodulated without knowledge of their corresponding phases, and a phase estimation scheme is proposed in this chapter which allows the received phases of bits between consecutive windows to be estimated while requiring no additional computations beyond those required for decorrelating the current window.

The system model for the fading channel is illustrated in Figure 3.1. Each user transmits a sequence of differentially encoded data bits through the channel. The ith differentially encoded bit of the kth user, $d_k(i)$, is related to the ith data bit of the kth user, $b_k(i)$, through the relationship

$$d_k(i) = d_k(i-1)b_k(i) \qquad (3.1)$$

The signature waveforms are now baseband polar sequences normalized to unit energy and zero outside the time interval $[0,T]$, where T is again the common symbol duration. Each user experiences statistically independent flat Rayleigh fading, represented as a time-varying multiplicative distortion of each user's transmitted signal. The multiplicative coefficients $a_k(i)$ are modeled as independent zero-mean, complex-valued Gaussian random variables. Since the fading processes of different users are statistically independent, the following equality holds

$$E\left\{a_j^*(i)a_k(i)\right\} = 0, \quad \forall j \neq k \qquad (3.2)$$
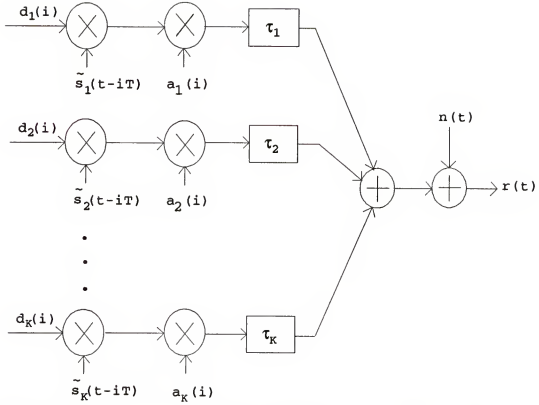
Figure 3.1 - System Model for Flat Rayleigh Fading Channel

The complex envelope of the received signal at the base station is written as

$$R(t) = S(t, \overline{d}) + N(t) \qquad (3.3)$$

where $N(t)$ is complex zero-mean Gaussian noise with power spectral density σ^2 and

$$S(t, b) = \sum_{i=1}^{M} \sum_{k=1}^{K} d_k(i) a_k(i) \sqrt{w_k(i)} \, \tilde{s}_k\big(t - iT - \tau_k\big) e^{j\phi_k(i)} \qquad (3.4)$$

where $\sqrt{w_k(i)}$ is the received power of the kth user in the ith symbol interval, $\tilde{s}_k(t)$ is the signature sequence of the kth user, and $\phi_k(i)$ is the received phase of the kth user in the ith symbol interval. The users are again ordered according to their relative time delays $0 < \tau_1 < \tau_2 < \cdots < \tau_K < T$.

The cross-correlation matrices are defined by their $(m,n)^{th}$ element as

$$R_{m,n}(1) = \int_{-\infty}^{\infty} \tilde{s}_m(t-\tau_m)\tilde{s}_n(t+1T-\tau_n)dt \qquad (3.5)$$

where it is again clear from the time-limited nature of the signature sequences that $R(1) = 0$ for $|1| > 1$ and $R(-1) = R^T(1)$.

The front end of the multiuser receiver will again consist of a matched filter bank, one filter being matched to each allowed signature waveform. The output of the kth user's matched filter sampled at the end of the ith bit interval is

$$y_k(i) = \int_{iT+\tau_k}^{(i+1)T+\tau_k} r(t)\tilde{s}_k(t-iT-\tau_k)dt \qquad (3.6)$$

The vector of matched filter outputs sampled at the end of the ith bit interval can be written as

$$\begin{aligned}\overline{y}(i) = &R(-1)W(i+1)\Phi(i+1)A(i+1)\overline{d}(i+1) + R(0)W(i)\Phi(i)A(i)\overline{d}(i) \\ &+ R(1)W(i-1)\Phi(i-1)A(i-1)\overline{d}(i-1) + \overline{n}(i)\end{aligned} \qquad (3.7)$$

where $\overline{d}(i) = [d_1(i), d_2(i), \cdots, d_k(i)]^T$, $A(i) = \mathrm{diag}[a_1(i), a_2(i), \cdots, a_k(i)]$, $W(i) = \mathrm{diag}[\sqrt{w_1(i)}, \sqrt{w_2(i)}, \cdots, \sqrt{w_K(i)}]$, $\Phi(i) = \mathrm{diag}[e^{j\phi_1(i)}, e^{j\phi_2(i)}, \cdots, e^{j\phi_K(i)}]$, and $\overline{n}(i) = [n_1(i), n_2(i), \cdots, n_K(i)]^T$. The covariance matrix of the matched filter output noise vector is

$$\tfrac{1}{2}E\{n^*(i)n^T(j)\} = \sigma^2 R(i-j) \qquad (3.8)$$

For an L bit wide window spanning bits i through i+L-1, the entire sequence of matched filter outputs can be written as

$$\overline{Y}_L = R_{LK}W_L\Phi_L A_L\overline{d}_L + \overline{n}_L + PW_e\Phi_e A_e\overline{d}_e \qquad (3.9)$$

where the quantities $W_L = \text{diag}[W(i), W(i+1), \cdots, W(i+L-1)]$,

$\Phi_L = \text{diag}[\Phi(i), \Phi(i+1), \cdots, \Phi(i+L-1)]$, $A_L = \text{diag}[A(i), A(i+1), \cdots, A(i+L-1)]$,

$\overline{d}_L = [\overline{d}(i)^T, \overline{d}(i+1)^T, \cdots, \overline{d}(i+L-1)^T]^T$, $\overline{n}_L = [\overline{n}(i)^T, \overline{n}(i+1)^T, \cdots, \overline{n}(i+L-1)^T]^T$,

$W_e = \text{diag}[W(i-1), W(i+L)]$, $\Phi_e = \text{diag}[\Phi(i-1), \cdots \Phi(i+L-1)]$,

$A_e = \text{diag}[A(i-1), A(i+L-1)]$, $\overline{d}_e = [\overline{d}(i-1)^T, \overline{d}(i+L)^T]^T$, and the LK by

LK and LK by 2K matrices R_{LK} and P are given by

$$R_{LK} = \begin{pmatrix} R(0) & R(-1) & 0 & \cdots & 0 \\ R(1) & R(0) & R(-1) & \ddots & \vdots \\ 0 & \ddots & \ddots & \ddots & 0 \\ \vdots & \ddots & R(1) & R(0) & R(-1) \\ 0 & \cdots & 0 & R(1) & R(0) \end{pmatrix} \quad \text{and} \quad P = \begin{pmatrix} R(1) & 0 \\ 0 & 0 \\ \vdots & \vdots \\ 0 & 0 \\ 0 & R(-1) \end{pmatrix}.$$

Proposed Multiuser Receiver Structure

The structure of the windowed decorrelator for a flat
Rayleigh fading channel is essentially the same as for an
AWGN channel, with two exceptions. First, the estimate of
the out-of-window MAI affecting each window must now include
an estimate of each user's phase immediately preceding and
following the window (recall that the phases were assumed to
be known in the AWGN channel). Secondly, each output vector
of the windowed decorrelator will contain differentially
encoded data bits of each user; therefore the windowed
decorrelating algorithm must be followed by a bank of
standard DPSK detectors, one for each user as shown in
Figure 3.2. The same technique can be used as in the AWGN
channel to form the required MAI estimates, only now the
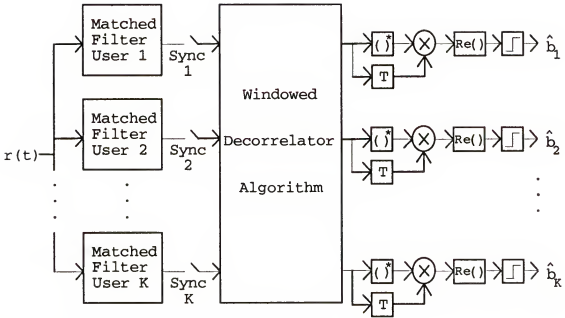intermediate decision statistic vector resulting from

Figure 3.2 - Multiuser Receiver Structure for Fading Channel

decorrelating each window will contain complex numbers. The
last K elements in the current window's intermediate
decision statistic vector will be used as the estimates of
the out-of-window MAI affecting the next window: the
magnitude of each complex number will be the estimated
magnitude of the corresponding user's MAI and the phase of
each complex number will be the estimated phase of the
corresponding user's MAI, as illustrated in Figure 3.3.
This estimation technique will, however, result in a 180°
phase ambiguity due to the fact that the polarity of the
differentially encoded data bits may be either +1 or -1 and
are unknown to the receiver. One way to remove this phase
ambiguity is to have the last bit of every user within each
window be a pilot bit. The polarities of the pilot bits are
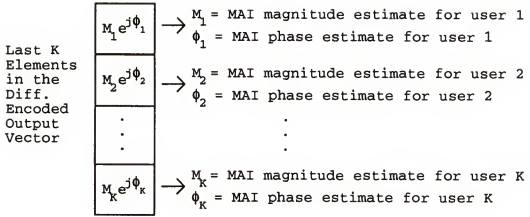known so there will be no phase ambiguity in the MAI

Figure 3.3 - MAI Estimation Technique of Fading Channel Windowed Decorrelator

estimates. Each user must still transmit a pilot bit between consecutive data windows so that the out-of-window MAI may be subtracted off properly, and thus each user in the fading channel must transmit two consecutive pilot bits after every block of L-1 data bits, as shown in Figure 3.4. The first pilot bit is grouped with the L-1 differentially encoded data bits to form a window L bits wide; this window is then decorrelated. The second pilot bit serves to separate the windows and will be discarded by the receiver, just as the lone pilot bit was in the AWGN analysis.

L-1 Data Bits	Pilot Bit	Pilot Bit	L-1 Data Bits	Pilot Bit	Pilot Bit	...

$\mid$ ←— Decorrelate —→ $\mid$ Discard $\mid$ ←— Decorrelate —→ $\mid$ Discard $\mid$
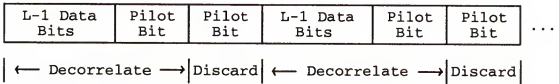
Figure 3.4 - Data Block Structure of the Mobile Units

The estimation technique described above will be referred to as a zeroth order scheme since it assumes each

user's fading process will be approximately constant over a
span of L+2 consecutive symbol intervals. A smarter
estimation technique might try to predict future fading
coefficients for each user based upon past values. In order
to choose an appropriate prediction algorithm, some
characteristics must be known about the fading processes. A
computer simulation of the magnitude and phase of a typical
flat Rayleigh fading process is shown in Figure 3.5 as a
function of the transmitted bit index. To represent numbers
which might be typical of a realistic wireless communication
system, a transmitted bit rate of 20 kbps and a carrier
frequency of 900 MHz were chosen. In addition, the user is
assumed to be traveling at a speed of 65 mph, thereby
representing the worst case fading which might be
encountered by a user in a cellular phone system. As can be
seen, in between the maxima and minima the curves are
approximately linear; for instance, between transmitted bits
460 and 540 of Figure 3.5. Linear extrapolation would
therefore seem a logical choice for a prediction technique.
Thus, as an alternative to using the zeroth order estimation
strategy, linear extrapolation could be employed. The
multiuser receiver would need to store the last K elements
in the previous window's decorrelated output vector. After
decorrelating the current window the receiver will have two
points, each a complex number, for each user from which it
can then compute a slope and an intercept. The estimate of
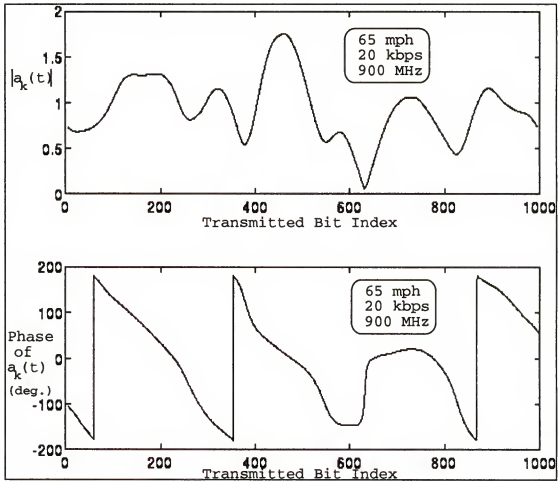each user's MAI contribution to the next window can then be

Figure 3.5 - Magnitude and Phase of a Flat Rayleigh Fading Process

determined by plugging the appropriate future transmitted bit indices into the equation for that user's line. Of course, this estimation scheme will produce poor estimates near the maxima and minima shown in Figure 3.5, but these points occur relatively infrequently, particularly for smaller window lengths. To facilitate the following performance analysis, the zeroth order estimation strategy will be assumed. The linear extrapolation method will be referred to as the first order scheme later in this chapter.

The overall block diagram of the windowed decorrelating receiver for flat Rayleigh fading channels is shown in Figure 3.6. The vector of decorrelated outputs is given by
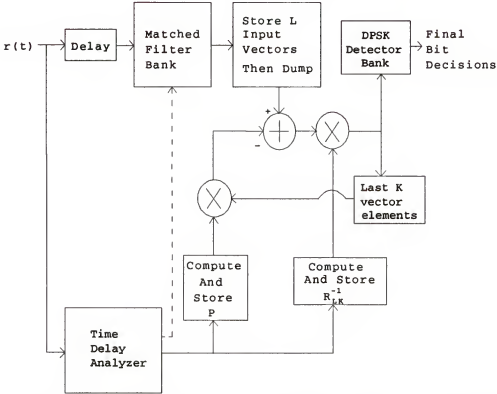

Figure 3.6 - Block Diagram of Fading Channel Windowed Decorrelator

$$\tilde{d}_L = R_{LK}^{-1}\left(\overline{Y}_L - P\hat{W}_e\hat{\Phi}_e\hat{A}_e\hat{\overline{d}}_e\right)$$

$$= W_L\Phi_L A_L\overline{d}_L + R_{LK}^{-1}\overline{n}_L + R_{LK}^{-1}P\left(W_e\Phi_e A_e\overline{d}_e - \hat{W}_e\hat{\Phi}_e\hat{A}_e\overline{d}_e\right) \qquad (3.10)$$

Defining

$$\overline{\gamma}_L = R_{LK}^{-1}\overline{n}_L \qquad (3.11)$$

the kth user's decorrelated intermediate decision statistic is given by

$$\tilde{d}_k(i) = \sqrt{w_k(i)}a_k(i)e^{j\phi_k(i)}d_k(i) + \gamma_k(i) + \left[R_{LK}^{-1}P\left(W_e\Phi_e A_e\overline{d}_e - \hat{W}_e\hat{\Phi}_e\hat{A}_e\overline{d}\right)\right]_v^u \qquad (3.12)$$

where as before the notation $[\bar{x}]_v^u$ represents the vth element in the uth window of the vector $\bar{x}$. As in the AWGN analysis, the window index u and the window element index v are given by equations (2.13) and (2.14), respectively. The final bit decisions are determined as

$$\hat{b}_k(i) = \text{sign}\left[\text{Re}\left\{\tilde{d}_k(i-1)\tilde{d}_k^*(i)\right\}\right] \tag{3.13}$$

Performance Analysis

The decision variable for the ith bit of the kth user given by equation (3.13) can be written in the form

$$D = \text{Re}\left\{XY^*\right\} \tag{3.14}$$

and therefore the probability of error is given by [55, Appendix B]

$$P_k(i) = \tfrac{1}{2}(1-\mu) \tag{3.15}$$

where

$$\mu = \frac{M_{xy} + M_{yx}}{\sqrt{\left(M_{xy} - M_{yx}\right)^2 + 4M_{xx}M_{yy}}} \tag{3.16}$$

and the covariances M_{xx}, M_{yy}, M_{xy}, and M_{yx} are given by

$$M_{xx} = \tfrac{1}{2}E\left\{XX^*\right\} \tag{3.17}$$

$$M_{yy} = \tfrac{1}{2}E\left\{YY^*\right\} \tag{3.18}$$

$$M_{xy} = \tfrac{1}{2}E\left\{XY^*\right\} \tag{3.19}$$

$$M_{yx} = \tfrac{1}{2}E\left\{YX^*\right\} \tag{3.20}$$

As a starting point, it is of interest to determine the best performance possible from the proposed windowed decorrelator, corresponding to the ideal scenario in which

the multiuser receiver has perfect knowledge (or perfect estimates) of the out-of-window MAI. In this scenario equation (3.12) reduces to

$$\tilde{d}_k(i) = \sqrt{w_k(i)}a_k(i)e^{j\phi_k(i)}d_k(i) + \gamma_k(i) \qquad (3.21)$$

From equations (3.13) and (3.14), the variables X and Y are then given by

$$X = \sqrt{w_k(i-1)}a_k(i-1)e^{j\phi_k(i-1)}d_k(i-1) + \gamma_k(i-1) \qquad (3.22)$$

$$Y = \sqrt{w_k(i)}a_k(i)e^{j\phi_k(i)}d_k(i) + \gamma_k(i) \qquad (3.23)$$

Applying equation (3.17) to find M_{xx} yields

$$M_{xx} = \tfrac{1}{2}w_k(i-1)E\{a_k(i-1)a_k^*(i-1)\} + \tfrac{1}{2}E\{\gamma_k(i-1)\gamma_k^*(i-1)\} \qquad (3.24)$$

where the fact that

$$E\{a_k(i)\gamma_k^*(j)\} = E\{a_k^*(i)\gamma_k(j)\} = 0 \quad \forall\, i,j \qquad (3.25)$$

has been used since the fading processes are statistically independent from the background noise.

The time autocorrelation function for the kth user's fading process is defined as

$$R_{a_k}(\tau) = \tfrac{1}{2}E\{a_k(t)a_k^*(t-\tau)\} \qquad (3.26)$$

and from equations (3.8) and (3.11)

$$\tfrac{1}{2}E\{\gamma_k(i-1)\gamma_k^*(i-1)\} = \sigma^2 c_{v-K,v-K} \qquad (3.27)$$

where as in the AWGN analysis, the $(m,n)^{th}$ element of the matrix R_{LK}^{-1} is denoted by $c_{m,n}$. Using equations (3.26) and (3.27), the expression for M_{xx} reduces to

$$M_{xx} = w_k(i-1)R_{a_k}(0) + \sigma^2 c_{v-K,v-K} \qquad (3.28)$$

Similarly, M_{yy} is found to be

$$M_{yy} = w_k(i)R_{a_k}(0) + \sigma^2 c_{v,v} \qquad (3.29)$$

Applying equation (3.19) to find M_{xy} results in

$$M_{xy} = \tfrac{1}{2}\sqrt{w_k(i-1)}\sqrt{w_k(i)}\, e^{j[\phi_k(i-1)-\phi_k(i)]} E\big\{a_k(i-1)a_k^*(i)\big\}d_k(i-1)d_k(i)$$
$$+ \tfrac{1}{2}E\big\{\gamma_k(i-1)\gamma_k^*(i)\big\} \qquad (3.30)$$

For convenience it will be assumed that the received energies and phases are constant over two consecutive signaling intervals, so that equation (3.30) simplifies to

$$M_{xy} = \tfrac{1}{2}w_k(i)b_k(i)R_{a_k}(T) + \sigma^2 c_{v-K,v} \qquad (3.31)$$

Similarly, M_{yx} is found to be

$$M_{yx} = \tfrac{1}{2}w_k(i)b_k(i)R_{a_k}(T) + \sigma^2 c_{v-K,v} \qquad (3.32)$$

which is identical to the expression found for M_{xy} in equation (3.31) and thus $M_{xy} = M_{yx}$. Plugging equations (3.28), (3.29), (3.31), and (3.32) into the expression for μ given by equation (3.16) yields

$$\mu = \frac{M_{xy}}{\sqrt{M_{xx}M_{yy}}} \qquad (3.33)$$

By symmetry, $\Pr(\text{error}) = \Pr\big(\text{error}\,|\,b_k(i)=1\big)$ and from equation (3.15) the probability of error will be given by

$$P_k(i)_{min} = \frac{1}{2}\left(1 - \frac{w_k(i)R_{a_k}(T) + \sigma^2 c_{v-K,v}}{\sqrt{\big(w_k(i)R_{a_k}(0) + \sigma^2 c_{v-K,v-K}\big)\big(w_k(i)R_{a_k}(0) + \sigma^2 c_{v,v}\big)}}\right) \qquad (3.34)$$

Equation (3.34) represents the probability of error obtained by an ideal windowed decorrelator with perfect estimates of the out-of-window MAI affecting each window. Define the kth user's average received signal-to-noise ratio as

$$SNR_k = \frac{w_k R_{a_k}(0)}{\sigma^2} \qquad (3.35)$$

and the kth user's fading correlation coefficient as

$$\rho_{a_k}(T) = \frac{R_{a_k}(T)}{R_{a_k}(0)} \qquad (3.36)$$

The fading correlation coefficient is a measure of how correlated the fading is between consecutive signaling intervals. If the fading was constant over two consecutive intervals, then $\rho_{a_k}(T)=1$. On the other hand, if the fading was completely uncorrelated from one interval to the next, then $\rho_{a_k}(T)=0$. Using the definitions given in equations (3.35) and (3.36), equation (3.34) may be re-written as

$$P_k(i)_{min} = \frac{1}{2}\left(1 - \frac{\rho_{a_k}(T) + (SNR_k)^{-1}c_{v-K,v}}{\left(1 + (SNR_k)^{-1}c_{v-K,v-K}\right)\left(1 + (SNR_k)^{-1}c_{v,v}\right)}\right) \qquad (3.37)$$

In the limit as the kth user's average signal-to-noise ratio becomes infinite, the windowed decorrelator's best possible probability of error will become

$$\lim_{SNR_k \to \infty} P_k(i)_{min} = \frac{1}{2}\left(1 - \rho_{a_k}(T)\right) \qquad (3.38)$$

The effect of the fading channel on the kth user's performance is readily apparent from equation (3.38). For $\rho_{a_k}(T) \neq 1$, there will be a fading-induced irreducible error floor, the level of which is dependent upon how highly correlated the fading is between consecutive signaling intervals. For instance, if $\rho_{a_k}(T)=0.99$, corresponding to fairly highly correlated fading, then the kth user will encounter an irreducible error floor of $5x10^{-3}$. Of course, the windowed decorrelator is not attempting to combat the effects of the fading; its goal is simply to eliminate the MAI and thereby achieve the same probability of error that a single user would have. To reduce the level of the error

floor imposed by the fading, diversity techniques may be employed [28]. For the multiuser scenario considered here, each user could repeat his or her message in frequency, time, or space. Referring to Figure 3.2, the appropriate re-combining of each user's replicas would then occur at the output of the decorrelating algorithm prior to the final data demodulation.

The probability of error obtained by a single user employing DPSK modulation in a flat Rayleigh fading channel is given by [28]

$$P_{e,single\ user} = \frac{1}{2}\left(1 - \frac{\rho_a(T)}{1 + (SNR_{eff})^{-1}}\right) \qquad (3.39)$$

In the limit as the single user's signal-to-noise ratio becomes infinite, the probability of error becomes

$$\lim_{SNR_{eff} \to \infty} P_{e,single\ user} = \frac{1}{2}(1 - \rho_a(T)) \qquad (3.40)$$

which is identical to the probability of error for the ideal windowed decorrelating given in equation (3.38), and thus the ideal windowed decorrelator is able to asymptotically achieve the same probability of error as a single user. The performance of the ideal windowed decorrelator is compared to that of the single user in Figure 3.7. A five user system with a five bit wide window was chosen for the windowed decorrelator. User two was chosen as the desired user and equal cross-correlations of $R_{jk}(0)=2/7$, $j \neq k$ and $R_{jk}(1)=1/7$, $j<k$ were assumed. The results displayed in Figure 3.7 are for window bit position v=7, corresponding to
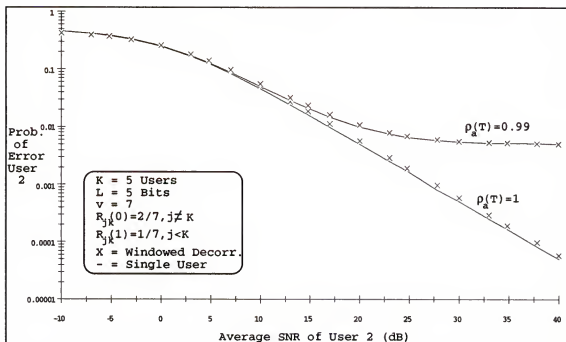
Figure 3.7 - Comparison of Ideal Windowed Decorrelator and Single User

the first data bit of the second user within the window (the second differentially encoded bit within the window). As can be seen, the windowed decorrelator with perfect knowledge of the out-of-window MAI is able to track the probability of error of a single user very closely. Interestingly, the results shown in Figure 3.7 were found to be almost identical for different values of window bit position v, indicating that the ideal windowed decorrelator's performance is for all practical purposes independent of bit position. This behavior is expected, since the ideal windowed decorrelator is able to completely subtract off the out-of-window MAI. Figure 3.7 also displays the error floor associated with the fading for $\rho_a(T) = 0.99$.

To analyze the performance of the windowed decorrelator which forms its MAI estimates according to the "dumb" estimation strategy described in section 3.2, the last term on the right hand side of equation (3.12) must be evaluated. To begin, consider the very first window (u=1). Since there have been no previous windows, the receiver's estimates are zero and the vth element of the MAI term becomes

$$\left[R_{LK}^{-1}PW_e\Phi_eA_e\overline{d}_e\right]_v^{u=1} = \sum_{l=1}^{K-1}\sum_{j=(L-1)K+1}^{LK}c_{v,j}R_{j-(L-1)K,l}(-1)\sqrt{w_1(L+1)}e^{j\phi_1(L+1)}a_1(L+1)$$

$$(3.41)$$

where it has again been assumed for convenience that all pilot bits have a polarity of +1, thus allowing the $\overline{d}_e$ terms to be dropped. For compactness, an interference vector is defined for the first window as

$$\overline{I_1(1)} = \left[R_{LK}^{-1}PW_e\Phi_eA_e\right]^{u=1}$$

$$(3.42)$$

The estimate of the kth user's contribution to the MAI affecting the second window is formed as

$$\hat{w}_k(L+1)e^{j\hat{\phi}_k(L+1)}\hat{a}_k(L+1) = \hat{w}_k(2L+2)e^{j\hat{\phi}_k(2L+2)}\hat{a}_k(2L+2)$$
$$= w_k(L)e^{j\phi_k(L+1)}a_k(L)+\gamma_k(L)+\left[\overline{I_1(1)}\right]_{(L-1)K+k}$$

$$(3.43)$$

Now consider the second window (u=2). Recall that the decorrelated output vector is given by equation (3.12), which is repeated below for convenience

$$\tilde{d}_k(i) = \sqrt{w_k(i)}a_k(i)e^{j\phi_k(i)}d_k(i)+\gamma_k(i)+\left[R_{LK}^{-1}P\left(W_e\Phi_eA_e\overline{d}_e - \hat{W}_e\hat{\Phi}_e\hat{A}_e\overline{d}\right)\right]_v^u \quad (3.12)$$

To proceed further, the last term on the right-hand side of equation (3.12) must be evaluated. This term represents the MAI corruption in the intermediate decision statistic

resulting from the fact that the channel characteristics immediately before and after the second window are not the same. By multiplying the matrices together, this MAI term may be expanded out as

$$\left(W_e\Phi_e A_e - \hat{W}_e\hat{\Phi}_e\hat{A}_e\right) = \begin{bmatrix} \sqrt{w_1(L+1)}e^{j\phi_1(L+1)}a_1(L+1) - \sqrt{w_1(L)}e^{j\phi_1(L)}a_1(L) - \gamma_1(L) - \boxed{I_1(1)}\Big|_{(L-1)K+1} \\ \sqrt{w_2(L+1)}e^{j\phi_2(L+1)}a_2(L+1) - \sqrt{w_2(L)}e^{j\phi_2(L)}a_2(L) - \gamma_2(L) - \boxed{I_1(1)}\Big|_{(L-1)K+2} \\ \vdots \\ \sqrt{w_K(L+1)}e^{j\phi_K(L+1)}a_K(L+1) - \sqrt{w_K(L)}e^{j\phi_K(L)}a_K(L) - \gamma_K(L) - \boxed{I_1(1)}\Big|_{LK} \\ \sqrt{w_1(2L+2)}e^{j\phi_1(2L+2)}a_1(2L+2) - \sqrt{w_1(L)}e^{j\phi_1(L)}a_1(L) - \gamma_1(L) - \boxed{I_1(1)}\Big|_{(L-1)K+1} \\ \sqrt{w_2(2L+2)}e^{j\phi_2(2L+2)}a_2(2L+2) - \sqrt{w_2(L)}e^{j\phi_2(L)}a_2(L) - \gamma_2(L) - \boxed{I_1(1)}\Big|_{(L-1)K+2} \\ \vdots \\ \sqrt{w_K(2L+2)}e^{j\phi_K(2L+2)}a_K(2L+2) - \sqrt{w_K(L)}e^{j\phi_K(L)}a_K(L) - \gamma_K(L) - \boxed{I_1(1)}\Big|_{LK} \end{bmatrix}$$

$$(3.44)$$

To simplify the math somewhat, it is necessary to make the assumption that the fading characteristics for each user will be approximately constant over two consecutive bit intervals. In other words, it will be assumed that

$$a_j(L+1) - a_j(L) \approx 0 \qquad (3.45)$$

Note that this assumption is justified in the sense that from equation (3.44), the receiver's performance will ultimately depend upon how small the quantity $a_j(L+2) - a_j(L)$ is. Thus, if the assumption given in equation (3.45) is not valid, then $a_j(L+2) - a_j(L)$ will not be very small and the receiver is doomed to fail. It is therefore only of practical interest to study the case in which the assumption is valid and to evaluate the receiver's performance as a

function of how correlated the fading process of each user is over a span of L+2 consecutive bit intervals.

Under the above assumption, the first K elements in the vector of equation (3.44) reduce to just the sum of the noise component and the initial MAI component; thus equation (3.44) simplifies to

$$
\left(W_e\Phi_e A_e - \hat{W}_e\hat{\Phi}_e\hat{A}_e\right) = \begin{bmatrix} -\gamma_1(L) - \left[\overline{I(1)}\right]_{(L-1)K+1} \\ -\gamma_2(L) - \left[\overline{I(1)}\right]_{(L-1)K+2} \\ \vdots \\ -\gamma_K(L) - \left[\overline{I(1)}\right]_{LK} \\ \sqrt{w_1(2L+2)}e^{j\phi_1(2L+2)}a_1(2L+2) - \sqrt{w_1(L)}e^{j\phi_1(L)}a_1(L) - \gamma_1(L) - \left[\overline{I_1(1)}\right]_{(L-1)K+1} \\ \sqrt{w_2(2L+2)}e^{j\phi_2(2L+2)}a_2(2L+2) - \sqrt{w_2(L)}e^{j\phi_2(L)}a_2(L) - \gamma_2(L) - \left[\overline{I_1(1)}\right]_{(L-1)K+2} \\ \vdots \\ \sqrt{w_K(2L+2)}e^{j\phi_K(2L+2)}a_K(2L+2) - \sqrt{w_K(L)}e^{j\phi_K(L)}a_K(L) - \gamma_K(L) - \left[\overline{I_1(1)}\right]_{LK} \end{bmatrix}
$$

$$(3.46)$$

To further evaluate the MAI term present after decorrelating the second window, the vector given in equation (3.46) must be pre-multiplied by $R_{LK}^{-1}P$. First, note that the vth element of the vector $\left[R_{LK}^{-1}P\overline{x}\right]$ will be of the form

$$
\left[R_{LK}^{-1}P\overline{x}\right]_v = \sum_{l=2}^{K}\sum_{j=1}^{l-1}c_{v,j}R_{j,1}(1)\left[\overline{x}\right]_1 + \sum_{l=1}^{K-1}\sum_{j=(L-1)K+1}^{LK}c_{v,j}R_{j-(L-1)K,1}(-1)\left[\overline{x}\right]_1 \qquad (3.47)
$$

where $\overline{x}$ is an arbitrary vector and as before $\left[\overline{x}\right]_m$ denotes the mth element in the vector. Indeed, it is the form of equation (3.47) which led to the recursion matrix for consecutive windows used in the AWGN analysis. Upon substituting $\overline{x} = \left(W_e\Phi_e A_e - \hat{W}_e\hat{\Phi}_e\hat{A}_e\right)$ into equation (3.47), the following result is obtained

$$\left[R_{LK}^{-1}P\left(W_e\Phi_e A_e - \hat{W}_e\hat{\Phi}_e\hat{A}_e\right)\right]_v^{u=2} = \sum_{l=2}^{K}\sum_{j=1}^{l-1}c_{v,j}R_{j,l}(1)\left\{-\gamma_1(L)-\left[\overline{I_1(1)}\right]_{1+(L-1)K}\right\}$$

$$+\sum_{l=1}^{K-1}\sum_{j=(l-1)K+1+L}^{LK}c_{v,j}R_{j-(l-1)K,1}(-1)\left\{W_e(2L+2)\Phi_e(2L+2)A_e(2L+2)-W_e(L)\Phi_e(L)A_e(L)-\gamma_1(L)-\left[\overline{I_1(1)}\right]_{1+(L-1)K}\right\}$$

$$(3.48)$$

By re-grouping terms, equation (3.48) may be re-written as

$$\left[R_{LK}^{-1}P\left(W_e\Phi_e A_e - \hat{W}_e\hat{\Phi}_e\hat{A}_e\right)\right]_v^{u=2} = -\sum_{l=2}^{K}\sum_{j=1}^{l-1}c_{v,j}R_{j,l}(1)\gamma_1(L)-\sum_{l=1}^{K-1}\sum_{j=(l-1)K+1+L}^{LK}c_{v,j}R_{j-(l-1)K,1}(-1)\gamma_1(L)$$

$$+\sum_{l=1}^{K-1}\sum_{j=(l-1)K+1+L}^{LK}c_{v,j}R_{j-(l-1)K,1}(-1)\left\{W_e(2L+2)\Phi_e(2L+2)A_e(2L+2)-W_e(L)\Phi_e(L)A_e(L)\right\}$$

$$-\sum_{l=2}^{K}\sum_{j=1}^{l-1}c_{v,j}R_{j,l}(1)\left[\overline{I_1(1)}\right]_{1+(L-1)K}-\sum_{l=1}^{K-1}\sum_{j=(l-1)K+1+L}^{LK}c_{v,j}R_{j-(l-1)K,1}(-1)\left[\overline{I_1(1)}\right]_{1+(L-1)K}$$

$$(3.49)$$

The first two terms on the right hand side of equation (3.49) are noise components. The third term is an "acquired" interference component introduced by the second window, and the last two terms are due to the "initial" interference introduced by the first window. To more clearly understand the significance of each of the two kinds of interference terms present in equation (3.49), suppose that there was no fading in the channel. Then equation (3.49) would still contain the "initial" interference terms since the first window would still have no previous estimates available with which it could attempt to subtract off its out-of-window MAI. The "initial" interference terms are thus inevitable for a windowed decorrelator operating in any channel. Now, however, the "acquired" interference term would not be present in equation (3.49) since in the absence of fading $a_j(2L+2)-a_j(L)\approx 0$ (for small L). Note that the

"initial" interference term has been reduced after the
second window has been decorrelated due to the
multiplication by $R_{LK}^{-1}P$. This is almost precisely the same
situation which occurred in the AWGN channel and thus the
"initial" interference term will become smaller and smaller
as more and more windows are processed until it finally
becomes negligible. The only difference between the
behavior of the "initial" interference term in the AWGN
channel and the flat fading channel is that in the former,
the worst case estimation errors of the uth window were
determined as a function of the worst case estimation errors
of the $(u-1)^{th}$ window, and so on. As a consequence of using
worst case estimation errors, the sign preceding the
recursion matrix A was always positive and thus equation
(2.53) was eventually arrived at. For the present fading
channel analysis, worst case estimates are not being used
since the estimates are no longer obtained simply by taking
the absolute value of the appropriate element in the
decorrelated output vector. Consequently, an equivalent
bound on the estimation errors cannot be found as in the
AWGN analysis. Now the actual errors are being used, and
decorrelating the first window yields an estimate which is
then subtracted from the second window's matched filter
output vector, thus reversing the sign on the "initial"
interference term. The estimate obtained from decorrelating
the second window is in turn subtracted from the third

window's matched filter output vector, thus reversing the sign on the "initial" interference term once again. This process repeats itself and as a result the fading channel counterpart to equation (2.53) is therefore

$$\overline{I_1'(u)} = (-1)^{u-1} A^{u-1} \overline{I_1'(1)} \qquad (3.50)$$

where $\overline{I_1'(u)}$ is a K element vector containing the last K elements of the interference vector $\overline{I_1(u)}$, and $\overline{I_1(1)}$ is defined in equation (3.42). The recursion matrix A is defined by its $(p,q)^{th}$ element as

$$a_{p,q} = \sum_{j=(L-1)K+1+q}^{LK} c_{p,j} R_{j-(L-1)K,q}(-1) + \sum_{j=1}^{q-1} c_{p,j} R_{j,q}(1) \qquad (3.51)$$

The matrix A in equation (3.50) should not be confused with the matrix of out-of-window fading coefficients A_e.

The real difference between the AWGN channel and the fading channel is the presence of the "acquired" interference term in equation (3.49). This term is a result of the fact that the fading characteristics of each user immediately before the second window are not the same as those immediately after the second window. For compactness define an interference vector due to the second window as

$$\left[\overline{I_2(2)}\right]_v = \sum_{l=1}^{K-1} \sum_{j=(L-1)K+1+1}^{LK} c_{v,j} R_{j-(L-1)K,1}(-1) \left[W_e(2L+2)\Phi_e(2L+2)A_e(2L+2) - W_e(L)\Phi_e(L)A_e(L)\right]$$

$$(3.52)$$

Note that this "acquired" interference term has the same form as the "initial" interference term did after the first window was decorrelated. Consequently the second window's "acquired" interference term will obey the same relationship

at the first window's "initial" interference term, except now the sign on this term will be positive after the second window, negative after the third window, positive after the fourth window, and so on. Thus

$$\overline{I_2'(u)} = (-1)^{u-2} A^{u-2} \overline{I_2'(2)}, \qquad u \geq 2 \qquad (3.53)$$

The structure of equation (3.49) will be the same for each additional window processed by the receiver; that is, after the nth window is decorrelated, the MAI term present in the decorrelated output vector will contain an "acquired" interference component introduced by the nth window as well as reduced versions of the "acquired" interference terms introduced by each of the preceding (n-2) windows. There will be also be a reduced version of the "initial" interference term introduced by the first window. From equations (3.50) and (3.53), the total MAI contained in the nth window's intermediate decision statistic vector will be

$$\left[R_{LK}^{-1}P\left(W_e\Phi_e A_e - \hat{W}_e\hat{\Phi}_e\hat{A}_e\right)\right]_{MAI}^{u=n} = (-1)^{n-1}A^{n-1}\overline{I_1'(1)} + (-1)^{n-2}A^{n-2}\overline{I_2'(2)}$$
$$+ (-1)^{n-3}A^{n-3}\overline{I_3'(3)} + \cdots + \overline{I_n(n)} \qquad (3.54)$$

Equation (3.54) can be written more compactly as

$$\left[R_{LK}^{-1}P\left(W_e\Phi_e A_e - \hat{W}_e\hat{\Phi}_e\hat{A}_e\right)\right]_{MAI}^{u=n} = \overline{I_n(n)} + \sum_{j=1}^{n-1}(-1)^{n-j}A^{n-j}\overline{I_j'(j)} \qquad (3.55)$$

where the "acquired" interference term introduced by the mth window is given by

$$\left[\overline{I_m(m)}\right]_v = \sum_{l=1}^{K-1}\sum_{j=(L-1)K+l+1}^{LK}c_{v,j}R_{j-(L-1)K,1}(-1)\left[W_e(m(L+1))\Phi_e(m(L+1))A_e(m(L+1))\right.$$
$$\left. -W_e((m-1)(L+1))\Phi_e((m-1)(L+1))A_e((m-1)(L+1))\right] \qquad (3.56)$$

and $\left[\overline{I_m'(m)}\right]$ contains the last K elements in $\left[\overline{I_m(m)}\right]$.

All that remains to be considered are the noise components in equation (3.49). Since these terms are identical to the "initial" interference terms in equation (3.49) with $\left[\overline{I_1(1)}\right]_1$ replaced by $\left[\overline{\gamma(1)}\right]_1$, they will behave in exactly the same manner. The MAI term in each additional window will contain a reduced noise component from each of the preceding windows. Therefore the total noise component contained in the MAI term of the nth window's intermediate decision statistic vector will be

$$\left[R_{LK}^{-1}P\left(W_e\Phi_eA_e - \hat{W}_e\hat{\Phi}_e\hat{A}_e\right)\right]_{Noise}^{u=n} = \sum_{j=1}^{n-1}(-1)^{n-j}A^{n-j}\overline{N_j(j)} \qquad (3.57)$$

where the noise vector $\overline{N_j(j)}$ is defined as

$$\left[\overline{N_j(j)}\right]_v = \sum_{l=2}^{K}\sum_{j=1}^{l-1}c_{v,j}R_{j,1}(1)\left[\overline{\gamma(j-1)}\right]_{(l-1)K+1}$$
$$+ \sum_{l=1}^{K-1}\sum_{j=(l-1)K+1+1}^{LK}c_{v,j}R_{j-(L-1)K,1}(-1)\left[\overline{\gamma(j-1)}\right]_{(l-1)K+1} \qquad (3.58)$$

Finally, by combining the MAI component and the noise component, the vth element of the MAI vector in the nth window's intermediate decision statistic vector is then given by

$$\left[R_{LK}^{-1}P\left(W_e\Phi_eA_e - \hat{W}_e\hat{\Phi}_e\hat{A}_e\right)\right]_v^{u=n} = \left[\overline{I_n(n)}\right]_v + \left[\sum_{j=1}^{n-1}(-1)^{n-j}A^{n-j}\overline{I_j'(j)}\right]_v$$
$$+ \left[\sum_{j=1}^{n-1}(-1)^{n-j}A^{n-j}\overline{N_j(j)}\right]_v \qquad (3.59)$$

Equations (3.14) through (3.20) can now be applied to obtain an expression for the probability of error resulting after decorrelating the nth window. Here the variable X in equation (3.14) will be given by

$$X = \sqrt{w_k(i-1)} e^{j\phi_k(i-1)} a_k(i-1) d_k(i-1) + \gamma_k(i-1)$$
$$+ \left[\overline{I_j(j)} + \sum_{j=1}^{n-1} (-1)^{n-j} A^{n-j} \left[\overline{I_j'(j)} + \overline{N_j(j)} \right] \right]_{v-\kappa} \qquad (3.60)$$

and the variable Y will be given by

$$Y = \sqrt{w_k(i)} e^{j\phi_k(i)} a_k(i) d_k(i) + \gamma_k(i)$$
$$+ \left[\overline{I_j(j)} + \sum_{j=1}^{n-1} (-1)^{n-j} A^{n-j} \left[\overline{I_j'(j)} + \overline{N_j(j)} \right] \right]_{v} \qquad (3.61)$$

It is clear from the preceding equations and discussion that unlike its AWGN counterpart, the fading channel windowed decorrelator will encounter an irreducible error floor due to the presence of the "acquired" interference introduced by the current window. In other words, even if a "steady-state" condition could be reached in which the influence of the out-of-window MAI encountered from all previous windows was negligible, the "acquired" MAI in the current window will introduce an irreducible error floor, thereby limiting the receiver's performance and resulting in a near-far resistance of zero. It therefore becomes important to determine what the near-far spread will be for the fading channel windowed decorrelator. The best possible performance for the fading channel windowed decorrelator with imperfect MAI estimates will correspond to the scenario in which all "acquired" MAI from previous windows is negligible, and thus only the MAI introduced by the current window will be considered. In reality, the effects of the MAI from the several most recent windows would probably not be negligible, but this analysis will provide an upper bound

on the receiver's performance. Ignoring the MAI introduced by previous windows, equation (3.59) becomes

$$\left[R_{LK}^{-1}P\left(W_e\Phi_e A_e - \hat{W}_e\hat{\Phi}_e\hat{A}_e\right)\right]_v^{u=n} = \left[\overline{I_n(n)}\right]_v \qquad (3.62)$$

For notational compactness, define

$$h_k(i) = \sqrt{w_k(i)}e^{j\phi_k(i)}a_k(i) \qquad (3.63)$$

and

$$\overline{S} = \left[R_{LK}^{-1}P\left(W_e\Phi_e A_e - \hat{W}_e\hat{\Phi}_e\hat{A}_e\right)\right] \qquad (3.64)$$

Then from equations (3.56), (3.63), and (3.64), equation (3.62) will become

$$\left[\overline{S}\right]_v^{u=n} = \sum_{l=1}^{K-1}\sum_{j=(L-1)K+1}^{LK}c_{v,j}R_{j-(L-1)K,1}(-1)\left[h_1(n(L+1)) - h_1((n-1)(L+1))\right] \quad (3.65)$$

The decision variables X and Y are then given by

$$X = h_k(i-1)d_k(i-1) + \gamma_k(i-1) + \left[\overline{S}\right]_{v-K}^n \qquad (3.66)$$

$$Y = h_k(i)d_k(i) + \gamma_k(i) + \left[\overline{S}\right]_v^n \qquad (3.67)$$

Finally, the covariances M_{xx}, M_{yy}, and M_{xy} are then

$$M_{xx} = 2w_k(i-1)R_{a_k}(0) + \sigma^2 c_{v-2,v-2} + E\left\{\left[\overline{S}\right]_{v-2}^n\left[\overline{S}^{*T}\right]_{v-2}^n\right\} \qquad (3.68)$$

$$M_{yy} = 2w_k(i)R_{a_k}(0) + \sigma^2 c_{v,v} + E\left\{\left[\overline{S}\right]_v^n\left[\overline{S}^{*T}\right]_v^n\right\} \qquad (3.69)$$

$$M_{xy} = 2\sqrt{w_k(i-1)}\sqrt{w_k(i)}R_{a_k}(T) + \sigma^2 c_{v-2,v} + E\left\{\left[\overline{S}\right]_{v-K}^n\left[\overline{S}^{*T}\right]_v^n\right\} \qquad (3.70)$$

where the notation $\overline{X}^{*T}$ represents the conjugate transpose operation. By symmetry, $M_{yx} = M_{xy}$. Next, the quantity $E\left\{\left[\overline{S}\right]_{v-K}^n\left[\overline{S}^{*T}\right]_{v-K}^n\right\}$ is found to be

$$E\left\{\left[\overline{S}\right]_{v-K}^n\left[\overline{S}^{*T}\right]_{v-K}^n\right\} = E\left\{\left(\sum_{l=1}^{K-1}\sum_{j=(L-1)K+1}^{LK}c_{v-K,j}R_{j-(L-1)K,1}(-1)\left[h_1(n(L+1)) - h_1((n-1)(L+1))\right]\right)\right.$$

$$\left.\left(\sum_{p=1}^{K-1}\sum_{q=(L-1)K+1}^{LK}c_{v-K,q}R_{q-(L-1)K,p}(-1)\left[h_p(n(L+1)) - h_p((n-1)(L+1))\right]\right)\right\}$$

$$(3.71)$$

which can be re-written as

$$E\left\{\left[\overline{S}\right]_{v-K}^n \left[\overline{S}^{*T}\right]_{v-K}^n\right\} = \sum_{l=1}^{K-1} \sum_{j=(L-1)K+1}^{LK} \sum_{p=1}^{K-1} \sum_{q=(L-1)K+1+p}^{LK} c_{v-K,j}R_{j-(L-1)K,1}(-1)c_{v-K,q}R_{q-(L-1)K,p}(-1) \cdot$$
$$E\left\{\left[h_1(n(L+1))-h_1((n-1)(L+1))\right]\left[h_p(n(L+1))-h_p((n-1)(L+1))\right]\right\}$$

(3.72)

Since the fading processes of different users are statistically independent,

$$E\left\{h_1(m)h_p^*(n)\right\} = 2\sqrt{w_1(m)}\sqrt{w_1(n)}R_{a_1}(m-n)\delta_{1p}$$ (3.73)

where the delta function is defined as

$$\delta_{ab} = \begin{cases} 1, & a=b \\ 0, & \text{otherwise} \end{cases}$$ (3.74)

Using equation (3.73), equation (3.72) simplifies to

$$E\left\{\left[\overline{S}\right]_{v-K}^n \left[\overline{S}^{*T}\right]_{v-K}^n\right\} = 4\sum_{l=1}^{K-1} w_1(i)\left[R_{a_1}(0)-R_{a_1}((L+2)T)\right]\left[\sum_{j=(L-1)K+1}^{LK} c_{v-K,j}R_{j-(L-1)K,1}(-1)\right]^2$$

(3.75)

where it has been assumed for simplicity that the received energies are constant over the span of L+2 bits; that is,

$$w_k((n-1)(L+1)) = w_k(n(L+1)) = w_k(i)$$ (3.76)

This assumption will be valid for small window lengths since the w_k represent received energies in the absence of fading. Similarly,

$$E\left\{\left[\overline{S}\right]_v^n \left[\overline{S}^{*T}\right]_v^n\right\} = 4\sum_{l=1}^{K-1} w_1(i)\left[R_{a_1}(0)-R_{a_1}((L+2)T)\right]\left[\sum_{j=(L-1)K+1}^{LK} c_{v,j}R_{j-(L-1)K,1}(-1)\right]^2$$ (3.77)

and

$$E\left\{\left[\overline{S}\right]_{v-K}^n \left[\overline{S}^{*T}\right]_v^n\right\} = 4\sum_{l=1}^{K-1} w_1(i)\left[R_{a_1}(0)-R_{a_1}((L+2)T)\right] \sum_{j=(L-1)K+1}^{LK} c_{v-K,j}R_{j-(L-1)K,1}(-1) \cdot$$
$$\sum_{q=(L-1)K+1+1}^{LK} c_{v,q}R_{q-(L-1)K+1+1}(-1)$$

(3.78)

The final expression for the kth user's probability of error
is then given by equation (3.15), with equations (3.75),
(3.77), and (3.78) appropriately substituted into equations
(3.68), (3.69), and (3.70). Note that the resulting
probability of error is a function of the bit position
within the window. Averaging the above mentioned
expression over all bit positions results in an average
probability of error

$$P_{k,avg} = \frac{1}{L-2} \sum_{v=k}^{(L-1)K+k} \frac{1}{2}\left(1 - \frac{M_{xy}(v)}{\sqrt{M_{xx}(v)M_{yy}(v)}}\right) \qquad (3.79)$$

Recall that the average probability of error given in
equation (3.79) is a lower bound due to the fact that only
the out-of-window MAI introduced by the current window is
considered. In order to determine how tight this bound is,
a computer simulation of an asynchronous DS-CDMA system
employing DPSK modulation through a flat Rayleigh fading
channel was created. In the simulation, each user
transmitted 100,000 bits through the channel and used the
windowed decorrelating receiver to decode the received bits.
The total number of errors was counted and then divided by
100,000 to determine the average probability of error. To
verify that the simulation was working properly, the number
of users was set equal to one and the resulting probability
of error performance was compared with equation (3.39). The
results are listed in Table 3.1 and plotted in Figure 3.8,
from which the validity of the simulation is confirmed.

Table 3.1 - Comparison of Computer Simulation Results with
True Single User Error Rates

Average SNR (dB)		Analytical Prob. of Error	Simulation Prob. of Error
0		0.25	0.2512
5		0.120126	0.12233
10		0.04545	0.046217
15		0.015327	0.014079
20		0.0049505	0.0050397
25		0.0015762	0.0014799
30		0.0004995	0.00043997
35		0.00015806	0.00015999
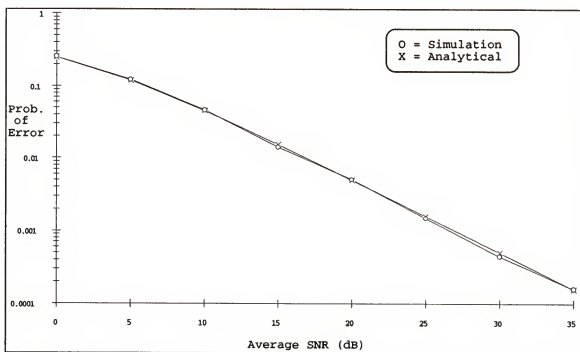
Figure 3.8 - Comparison of Computer Simulation Results with
True Single User Error Rates

Figure 3.9 compares the simulation with the lower bound for

the case of two active users with cross-correlations

$R_{12}(0)=\frac{2}{3}$ and $R_{12}(1)=\frac{1}{3}$. A nineteen bit wide window was used,

resulting in a 10% overhead for each user. To model the

fading, both users were assumed to be traveling at 65 mph,

transmitting a bit rate of 20 kbps, and using a carrier
frequency of 900 MHz. User two was designated as the
desired user and given an average received signal-to-noise
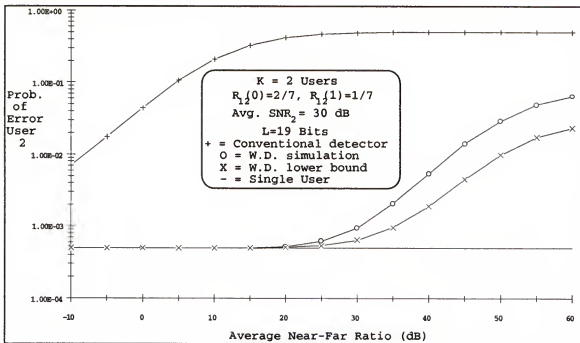ratio of 30 dB. As can be seen from Figure 3.9, the

Figure 3.9 - Comparison of Analytical Lower Bound with
Computer Simulation

simulation indicates a larger probability of error than the
lower bound. This is expected, of course, since the
simulation will contain the out-of-window MAI influence from
all previous windows. Both the simulation and the lower
bound indicate that the windowed decorrelator can track the
single user error probability for near-far effects of
approximately 20 dB or less. For larger near-far effects,
the windowed decorrelator's error probability diverges from
that of the single user and eventually approaches a value of

one-half. For comparison purposes, the performance of the conventional DS-CDMA detector is also displayed in Figure 3.9.

Figure 3.10 displays the probability of error for user two versus the average signal-to-noise ratio of user two. Here the average near-far effect is held at 30 dB. Note that the lower bound is not too far off from the computer simulation. The simulation reveals an error floor of
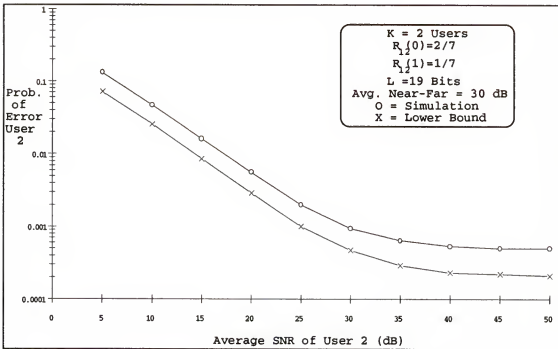

Figure 3.10 - Error Floors of Lower Bound and Simulation for a 30 dB Near-Far Ratio

approximately 5×10^{-4} whereas the lower bound predicts an error floor of approximately 2×10^{-4}. Figure 3.11 displays the same scenario as in Figure 3.10, except now the average near-far effect is increased to 40 dB. The result is that the lower bound is not as tight as before: the simulation

shows an error floor of approximately 5×10^{-3} whereas the lower bound predicts an error floor of approximately 1×10^{-3}. This increase is expected, however, since the MAI acquired by past windows will become less negligible as the severity of the near-far effect increases.
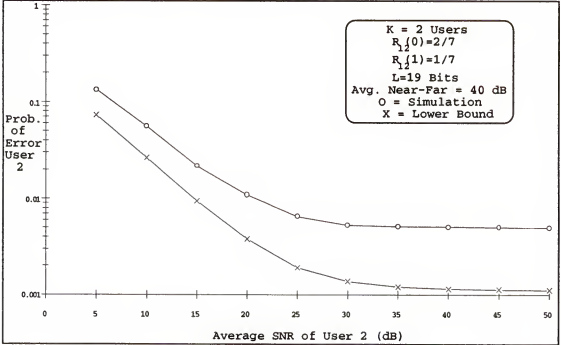

Figure 3.11 - Error Floors of Lower Bound and Simulation for a 40 dB Near-Far Ratio

The lower bound derived in the preceding analysis may be tightened by extending the previous analysis to include the effects of the out-of-window MAI acquired from the window immediately preceding the current window, since this window's MAI influence will be the next largest after that of the current window. Equation (3.59) will then become

$$\left[\overline{S}\right]_v^n = \left[R_{LK}^{-1} P\left(W_e \Phi_e A_e - \hat{W}_e \hat{\Phi}_e \hat{A}_e\right)\right]_v^{u=n} = \left[\overline{I_n(n)}\right]_v - \left[\overline{A I_{n-1}'(n-1)}\right]_v + \left[\overline{N_{n-1}(n-1)}\right]_v \quad (3.80)$$

Using equation (3.58) to expand out the noise term on the right hand side of equation (3.80), the expression for the noise component in the MAI term contained in the nth window's intermediate decision statistic vector becomes

$$\left[\overline{N_{n-1}(n-1)}\right]_v = -\sum_{l=2}^{K}\sum_{j=1}^{l-1}c_{v,j}R_{j,1}(1)\gamma_1\big((n-1)(L+1)-1\big)$$
$$-\sum_{l=1}^{K-1}\sum_{j=(L-1)K+1+1}^{LK}c_{v,j}R_{j-(L-1)K,1}(-1)\gamma_1\big((n-1)(L+1)-1\big) \qquad (3.81)$$

The middle term on the right hand side of equation (3.80) represents the MAI acquired from the $(n-1)^{st}$ window; expanding out this term results in

$$\left[A\overline{I_{n-1}(n-1)}\right]_v = \sum_{q=1}^{K}a_{v,q}\sum_{l=1}^{K-1}\sum_{j=(L-1)K+1+1}^{LK}c_{(L-1)K+q,j}R_{j-(L-1)K,1}(-1)\cdot$$
$$\left[h_1\big((n-1)(L+1)\big)-h_1\big((n-2)(L+1)-1\big)\right] \qquad (3.82)$$

The first term on the right hand side of equation (3.80) represents the out-of-window MAI acquired by the nth window and as before it is given by equation (3.65).

   Recall that the average probability of error for the fading channel windowed decorrelator is given by equation (3.79). The decision variables X and Y are again given by equations (3.66) and (3.67) and the covariances M_{xx}, M_{yy}, and M_{xy} are again given by equations (3.68) through (3.70). The only difference in the analysis of the second lower bound is that the expression for $\left[\overline{S}\right]_v^n$ given in equation (3.80) contains more terms than it did for the first lower bound, thereby resulting in more complicated expressions for the covariances. Repeating the same procedure used to derive

equations (3.71) through (3.78) yields

$$
\begin{aligned}
E\left\{\left[\bar{S}\right]^n_{v-K}\left[\bar{S}^{*T}\right]^n_{v-K}\right\} = &\ 4\sum_{i=1}^{K-1} w_1(i)\left[R_{a_i}(0)-R_{a_i}((L+2)T)\right]\left[\sum_{j=(L-1)K+1+1}^{LK} c_{v-K,j}R_{j-(L-1)K,1}(-1)\right]^2 \\
&+4\sum_{i=1}^{K-1} w_1(i)\left[R_{a_i}(0)-R_{a_i}((L+2)T)\right]\left[\sum_{q=1}^{K} a_{v-K,q}\sum_{j=(L-1)K+1+1}^{LK}c_{(L-1)K+q,j}R_{j-(L-1)K,1}(-1)\right]^2 \\
&-4\sum_{i=1}^{K-1} w_1(i)\left[2R_{a_i}((L+1)T)-R_{a_i}(T)-R_{a_i}((2L+1)T)\right]\cdot \\
&\left[\sum_{q=1}^{K}a_{v-K,q}\sum_{j=(L-1)K+1+1}^{LK}c_{(L-1)K+q,j}R_{j-(L-1)K,1}(-1)\right]\left[\sum_{s=(L-1)K+1+1}^{LK}c_{v-K,s}R_{s-(L-1)K,1}(-1)\right] \\
&+\sigma^2\sum_{l=2}^{K}\sum_{r=2}^{K}c_{(L-1)K+1,(L-1)K+r}\sum_{j=1}^{l-1}\sum_{s=1}^{r-1}c_{v-K,j}c_{v-K,s}R_{j,1}(1)R_{a,r}(1) \\
&+\sigma^2\sum_{l=1}^{K-1}\sum_{r=1}^{K-1}c_{(L-1)K+1,(L-1)K+r}\sum_{j=(L-1)K+1+1}^{LK}\sum_{s=(L-1)K+1+r}^{LK}c_{v,j}c_{v,s}R_{j-(L-1)K,1}(-1)R_{s-(L-1)K,r}(-1) \\
&+2\sigma^2\sum_{l=2}^{K}\sum_{r=1}^{K-1}c_{(L-1)K+1,(L-1)K+r}\sum_{j=1}^{l-1}\sum_{a=(L-1)K+1+r}^{LK}c_{v,j}c_{v,a}R_{j,1}(1)R_{a-(L-1)K,r}(-1)
\end{aligned}
$$

(3.83)

$$
\begin{aligned}
E\left\{\left[\bar{S}\right]^n_{v-K}\left[\bar{S}^{*T}\right]^n_{v-K}\right\} = &\ 4\sum_{i=1}^{K-1} w_1(i)\left[R_{a_i}(0)-R_{a_i}((L+2)T)\right]\sum_{j=(L-1)K+1+1}^{LK}c_{v,j}R_{j-(L-1)K,1}(-1)\cdot \\
&\sum_{s=(L-1)K+1+1}^{LK}c_{v,a}R_{s-(L-1)K,1}(-1)+4\sum_{i=1}^{K-1} w_1(i)\left[R_{a_i}(0)-R_{a_i}((L+2)T)\right]\cdot \\
&\sum_{q=1}^{K}a_{v-K,q}\sum_{j=(L-1)K+1+1}^{LK}c_{(L-1)K+q,j}R_{j-(L-1)K,1}(-1)\sum_{r=1}^{K}a_{v,r}\sum_{s=(L-1)K+1+1}^{LK}c_{r,s}R_{s-(L-1)K,1}(-1) \\
&-2\sum_{i=1}^{K-1} w_1(i)\left[2R_{a_i}((L+1)T)-R_{a_i}(T)-R_{a_i}((2L+1)T)\right]\cdot \\
&\left[\sum_{q=1}^{K}a_{v-K,q}\sum_{j=(L-1)K+1+1}^{LK}c_{(L-1)K+q,j}R_{j-(L-1)K,1}(-1)\right]\left[\sum_{s=(L-1)K+1+1}^{LK}c_{v,a}R_{a-(L-1)K,1}(-1)\right] \\
&+\sigma^2\sum_{l=2}^{K}\sum_{r=2}^{K}c_{(L-1)K+1,(L-1)K+r}\sum_{j=1}^{l-1}\sum_{s=1}^{r-1}c_{v-K,j}c_{v,a}R_{j,1}(1)R_{a,r}(1) \\
&+\sigma^2\sum_{l=1}^{K-1}\sum_{r=1}^{K-1}c_{(L-1)K+1,(L-1)K+r}\sum_{j=(L-1)K+1+1}^{LK}\sum_{s=(L-1)K+1+r}^{LK}c_{v-K,j}c_{v,s}R_{j-(L-1)K,1}(-1)R_{s-(L-1)K,r}(-1) \\
&+2\sigma^2\sum_{l=2}^{K}\sum_{r=1}^{K-1}c_{(L-1)K+1,(L-1)K+r}\sum_{j=1}^{l-1}\sum_{a=(L-1)K+1+r}^{LK}c_{v-K,j}c_{v,a}R_{j,1}(1)R_{a-(L-1)K,r}(-1)
\end{aligned}
$$

(3.84)

The expression for $E\left\{\left[\bar{S}\right]^n_{v}\left[\bar{S}^{*T}\right]^n_{v}\right\}$ will be identical to equation (3.83), except the subscript v-K will be replaced with v.

The resulting lower bound on the average probability of error is then found by using equations (3.83) and (3.84) in the expressions for M_{xx}, M_{yy}, and M_{xy} given by equations (3.68) through (3.70), which in turn are substituted into equation (3.79).

The second lower bound is compared to the first lower bound and the simulation results in Figures 3.12, 3.13, and 3.14. In Figure 3.12, the second lower bound is seen to represent a substantial improvement over the first lower bound: approximately half of the total out-of-window MAI influence due to all previous windows is accounted for by
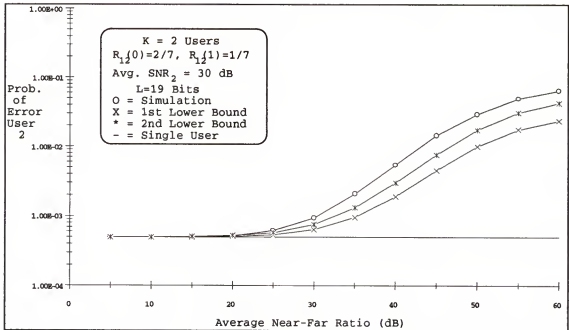

Figure 3.12 - Comparison of Second Lower Bound with First Lower Bound and Simulation

the MAI incurred from the most previous window. In Figure 3.13, the second lower bound predicts an error floor of

approximately 3.3×10^{-4} which compares very favorably with the error floor of 5×10^{-4} indicated by the simulation. Similarly, Figure 3.14 also shows a substantial improvement in the second lower bound over the first: an error floor of approximately 2.3×10^{-3} is now predicted which is not too far off from the simulation's value of 5×10^{-3}.

The second lower bound could be tightened by extending the previous analysis to include the effects of out-of-window MAI from even more past windows; however, such an analysis would soon become analytically intractable. Therefore, the second lower bound will be used as an approximation for the average probability of error of the
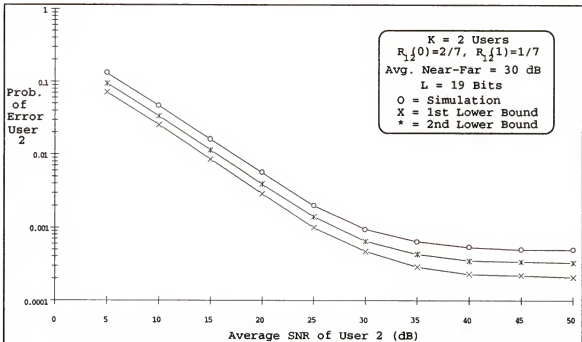

Figure 3.13 - Error Floors of Second Lower Bound, First Lower Bound, and Simulation for an Average Near-Far Ratio of 30 dB
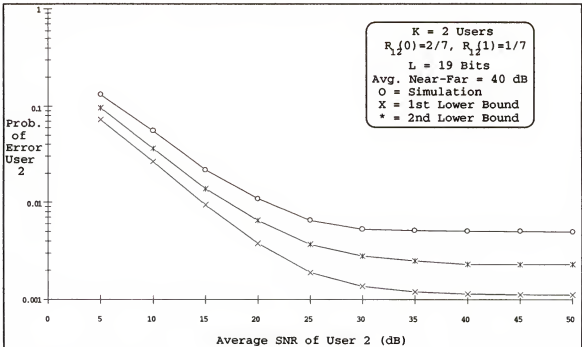
Figure 3.14 - Error Floors of Second Lower Bound, First Lower Bound, and Simulation for an Average Near-Far Ratio of 40 dB

windowed decorrelator. Of course, another way to view the results presented in this section is that the lower bounds serve to further confirm the validity of the computer simulation; therefore, the simulation will be used as well in obtaining performance results for the windowed decorrelator in a flat Rayleigh fading channel.

Unfortunately, equations (3.83) and (3.84) are so unwieldy that they preclude the possibility of using equation (2.10) to solve for the fading channel windowed decorrelator's asymptotic efficiency. The results shown in Figures 3.9 and 3.12, however, are sufficient to allow the performance of the windowed decorrelator to be completely characterized; moreover, they suggest that the overall

system structure proposed previously will require modification in order for the fading channel windowed decorrelator to be near-far resistant.

Modified Multiuser Receiver Structure

Figures 3.9 and 3.12 show that the windowed decorrelator is capable of tracking the bit error rate of a single user up to a certain level of near-far effect (about 20 dB for the system considered in Figure 3.9); for greater near-far effects, the windowed decorrelator loses this ability. This observation leads to the conclusion that the multiuser receiver structure presented earlier requires some modification in order to become near-far resistant; namely, an average power control scheme is required which would function to keep the average received power levels of all users to within a certain range of one another (20 dB in Figure 3.9). At first, the idea of using a power control scheme in conjunction with the windowed decorrelator may seem self-defeating, since the original goal of this work was to overcome the near-far problem without the use of conventional power control; however, this combination is not self-defeating for three important reasons. First, the fading channel windowed decorrelator requires an average power control scheme, not a bit-by-bit power control scheme as is required by the conventional DS-CDMA receiver. Thus the rate at which the power control updates must be made

will be much less for the windowed decorrelator, thereby overcoming the necessity of updating powers during fast fading. Secondly, the conventional DS-CDMA receiver requires a difference of 0 dB between all received signals for optimum performance; as the difference in received powers increases, the performance of the conventional detector degrades. On the contrary, as demonstrated by Figures 3.9 and 3.12, the windowed decorrelator's performance remains unaffected by changes in the received powers as long as they are all within the required range (20 dB in this case). Of course, the exact power control range required will depend upon the number of active users and the magnitudes of their signature waveform cross-correlations. Finally, even if perfect bit-by-bit power control was achievable for the conventional detector, there would still be an irreducible error floor due to the presence of the MAI component in each user's decision statistic. As seen in Figure 3.9, for a near-far effect of 0 dB the conventional detector can only achieve a bit error rate of 4.5×10^{-2}. On the contrary, as long as the average received energies are kept within 20 dB of one another, the windowed decorrelator is able to remove the MAI and approach the single user error rate.

To summarize, the windowed decorrelating receiver for flat Rayleigh fading channels must be used in conjunction with an average received power control scheme. The estimates of each user's received power level may be

obtained by the MAI estimation procedure illustrated in Figure 3.3 and thus no additional computational complexity is required to track the received power levels. The multiuser receiver can simply compare the magnitudes obtained from the estimation procedure and then send out appropriate control signals to the users, instructing them to adjust their transmitter output powers accordingly. The block diagram of the fading channel windowed decorrelator incorporating power control is shown in Figure 3.15.
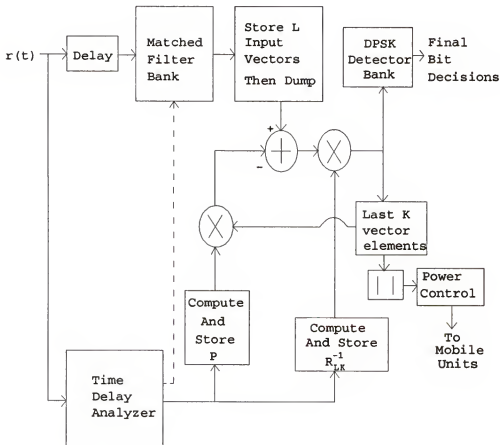

Figure 3.15 - Block Diagram of Fading Channel Windowed Decorrelator Incorporating Power Control

Numerical Examples

Numerical examples are presented in this section to highlight the performance of the windowed decorrelator in flat Rayleigh fading channels. The results for two users displayed in Figures 3.16 through 3.20 were obtained from the computer simulation discussed previously. The results for more than two users presented in Figures 3.21 through 3.25 were obtained from the second lower bound derived earlier in this chapter.

The performance of the windowed decorrelator as a function of the window length was investigated; the results are displayed in Figure 3.16 for window lengths of 19 bits (10% overhead) and 5 bits (33% overhead). Here zeroth
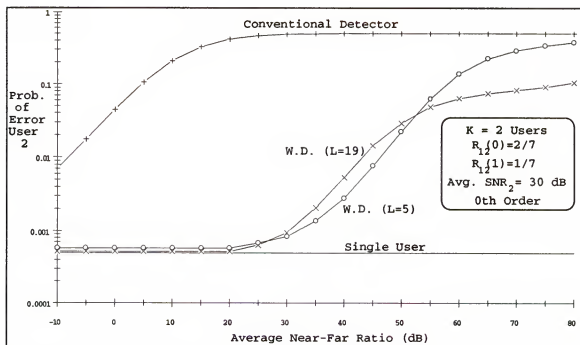

Figure 3.16 - Performance of the Windowed Decorrelator as a Function of the Window Length with Zeroth Order Estimation

order estimation was employed. For error rates of 1×10^{-3} or
less, both window sizes yield almost identical performance.
For the two user system considered here, the power control
scheme would need to keep the average received power levels
to within about 20 dB of one another in order to achieve an
error rate approaching that of a single user.

Figure 3.17 compares the zeroth order and first order
MAI estimation strategies when a window length of nineteen
bits is used. Interestingly, for error rates of 1×10^{-3} or
less there is no noticeable difference in the receiver's
performance; thus, the zeroth order technique would be
preferred since it results in computational savings over the
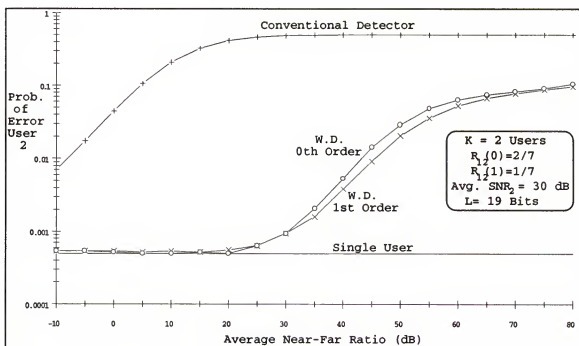use of linear extrapolation.

Figure 3.17 - Comparison of Zeroth Order and First Order
Estimation Techniques for a Window Length of Nineteen Bits

Figure 3.18 compares the zeroth order and first order MAI estimation strategies when a window length of five bits is used. Now there is a significant difference in performance. Note that when the zeroth order strategy is used, the power scheme must keep the averaged received power levels to within about 32 dB of one another to obtain a 1×10^{-3} error rate. The first order strategy only requires the average received power levels to be within about 40 dB to achieve the same level of performance, and so for this scenario the first order technique would be preferred.

Figure 3.19 compares window lengths of five bits and nineteen bits when the first order estimation strategy is employed. For a window length of nineteen bits, a power control range of about 32 dB is required to achieve a 1×10^{-3}
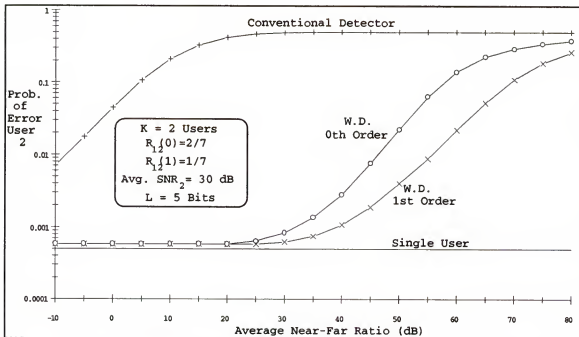

Figure 3.18 - Comparison of Zeroth Order and First Order Estimation Techniques for a Window Length of Five Bits
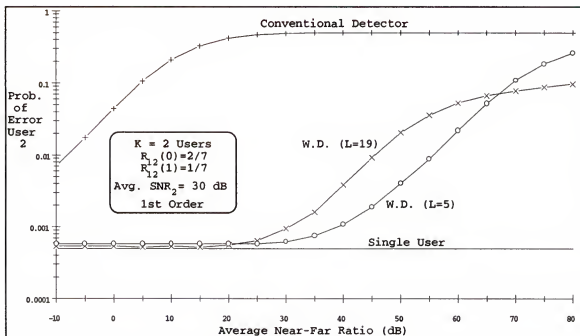
Figure 3.19 - Performance of the Windowed Decorrelator as a Function of Window Length When First Order Estimation is Used

error rate, whereas for a window length of five bits this range becomes about 40 dB. The conclusion from Figures 3.15 through 3.18 is that for smaller window lengths, the first order MAI estimation strategy (linear extrapolation) can significantly relax the level of average power control required by the system. As the window length increases, the advantage offered by the first order strategy becomes smaller.

The irreducible error floors encountered by the fading channel windowed decorrelator for various average near-far effects are displayed in Figure 3.20. As can be seen, an error rate of 1×10^{-3} or less may be achieved as long as the average near-far ratio is kept to within roughly 30 dB or less.
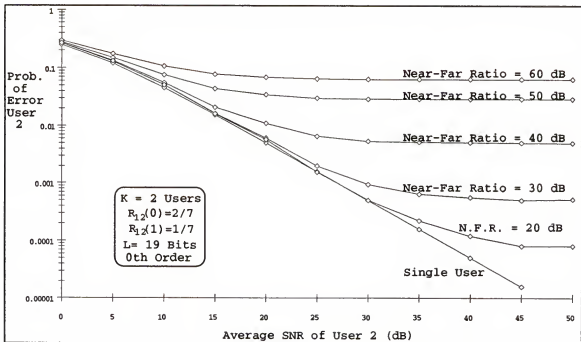
Figure 3.20 – Error Floors of the Windowed Decorrelator for Various Average Near-Far Ratios

The performance of the windowed decorrelator as a function of the number of active users is examined in Figures 3.21 through 3.25. In Figure 3.21, Gold codes of length seven chips were used for the signature sequences. The results indicate that average near-far ratios of less than 35 dB, 25 dB, and 17.5 dB are required in order for the receiver to obtain a 1×10^{-3} error rate for two, three, and four active users, respectively. In Figure 3.22, Gold codes of length 31 chips were used for the signature sequences, resulting in lower cross-correlation magnitudes. Here it is seen that average near-far ratios of less than 57.5 dB, 42 dB, and 22 dB are required in order for the receiver to maintain a 1×10^{-3} error rate for two, three, and four active users, respectively. The conclusion from Figures 3.21 and
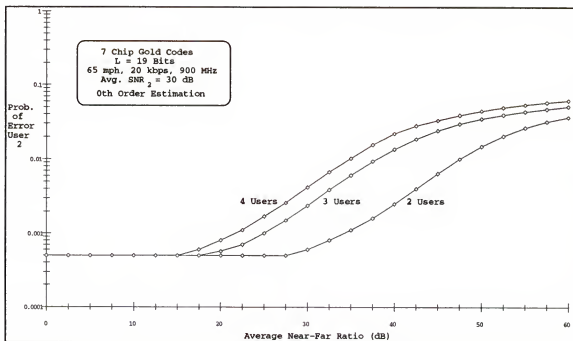
Figure 3.21 - Error Rate of the Windowed Decorrelator vs. the Number of Active Users for Gold Codes of Length Seven Chips and 65 mph User Speed
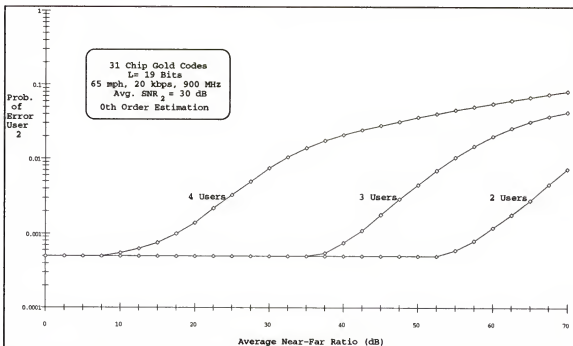

Figure 3.22 - Error Rate of the Windowed Decorrelator vs. the Number of Active Users for Gold Codes of Length Thirty-one Chips and 65 mph User Speed

3.22, therefore, is that even when a decorrelating strategy
is used, it is still important to choose signature waveforms
with low cross-correlations; specifically, lower cross-
correlation magnitudes will result in a relaxation of the
power control range required by the communication system.

Figures 3.21 and 3.22 were obtained by assuming that
each user was moving at a speed of 65 mph, corresponding to
a cellular telephone scenario. For many applications,
however, such as personal communication systems or indoor
wireless networks, the mobile units will be traveling at
much lower speeds. Since the rapidity of the fading
processes is a function of the speed of the mobile units
[28], the fading will occur at a much slower rate in such
communication systems. As a result of the slower fading,
the estimates of the future MAI should become better, and
the performance of the windowed decorrelator would be
expected to improve. Figure 3.23 compares a computer
simulation of the time autocorrelation function of a typical
flat Rayleigh fading process for user speeds of 65 mph and
15 mph. Indeed, for the user traveling at the slower speed,
the fading process remains highly correlated over a much
wider time span. Figure 3.24 repeats the system of Figure
3.19 (Gold codes of length seven chips) but with the users
moving at 15 mph instead of 65 mph. Likewise, Figure 3.25
repeats the system of Figure 3.20 (Gold codes of length
thirty-one chips) but with user speeds of 15 mph. Clearly,
there is a noticeable improvement in performance as the
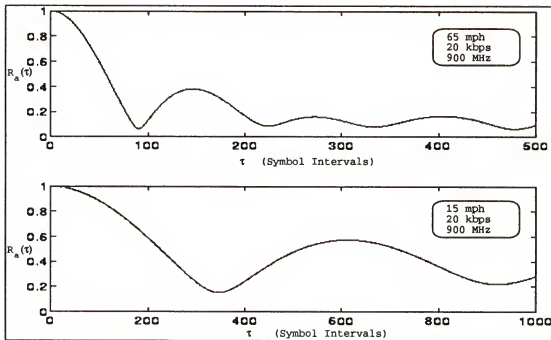
Figure 3.23 - Comparison of the Autocorrelation Functions of Flat Rayleigh Fading Processes for User Speeds of 65 mph and 15 mph
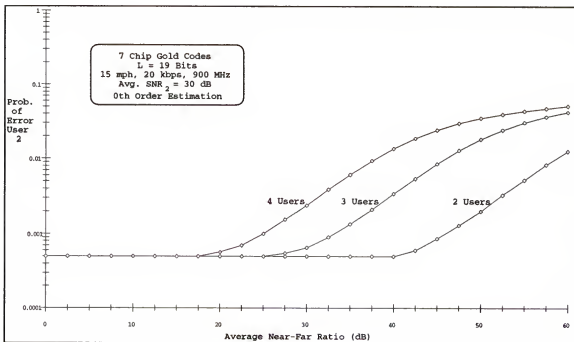
Figure 3.24 - Error Rate of the Windowed Decorrelator vs. the Number of Active Users for Gold Codes of Length Seven Chips and User Speeds of 15 mph
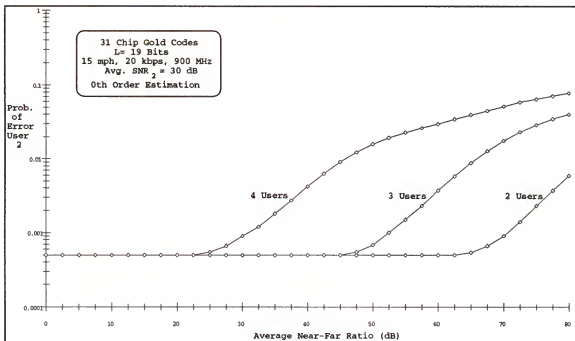
Figure 3.25 - Error Rate of the Windowed Decorrelator vs. the Number of Active Users for Gold Codes of Length Thirty-one Chips and User Speeds of 15 mph

speed of the mobile units decreases; specifically, the required power control range is relaxed. It is reasonable, therefore, to expect that the windowed decorrelator would tend to be more robust in a personal communication system or indoor wireless network than in a cellular telephone system.

CHAPTER 4
IMPLEMENTATIONAL CONSIDERATIONS

In this chapter, two important practical considerations related to the implementation of a windowed decorrelating receiver are examined. First, the sensitivity of the receiver to errors in the timing information is investigated. Secondly, the computational requirements for computing the inverse of the cross-correlation matrix are examined.

Sensitivity to Propagation Delay Estimation Errors

In the previous chapters, the performance analyses of the windowed decorrelator for AWGN and frequency nonselective Rayleigh fading channels assumed that the multiuser receiver had perfect knowledge of the propagation delay from each user to the base station. In practice it will not be possible for the receiver to obtain perfect estimates; even if the MAI corruption could be removed, the background noise would still result in estimation errors. It is therefore of interest to determine how the windowed decorrelator's performance will be affected by imperfect timing information.

Imperfect timing information will affect the windowed decorrelator in two ways: the vector of matched filter

sampled outputs will be different than before, and the computed inverse cross-correlation matrix will no longer represent the inverse of the true cross-correlation matrix. It should be noted that the operation of windowing the received sequences does not in any way affect the decorrelator's sensitivity to timing errors; in other words, the windowed decorrelator should have the same sensitivity to timing errors as does the full-length decorrelator. Also, since the decorrelating operation itself is the same for both the AWGN and flat Rayleigh fading channels, the following analysis will be for a full-length decorrelator operating in an AWGN channel. A similar analysis has been presented by Strom [59], although in that work Monte Carlo simulations were used to obtain results. The goal here will be to derive an analytical expression for the asymptotic efficiency of a decorrelating receiver as a function of the severity of the timing estimation errors.

For convenience, the notation introduced by Strom [59] will be adopted. The system is essentially described by the same notation as in chapter 2, but now only one window of length M bits is transmitted and decorrelated. Of course, pilot bits are no longer employed since no windowing is being done. The received signal at the base station is

$$r(t) = S(t, \overline{b}) + n(t) \tag{4.1}$$

where $n(t)$ is white Gaussian noise with power spectral density σ^2 and

$$S(t, \overline{b}) = \sum_{i=1}^{M} \sum_{k=1}^{K} \sqrt{w_k(i)} \, b_k(i) \tilde{s}_k(t - iT - \tau_k) \qquad (4.2)$$

where as before $w_k(i)$ is the received energy of the kth user during the ith interval, $b_k(i) \in \{\pm 1\}$ is the polarity of the kth user's i^{th} bit, and $\tilde{s}_k(t)$ is the kth user's RF signature waveform normalized to unit energy and zero outside the time interval $[0, T]$.

Let the time delay analyzer shown in Figure (2.7) produce an estimate of the kth user's propagation delay denoted by $\hat{\tau}_k$. It will be assumed that $\hat{\tau}_k \in [0, T)$. The ith sampled output of the kth user's matched filter now becomes

$$
\begin{aligned}
y_k(i) &= \int_{iT + \hat{\tau}_k}^{(i+1)T + \hat{\tau}_k} r(t) \tilde{s}_k(t - iT - \hat{\tau}_k) dt \\
&= \int_{iT + \hat{\tau}_k}^{(i+1)T + \hat{\tau}_k} S(t, \overline{b}) \tilde{s}_k(t - iT - \hat{\tau}_k) dt + n_k(i)
\end{aligned}
\qquad (4.3)
$$

where

$$n_k(i) = \int_{iT + \hat{\tau}_k}^{(i+1)T + \hat{\tau}_k} n(t) \tilde{s}_k(t - iT - \hat{\tau}_k) dt \qquad (4.4)$$

is a zero-mean Gaussian random variable with cross-correlation given by

$$E[n_k(i) n_l(j)] = \sigma^2 \int_{-\infty}^{\infty} \tilde{s}_k(t - iT - \hat{\tau}_k) \tilde{s}_l(t - jT - \hat{\tau}_l) dt \qquad (4.5)$$

Next, the following two cross-correlation matrices are defined by their $(k, j)^{th}$ elements

$$\hat{\hat{R}}_{kj}(1) = \int_{-\infty}^{\infty} \tilde{s}_k(t - \hat{\tau}_k) \tilde{s}_j(t + 1T - \hat{\tau}_j) dt \qquad (4.6)$$

$$\hat{R}_{kj}(1) = \int_{-\infty}^{\infty} \tilde{s}_k(t - \hat{\tau}_k) \tilde{s}_j(t + 1T - \tau_j) dt \qquad (4.7)$$

so that equation (4.5) may be rewritten as

$$E\big[n_k(i)n_j(j)\big] = \sigma^2 \hat{R}_{kj}(i-j) \tag{4.8}$$

Due to the time-limited nature of the signature waveforms, it is again clear that $\hat{R}_{kj}(l) = \hat{R}_{kj}(l) = 0$ for $|l| > 1$. Upon substituting for $S(t,\overline{b})$, equation (4.3) becomes

$$
\begin{aligned}
y_k(i) = n_k(i) + \sum_{l=1}^{K} b_l(i-1)\sqrt{w_l(i-1)}\hat{R}_{kl}(1) \\
+ \sum_{l=1}^{K} b_l(i)\sqrt{w_l(i)}\hat{R}_{kl}(0) + \sum_{l=1}^{K} b_l(i+1)\sqrt{w_l(i+1)}\hat{R}_{kl}(-1)
\end{aligned}
\tag{4.9}
$$

where the fact that $b_k(0) = b_k(M+1) = 0$ has been used. Following the same steps as in chapter 2, the complete vector of matched filter sampled outputs can be written as

$$\overline{Y} = \hat{R}W\overline{b} + \overline{n} \tag{4.10}$$

where $\overline{Y} = \big[\overline{y}^T(1), \overline{y}^T(2), \cdots, y^T(M)\big]^T$, $\overline{y}(i) = \big[y_1(i), y_2(i), \cdots, y_K(i)\big]^T$, $\overline{n} = \big[\overline{n}^T(1), \overline{n}^T(2), \cdots, \overline{n}^T(M)\big]^T$, $\overline{n}(i) = \big[n_1(i), n_2(i), \cdots, n_K(i)\big]^T$, $W = \text{diag}[W(1), W(2), \cdots, W(M)]$, $W(i) = \text{diag}\big[\sqrt{w_1(i)}, \sqrt{w_2(i)}, \cdots, \sqrt{w_K(i)}\big]$, and

$$
\hat{R} = \begin{bmatrix}
\hat{R}(0) & \hat{R}(1) & 0 & \cdots & 0 \\
\hat{R}(1) & \hat{R}(0) & \hat{R}(-1) & & \vdots \\
0 & \hat{R}(1) & \hat{R}(0) & \ddots & 0 \\
\vdots & & \ddots & \ddots & \hat{R}(-1) \\
0 & \cdots & 0 & \hat{R}(1) & \hat{R}(0)
\end{bmatrix}.
$$

The noise vector $\overline{n}$ is a Gaussian zero-mean vector with a covariance matrix given by

$$E\big[\overline{n}\,\overline{n}^T\big] = \sigma^2 \hat{\hat{R}} \tag{4.11}$$

where the matrix $\hat{\hat{R}}$ is defined as $\hat{R}$ with the appropriate substitutions.

Recall that the goal of the multiuser receiver is to determine the vector of transmitted polarities $\overline{b}$ from the

vector of matched filter sampled outputs $\overline{Y}$ given by
equation (4.10). The matrix $\hat{R}$ is unknown to the receiver,
however, since its elements are functions of the true time
delays through equation (4.7); thus, the receiver cannot
compute $\hat{R}^{-1}$. Of course, the multiuser receiver does not
know that its timing information is in error, and thus it
will form its decisions according to

$$\hat{\overline{b}} = sign\left[\hat{R}^{-1}\hat{R}W\overline{b} + \hat{R}^{-1}\overline{n}\right] \tag{4.12}$$

It is immediately clear from equation (4.12) that since
$\hat{R}^{-1}\hat{R} \neq I$, the multiuser receiver will not be able to
completely decorrelate the received signals and will
consequently have a near-far resistance of zero. It is of
interest, then, to determine the near-far spread obtainable
by the receiver. Define the matrix

$$E = \hat{R}^{-1}\hat{R} = \begin{bmatrix} e_{1,1} & e_{1,2} & \cdots & e_{1,MK} \\ e_{2,1} & e_{2,2} & \cdots & e_{2,MK} \\ \vdots & \vdots & \ddots & \vdots \\ e_{MK,1} & e_{MK,2} & \cdots & e_{MK,MK} \end{bmatrix} \tag{4.13}$$

and the vector

$$\overline{\gamma} = \hat{R}^{-1}\overline{n} \tag{4.14}$$

Then equation (4.12) becomes

$$\hat{\overline{b}} = sign\left[EW\overline{b} + \overline{\gamma}\right] \tag{4.15}$$

and the estimate of the ith bit of the kth user is

$$\hat{b}_k(i) = sign\left[\sum_{l=1}^{MK} e_{v,l}\left[W\overline{b}\right]_l + \left[\overline{\gamma}\right]_v\right]$$

$$= sign\left[e_{v,v}\sqrt{w_k(i)}\,b_k(i) + \sum_{\substack{l=1 \\ l \neq v}}^{MK} e_{v,l}\left[W\overline{b}\right]_l + \left[\overline{\gamma}\right]_v\right] \tag{4.16}$$

where as before the vector element v is related to the bit index i through equation (2.14) and the notation $[\overline{x}]_1$ denotes the 1th element in the vector $\overline{x}$.

The conditional probability of bit error will then be given by

$$P_k\left(i|\overline{b}\right) = \Pr\left\{\hat{b}_k(i) > 0 \middle| b_k(i) = -1, \overline{b}\right\}$$

$$= \Pr\left\{[\tilde{\gamma}]_v > e_{v,v}\sqrt{w_k(i)} - \sum_{\substack{l=1 \\ l \neq v}}^{MK} e_{v,l}[W\overline{b}]_l\right\}$$

$$= Q\left(\sqrt{\frac{e_{v,v}\sqrt{w_k(i)} - \sum_{\substack{l=1 \\ l \neq v}}^{MK} e_{v,l}[W\overline{b}]_l}{\sigma^2\left[\hat{\overline{R}}^{-1}\right]_{v,v}}}\right) \tag{4.17}$$

where the notation $\left[\hat{\overline{R}}^{-1}\right]_{m,n}$ denotes the element in the mth row and n^{th} column of the matrix $\hat{\overline{R}}^{-1}$. The average probability of error is found by averaging equation (5.17) over all possible vectors $\overline{b}$ with $b_k(i) = -1$. Doing so yields

$$P_k\left(i|\overline{b}\right) = \frac{1}{2^{MK-1}} \sum_{\substack{\overline{b} \in \{\pm 1\}^{MK} \\ b_k(i) = -1}} Q\left(\sqrt{\frac{e_{v,v}\sqrt{w_k(i)} - \sum_{\substack{l=1 \\ l \neq v}}^{MK} e_{v,l}[W\overline{b}]_l}{\sigma^2\left[\hat{\overline{R}}^{-1}\right]_{v,v}}}\right) \tag{4.18}$$

Since computing equation (4.18) will not be practical for large MK, the performance measure of choice becomes asymptotic efficiency. In the limit as $\sigma \to 0$, the summation in equation (4.18) will be dominated by the Q-function with the smallest argument, thus

$$\lim_{\sigma \to 0} P_{e,avg} \approx Q\left(\sqrt{\frac{\left|e_{v,v}\sqrt{w_k(i)} - \sum_{\substack{j=1 \\ j \neq v}}^{MK} \left|e_{v,1}\left[\overline{W}_b\right]_1\right|\right|}{\sigma^2\left[\hat{\overline{R}}^{-1}\right]_{v,v}}}\right) \qquad (4.19)$$

where the vector $\overline{W}_b$ has been defined as

$$\overline{W}_b = \left[\sqrt{w_1(1)}, \sqrt{w_2(1)}, \cdots, \sqrt{w_K(1)}, \sqrt{w_1(2)}, \sqrt{w_2(2)}, \cdots, \sqrt{w_K(2)}, \cdots, \sqrt{w_1(M)}, \sqrt{w_2(M)}, \cdots, \sqrt{w_K(M)}\right]^T.$$

From equation (2.10) the asymptotic efficiency for the windowed decorrelator with imperfect timing estimates is

$$\eta_k(i) = \max^2\left\{0, \frac{1}{\sqrt{\left[\hat{\overline{R}}^{-1}\right]_{v,v}}}\left(\left|e_{v,v}\right| - \sum_{\substack{j=1 \\ j \neq v}}^{MK} \frac{\left|e_{v,1}\left[\overline{W}_b\right]_1\right|}{\sqrt{w_k(i)}}\right)\right\} \qquad (4.20)$$

Of course, if the receiver's timing estimates were perfect then $E = I$, $\left[\hat{\overline{R}}^{-1}\right]_{v,v} = c_{v,v}$, and equation (4.20) would reduce to the expression found by Lupas [38] for the full-length decorrelator.

To obtain some insight into the sensitivity of the decorrelator to timing errors, equation (4.20) was evaluated for a three user system employing Gold codes of length 31 chips. Each user transmitted a total of five bits. Three of the possible 33 Gold codes were chosen at random, and three true propagation delays were randomly chosen to be $\tau_1 = 17.1921$ chips, $\tau_2 = 23.1971$ chips, and $\tau_3 = 29.6162$ chips. The asymptotic efficiency of user two was computed for the third transmitted bit (v=8); this was an arbitrary choice since there is no reason why the timing sensitivity should

be dependent upon the bit index, even though the value of asymptotic efficiency will be. The results are displayed in Figure 4.1 for three different timing error scenarios: $\hat{\tau}_k = \tau_k \pm 0.1$ chips, $\hat{\tau}_k = \tau_k \pm 0.01$ chips, and $\hat{\tau}_k = \tau_k \pm 0.001$ chips.
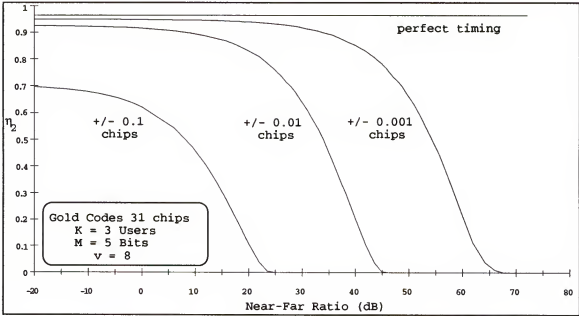

Figure 4.1 - Sensitivity of Decorrelator to Timing Errors for One Particular Timing Configuration

As can be seen from Figure 4.1, when the timing estimates are perfect, the decorrelator has an asymptotic efficiency of 0.967 and a near-far spread of infinity. When the timing estimates of all users are off by one-thousandth of a chip, the decorrelator's asymptotic efficiency drops slightly to 0.95 and its near-far spread becomes approximately 67 dB. When the timing estimates of all users are off by one-hundredth of a chip, the decorrelator's asymptotic efficiency drops to 0.925 and its near-far spread becomes approximately 45 dB. Finally, when the timing estimates of

all users are off by one-tenth of a chip, the decorrelator's asymptotic efficiency drops to 0.7 and its near-far spread becomes approximately 24 dB.

The results displayed in Figure 4.1 are for one particular timing configuration; that is, the three chosen Gold codes and the three chosen true propagation delays. Of course, different Gold codes and different propagation delays will result in different cross-correlations which in turn will result in different values of asymptotic efficiency. It is therefore of interest to average the decorrelator's timing sensitivity over all possible timing configurations; however, since an infinite number of timing configurations exist, the asymptotic efficiency was averaged over 1000 different timing configurations. For each configuration, three of the 33 possible Gold codes were chosen at random along with three true propagation delays. The resulting average asymptotic efficiency for the third bit of user two is displayed in Figure 4.2 for the same timing error scenarios as in Figure 4.1. Interestingly, the results shown in Figure 4.1 are fairly representative of the average timing sensitivity of the decorrelator. Note from Figures 4.1 and 4.2 that for this three user system, as long as the received energies are kept within about 25 dB of one another, then a nonzero asymptotic efficiency is achievable when each user's propagation delay estimate is off by as much as a tenth of a chip. The conclusion, therefore, is that the use of a transmitter power control scheme in
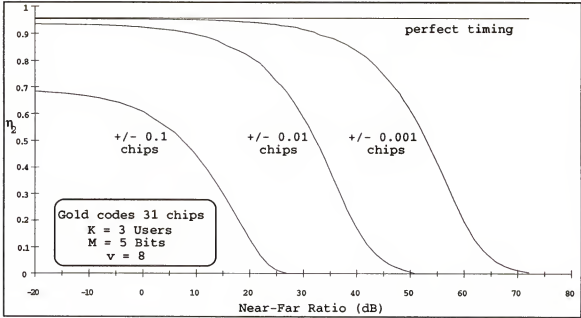
Figure 4.2 - Sensitivity of Decorrelator to Timing Errors
Averaged Over 1000 Timing Configurations

conjunction with the windowed decorrelator will relax the
accuracy requirements of the timing information. Thus, even
in an AWGN channel, a practical decorrelating receiver will
need to include an average power control scheme.

The fact that the decorrelating strategy is sensitive
to errors in the timing information should not be
surprising, as a decorrelating receiver is essentially
performing the operation of inverse filtering. The cross-
correlation matrix R_{LK} may be thought of as the transfer
matrix of the multi-input/multi-output channel. In order to
successfully compute the inverse of the channel transfer
matrix, perfect timing information will be necessary. An
important conclusion, therefore, is that for channels in
which it is not feasible to obtain reliable timing
information, a method other than a decorrelating strategy

should be considered for demodulating the received signals. Of course, any demodulation method which includes a matched filter bank inherently requires knowledge of the system timing configuration.

Inversion of the Cross-correlation Matrix

The windowed decorrelator needs to compute the inverse of the symmetric block tri-diagonal Toeplitz matrix R_{LK}, which is of dimension LK by LK where L is the window length in symbols and K is the number of active users. As noted by Lupas [61], the straightforward inversion of R_{LK} by Cholesky decomposition or Gaussian elimination will require on the order of $2(LK)^3$ operations. To obtain some numerical results on the computational complexity of performing the matrix inversion, the computer mathematical modeling package MATLAB was utilized. A useful feature of MATLAB is its ability to count the number of floating point operations (flops) it performs. Additions and subtractions are each one flop if real and two if complex. Multiplications and divisions count one flop each if the result is real and six flops if it is complex.

A two user asynchronous system was constructed and the matrix R_{LK} was inverted for various window lengths. The results are summarized in Table 4.1. MATLAB was then used on the data in Table 4.1 to determine a polynomial curve fit of order three. The result is

Table 4.1 - Number of Flops Required to Invert R_{LK} for Two
Users with Various Window Lengths

L	LK	Flops
2	4	179
3	6	495
4	8	1047
5	10	1899
6	12	3115
7	14	4759
8	16	6895

$$\text{No. of flops} = 1.3333(LK)^3 + 5.5(LK)^2 - 1.6667(LK) - 1 \qquad (4.21)$$

Note that equation (4.21) is an exact curve fit, not an
approximation. In a practical multiple access communication
system, many users may be simultaneously active. For
instance, if K = 35 users and L = 8 bits then from equation
(4.21) the computation of the inverse of R_{280} will require
29,699,334 flops.

One simple way to reduce the number of flops required
to compute R_{LK}^{-1} is to choose a small window length . If a
window length of L = 4 bits is used in the previous example,
then the number of flops required to invert R_{140} is
3,766,141, or approximately one-eighth of the number of
flops required when the window length was twice as wide.
Keeping the window length small will also result in better

estimates of future MAI since the received energies and phases will have had less time to change since being estimated. Of course, the major disadvantage in choosing a small window length is that the percentage of overhead will increase due to the presence of the pilot bits.

The formula presented in equation (4.21) is based upon straightforward computation of the matrix inverse. An iterative algorithm has been found which can reduce the number of computations from approximately $2(LK)^3$ to $n(LK)^2$, where n is a number which depends upon the eigenvalue spread of the matrix R_{LK} [61]. Other methods also exist for reducing the computational complexity of inverting Toeplitz matrices [62].

Finally, it should be recalled that the matrix R_{LK} only requires inverting when the multiuser receiver detects a change in either the number of active users or their relative time delays. For indoor wireless communication networks and personal communication systems, these quantities may remain static for much of the duration of a user's message.

CHAPTER 5
CONCLUSIONS

Summary of Time-Windowed Decorrelating Receivers

In this work, a unique method of implementing a multiuser decorrelating receiver for asynchronous DS-CDMA channels was presented. Unlike the original full-length decorrelator, the time-windowed decorrelator proposed here has a small decoding delay (on the order of L bits, where L may be chosen as desired), only needs to store LK elements in memory (where K is the number of active users), and only needs to invert a matrix of dimension LK by LK.

In chapter two, a windowed decorrelating multiuser receiver was proposed and analyzed for AWGN channels. The front-end of the receiver is a matched filter bank. The receiver stores L consecutive vectors of matched filter sampled outputs, thus forming a "window". Estimates of the out-of-window multiple-access-interference (MAI) affecting the current window are then subtracted from the current window vector. The resulting modified window vector is then decorrelated (i.e., multiplied by the inverse of the system cross-correlation matrix). Sign decisions are then made upon the resulting decorrelated output vector to determine the transmitted polarities. To form the required out-of-

window MAI estimates, each mobile transmitter inserts a
pilot bit into its transmitted sequence after every L data
bits. Knowledge of the polarities of the pilot bits thus
provides the multiuser receiver with knowledge of the
polarities of the out-of-window MAI components. The
magnitudes of the last bit of each user contained within the
previous window, obtained from the previous window's
decorrelating solution, are used as the estimates of the
out-of-window MAI magnitudes affecting the current window.
The out-of-window MAI phases are known since it was assumed
that the carrier phases of the users were being tracked for
the purpose of coherent BPSK demodulation.

    The asymptotic efficiency of the proposed window
decorrelator was then found. It was observed that under
certain conditions imposed upon the signature waveform
cross-correlations, the asymptotic efficiency will converge
to a constant value. For the special case of two users, the
condition necessary for convergence was shown to be
identical to the condition necessary for the existence of a
full-length decorrelator in the limit as the message length
approaches infinity. For the more general K user scenario,
the condition required for convergence could not be
analytically derived; however, the results of a numerical
analysis suggest that the same condition as found for the
two user case also applies to the K user case. It is
therefore conjectured that the windowed decorrelator will be

applicable for any communication system for which the full-length decorrelator is applicable.

The asymptotic efficiency of the windowed decorrelator was then evaluated for several numerical examples and seen to provide a near-far resistant solution up to a certain level of near-far effect when a finite number of windows was processed. A new performance measure, the receiver's near-far spread, was defined as the largest difference in received energies for which the receiver could operate at a nonzero asymptotic efficiency. It was demonstrated that as the number of active users increases, the windowed decorrelator maintains its ability to achieve any desired level of near-far spread, but the number of windows which must be processed first increases accordingly.

In chapter three, a windowed decorrelator was proposed and analyzed for a communication channel in which each user experiences statistically independent frequency nonselective Rayleigh fading. Differential phase shift keying (DPSK) was chosen as the modulation technique so that tracking of each user's carrier phase is not required. The overall receiver strategy is similar to that for the AWGN channel, but now each mobile transmitter must insert two pilot bits between every block of L-1 data bits. The first pilot bit is grouped with the L-1 data bits to form a window L bits wide. Estimates of the out-of-window MAI are subtracted from the matched filter sampled output vector, and the resulting modified vector is decorrelated. Standard DPSK detection is

then done on the resulting decorrelated output vector to determine the polarities of the transmitted bit sequences. The out-of-window MAI estimates are complex numbers; that is, they must include a magnitude and phase. These estimates are obtained as in the AWGN scenario, only now the last K elements in the previous decorrelated output vector, corresponding to the first of the two consecutive pilot bits, are used as the MAI estimates rather than their magnitudes.

Asymptotic efficiency was found to be analytically intractable, so the performance measure became probability of bit error. It was shown through numerical examples that the windowed decorrelator could approach the single user bit error rate up to a certain level of average near-far effect. This observation led to the incorporation of an average power control scheme into the overall communication system.

In chapter four, the sensitivity of the decorrelating strategy to errors in the timing information was investigated. The asymptotic efficiency of a full-length decorrelator operating in an AWGN channel was derived as a function of the error matrix resulting from incorrectly inverting the true cross-correlation matrix. It was found that the decorrelating strategy is sensitive to timing errors; the degree of sensitivity increases as the near-far effect increases and as the magnitude of the timing errors increases. The use of power control will therefore also

help to relax the level of precision needed for the propagation delay estimates.

A brief discussion of the computational complexity involved in computing the inverse of the cross-correlation matrix was also addressed in chapter four. It was demonstrated that straightforward inversion of the LK by LK symmetric tri-block-diagonal Toeplitz matrix requires on the order of $2(LK)^3$ floating point operations. References were given which discuss more computationally efficient algorithms, although an in-depth treatment of such algorithms is beyond the scope of this work.

Areas For Future Work

In this section several areas for further work related to the windowed decorrelator are suggested. A fundamental requirement of any decorrelating receiver is the knowledge of the propagation delay from each user (i.e., the system timing configuration). It was assumed in this work that an ideal time delay analyzer was available to provide the windowed decorrelator with perfect timing information. In practice, of course, such a device must be built and thus methods for obtaining knowledge of the timing configuration need to be developed.

Another area for future work is the modification and performance analysis of the windowed decorrelator for frequency selective fading channels. RAKE receivers are

often suggested for use in frequency selective fading
channels [25], [59]. In the multiuser context, the matched
filter bank would be replaced with a bank of RAKE filters,
one for each user [50], [51]. The decorrelating algorithm
would then decorrelate all the received replicas from each
user, and appropriate recombining of the decorrelated
replicas would then occur before final decisions are made.
Of course, a RAKE receiver requires a lot of side
information which may not be readily available. Acquisition
of any required side information should therefore be
addressed. Also, intersymbol interference is a common
result of digital communication systems operating in
frequency selective fading channels and would therefore need
to be addressed as well.

In many communication networks, data and video
transmissions are present in addition to voice
transmissions. Such systems would typically allow the users
to have different data rates, depending upon the type of
information they were transmitting. Varying data rates
among the users changes some of the basic system assumptions
made by a decorrelating receiver; thus, modifying the
decorrelator to be capable of operating in an environment
with varying data rates should also be investigated.

APPENDIX A
PROOF OF EQUATION (2.40)

In this appendix, the upper and lower bounds given in equation (2.40) are proven. Although the proof is straightforward, it is included here for completeness.

<u>Claim:</u> $\quad -|I| \le \sqrt{w} - |\pm\sqrt{w} \pm I| \le |I|$

<u>Proof:</u> The proof consists of considering the four possible combinations of the signs inside the absolute value.

Case I: $\quad +\sqrt{w}, +I$

The quantity inside the absolute value is $\sqrt{w} + I$ so that $\left|\sqrt{w} + I\right| = \sqrt{w} + I$ and the result of the subtraction is then $\sqrt{w} - \left(\sqrt{w} + I\right) = -I$.

Case II: $\quad -\sqrt{w}, -I$

The quantity inside the absolute value is $-\sqrt{w} - I$ so that $\left|-\sqrt{w} - I\right| = \sqrt{w} + |I|$ and the result of the subtraction is then $\sqrt{w} - \left(\sqrt{w} + |I|\right) = -|I|$.

Case III: $+\sqrt{w}, -I$

The quantity inside the absolute value is $\sqrt{w} - I$.

If $\sqrt{w} > |I|$ then $\left|\sqrt{w} - I\right| = \sqrt{w} - |I|$ and the result of the subtraction is then $\sqrt{w} - \left(\sqrt{w} - |I|\right) = +|I|$.

If $\sqrt{w} < |I|$ then $\left|\sqrt{w} - I\right| = |I| - \sqrt{w}$ and the result of the subtraction is then $\sqrt{w} - \left(|I| - \sqrt{w}\right) = 2\sqrt{w} - |I| < 2|I| - |I| = |I|$.

<u>Case IV:</u> $-\sqrt{w},+I$

The quantity inside the absolute value is $I-\sqrt{w}$.

If $I>\sqrt{w}$ then $\left|I-\sqrt{w}\right|=|I|-\sqrt{w}$ and the result of the subtraction is then $\sqrt{w}-\left(|I|-\sqrt{w}\right)=2\sqrt{w}-|I|<2|I|-|I|=|I|$.

If $I<\sqrt{w}$ then $\left|I-\sqrt{w}\right|=\sqrt{w}-|I|$ and the result of the subtraction is then $\sqrt{w}-\left(\sqrt{w}-|I|\right)=|I|$.

APPENDIX B

DIAGONALIZATION OF THE RECURSION MATRIX FOR TWO ACTIVE USERS

In this appendix it is shown that the matrix A, defined in equation (2.52), will always be diagonalizable for the case of two active users. For convenience a window length of three bits is chosen. The matrix A will be diagonalizable if its determinant is nonzero [60]; therefore

$$\det[A] = \left|c_{5,6}\rho_{21}\right|\left|c_{6,1}\rho_{21}\right| - \left|c_{5,1}\rho_{21}\right|\left|c_{6,6}\rho_{21}\right| \neq 0 \qquad (B.1)$$

which produces the condition

$$\left|c_{5,6}\right|\left|c_{6,1}\right| \neq \left|c_{5,1}\right|\left|c_{6,6}\right| \qquad (B.2)$$

where it has been assumed that $\left|\rho_{21}\right| \neq 0$ since this would result in the matrix A being identically zero and thus the windowed decorrelator would already be near-far resistant from equation (2.55). Expanding out the equation $RR^{-1} = I$, where I is the identity matrix, yields

$$\begin{bmatrix} 1 & \rho_{12} & 0 & 0 & 0 & 0 \\ \rho_{12} & 1 & \rho_{21} & 0 & 0 & 0 \\ 0 & \rho_{21} & 1 & \rho_{12} & 0 & 0 \\ 0 & 0 & \rho_{12} & 1 & \rho_{21} & 0 \\ 0 & 0 & 0 & \rho_{21} & 1 & \rho_{12} \\ 0 & 0 & 0 & 0 & \rho_{12} & 1 \end{bmatrix} \begin{bmatrix} c_{1,1} & c_{1,2} & c_{1,3} & c_{1,4} & c_{1,5} & c_{1,6} \\ c_{2,1} & c_{2,2} & c_{2,3} & c_{2,4} & c_{2,5} & c_{2,6} \\ c_{3,1} & c_{3,2} & c_{3,3} & c_{3,4} & c_{3,5} & c_{3,6} \\ c_{4,1} & c_{4,2} & c_{4,3} & c_{4,4} & c_{4,5} & c_{4,6} \\ c_{5,1} & c_{5,2} & c_{5,3} & c_{5,4} & c_{5,5} & c_{5,6} \\ c_{6,1} & c_{6,2} & c_{6,3} & c_{6,4} & c_{6,5} & c_{6,6} \end{bmatrix} = \begin{bmatrix} 1 & 0 & 0 & 0 & 0 & 0 \\ 0 & 1 & 0 & 0 & 0 & 0 \\ 0 & 0 & 1 & 0 & 0 & 0 \\ 0 & 0 & 0 & 1 & 0 & 0 \\ 0 & 0 & 0 & 0 & 1 & 0 \\ 0 & 0 & 0 & 0 & 0 & 1 \end{bmatrix} \qquad (B.3)$$

It is evident from equation (B.3) that

$$\rho_{12}c_{5,1} + c_{6,1} = 0 \qquad (B.4)$$

and

$$\rho_{12}c_{5,6} + c_{6,6} = 1 \qquad (B.5)$$

Solving equations (B.4) and (B.5) for $c_{6,1}$ and $c_{6,6}$, respectively, and substituting the results into equation (B.2), the following condition is obtained

$$\left| c_{5,6} \rho_{12} c_{5,1} \right| \neq \left| c_{5,1} - c_{5,1} \rho_{12} c_{5,6} \right| \qquad (B.6)$$

which is satisfied as long as

$$c_{5,1} \neq 0 \qquad (B.7)$$

To proceed further, it will be necessary to determine $c_{5,1}$ as a function of the cross-correlations ρ_{12} and ρ_{21}. From equation (B.3) it is seen that

$$c_{1,1} + \rho_{12} c_{2,1} = 1 \qquad (B.8)$$

and

$$\rho_{12} c_{1,1} + c_{2,1} + \rho_{21} c_{3,1} = 0 \qquad (B.9)$$

Solving equations (B.8) and (B.9) for $c_{1,1}$ and $c_{2,1}$, respectively, and substituting the result of equation (B.8) into equation (B.9) produces

$$c_{2,1} = \frac{\rho_{12} + \rho_{21} c_{3,1}}{\rho_{12}^2 - 1} \qquad (B.10)$$

Next, from equation (B.3) it is clear that

$$\rho_{21} c_{2,1} + c_{3,1} + \rho_{12} c_{4,1} = 0 \qquad (B.11)$$

Substituting equation (B.10) into equation (B.11) and solving for $c_{3,1}$ yields

$$c_{3,1} = \left[\frac{\rho_{12}\left(\rho_{12}^2 - 1 \right)}{1 - \rho_{12}^2 - \rho_{21}^2} \right] c_{4,1} + \frac{\rho_{12}\rho_{21}}{1 - \rho_{12}^2 - \rho_{21}^2} \qquad (B.12)$$

Repeating this procedure by solving for $c_{4,1}$ in terms of $c_{5,1}$ and then using the relationship given by equation (B.4) to eliminate $c_{6,1}$, the following result is obtained

$$c_{5,1} = \frac{\rho_{12}^2 \rho_{21}^2}{\rho_{12}^6 - 3\rho_{12}^4 - \rho_{21}^4 + 3\rho_{12}^2 - 2\rho_{12}^2\rho_{21}^2 + 2\rho_{21}^2 - 1} \qquad (B.13)$$

Applying the condition that $c_{5,1} \neq 0$ given by equation (B.7), it is obvious that the matrix A will be diagonalizable if and only if

$$\rho_{12}^2 \rho_{21}^2 \neq 0 \qquad (B.14)$$

which is equivalent to the condition

$$\rho_{12}\rho_{21} \neq 0 \qquad (B.15)$$

Since the cross-correlations are functions of the relative delay between the received signals of user 1 and user 2, and since the delay is defined along a continuum of values, the converse of equation (B.15) will occur with probability zero. In the event that $\rho_{12}\rho_{21} = 0$, one of three possible situations has occurred: $\rho_{12} = 0$, $\rho_{21} = 0$, or $\rho_{12} = \rho_{21} = 0$. If either of the latter two situations occurs, then the windowed decorrelator will be near-far resistant for the duration of the occurrence since the matrix A will be identically zero. If the first situation should arise, then from equations (B.13) and (B.4) $c_{5,1} = 0$ and $c_{6,1} = 0$ so that the matrix A will then become

$$A = \begin{bmatrix} |c_{5,6}\rho_{21}| & 0 \\ |c_{6,6}\rho_{21}| & 0 \end{bmatrix} \qquad (B.16)$$

To proceed, it will be necessary to solve for $c_{5,6}$ in terms of ρ_{12} and ρ_{21}. This can be accomplished by repeating the procedure used to obtain equation (B.13) but using the identity $R^{-1}R = I$. Doing so results in

$$c_{5,6} = \frac{\rho_{12}^5 - 2\rho_{12}^3 - \rho_{21}^2\rho_{12} + \rho_{12}}{\rho_{12}^6 - 3\rho_{12}^4 - \rho_{21}^4 - 2\rho_{12}^2\rho_{21}^2 + 3\rho_{12}^2 + 2\rho_{21}^2 - 1} \qquad (B.17)$$

From equation (B.17), it is clear that $c_{5,6}$ will equal zero for $\rho_{12} = 0$; thus, from equation (B.16) the matrix A will identically be zero and again the windowed decorrelator will be near-far resistant. Therefore, for the case of two users, the matrix A will always be diagonalizable except for the trivial case when $\rho_{12}\rho_{21} = 0$, for which the matrix A is identically zero and the windowed decorrelator is near-far resistant.

LIST OF REFERENCES

1. W. C. Lee, "Overview of Cellular CDMA," IEEE Trans. on Vehicular Technology, Vol. 40, No. 2, pp. 291-302, May 1991.

2. K. S. Gilhousen, I. M. Jacobs, R. Padovani, A. J. Viterbi, L. A. Weaver, Jr., and C. E. Wheatley III, "On the Capacity of a Cellular CDMA System," IEEE Trans. on Vehicular Technology, Vol. 40, No. 2, pp. 303-312, May 1991.

3. R. L. Pickholtz, L. B. Milstein, and D. L. Schilling, "Spread Spectrum for Mobile Communications," IEEE Trans. on Vehicular Technology, Vol. 40, No. 2, pp. 313-322, May 1991.

4. L. Milstein, T. Rappaport, R. Barghouti, "Performance Evaluation for Cellular CDMA," IEEE Journal on Selected Areas in Communications, Vol. 10, No. 4, pp. 680-689, May 1992.

5. M. Kavehrad, B. Ramamurthi, "Direct-Sequence Spread Spectrum with DPSK Modulation and Diversity for Indoor Wireless Communications," IEEE Trans. on Communications, Vol. COM-35, No. 2, pp. 224-236, February 1987.

6. W. Lam, R. Steele, "Performance of Direct Sequence Spread Spectrum Multiple-Access Systems in Mobile Radio," IEE Proc.-I, Vol. 138, No. 1, pp. 1-14, February 1991.

7. K. Johannsen, "Code Division Multiple Access Versus Frequency Division Multiple Access Channel Capacity in Mobile Satellite Communication," IEEE Trans. on Vehicular Technology, Vol. 39, No. 1, pp. 17-26, February 1990.

8. K. Gilhouse, I. Jacobs, R. Padovani, and L. Weaver, "Increased Capacity Using CDMA for Mobile Satellite Communication," IEEE Journal on Selected Areas in Communcations, Vol. 8, No. 4, pp. 503-513.

9. M. Soroushnejad, E. Geraniotis, "Performance Comparison of Different Spread-Spectrum Signaling Schemes for Cellular Mobile Radio Networks," IEEE Trans. on Communications, Vol. 40, No. 5, pp. 947-956, May 1992.

10. B. Vojcic, R. Pickholtz, I. Stojanovic, "A Comparison of TDMA and CDMA in Microcellular Radio Channels," Proceedings ICC '91, pp. 866-870.

11. R. De Gaudenzi, C. Elia, R. Viola, "Bandlimited Quasi-Synchronous CDMA: A Novel Satellite Access Technique for Mobile and Personal Communication Systems," IEEE Journal on Selected Areas in Communications, Vol. 10, No. 2, pp. 328-343, February 1992.

12. A. J. Viterbi, "When Not to Spread Spectrum -- A Sequel," IEEE Communications Magazine, Vol. 23, pp. 12-17, April 1985.

13. A. J. Viterbi, "Spread Spectrum Communications -- Myths and Realities," IEEE Communications Magazine, pp. 11-18, May 1979.

14. G. R. Cooper, R. W. Nettleton, "A Spread-Spectrum Technique for High Capacity Mobile Communications," IEEE Trans. on Vehicular Technology, Vol. VT-27, pp. 264-275, November 1978.

15. D. Goodman, "Second Generation Wireless Information Networks," IEEE Trans. on Vehicular Technology, Vol. 40, No. 2, pp. 366-374, May 1991.

16. M. Kavehrad, P. J. Mclane, "Performance of low-complexity channel coding and diversity for spread-spectrum in indoor, wireless communication," AT&T Technical Journal, Vol. 64, pp. 1927-1965, October 1985.

17. L. B. Milstein, "Interference Rejection Techniques in Spread Spectrum Communications," Proc. IEEE, Vol. 76, pp. 657-671, June 1988.

18. R. Iltis, L. B. Milstein, "Performance Analysis of Narrowband Interference Rejection Techniques in DS Spread Spectrum Systems," IEEE Trans. on Communications, Vol. COM-32, pp. 1169-1177, Nov. 1984.

19. R. Vijayan, H. V. Poor, "Nonlinear Techniques for Interference Suppression in Spread Spectrum Systems,"

IEEE Trans. on Communications, Vol. COM-38, pp. 1060-1065, July 1991.

20. L. B. Milstein, "On the Feasibility of a CDMA Overlay for Personal Communication Networks," IEEE Journal on Selected Areas in Communications, Vol.10, pp. 655-668, May 1992.

21. D. Schiling, E. Kanterakis, "Broadband CDMA Overlay of FM or TDMA in the Cellular System," Conference Record of the Communication Theory Mini-Conference (in conjunction with GLOBECOM '92), Orlando, Florida, December 1992, pp. 61-65.

22. L. A. Rusch, H. V. Poor, "Narrowband Interference Suppression in CDMA Spread Spectrum Communications," IEEE Trans. on Communications, Vol. 42, No. 2, pp. 1969-1979, April 1994.

23. J. Ketchum, J. G. Proakis, "Adaptive Algorithms for Estimating and Suppressing Narrowband Interference in PN Spread Spectrum Systems," IEEE Trans. on Communications, Vol. COM-30, pp. 913-924, May 1982.

24. G. J. Saulnier, "Suppression of Narrowband Jammers in a Spread Spectrum Receiver Using Transform-Domain Adaptive Filtering," IEEE Journal on Selected Areas in Communications, Vol. 10, No. 4, pp. 742-749, 1992.

25. G. Turin, "Introduction to Spread-Spectrum Antimultipath Techniques and Their Application to Urban Digital Radio," Proceedings of the IEEE, Vol. 68, pp. 328-353, March 1980.

26. K. Simon, J. Omura, R. Scholtz, B. Levitt, Spread Spectrum Communications Vol III, Rockville, MD: Computer Science Press 1985.

27. J. Lehnert, M. Pursley, "Multipath Diversity Reception of Spread Spectrum Multiple-Access Communications," IEEE Trans. on Communications, Vol. COM-35, pp. 1189-1198, November 1987.

28. J. Proakis, Digital Communications, New York: McGraw Hill, 1989, second edition.

29. S. Verdu, "Minimum Probability of Error for Asynchronous Gaussian Mulitple-Access Channels," IEEE Trans. on Information Theory, Vol. 32, No. 1, pp. 85-96, January 1986.

30. E. A. Geraniotis, M. B. Pursley, "Error Probability for Direct-Sequence Spread-Spectrum Multiple-Access Communications--Part II: Approximations," IEEE Trans. on Communications, Vol. COM-30, pp. 985-995, May 1982.

31. M. B. Pursley, D. V. Sawarte, W. E. Stark, "Error Probability for Direct-Sequence Spread-Spectrum Multiple-Access Communications--Part I: Upper and Lower Bounds," IEEE Trans. on Communications, Vol. COM-30, pp. 975-984, May 1982.

32. J. S. Lehnert, M. B. Pursley, "Error Probabilities for Binary Direct-Sequence Spread-Spectrum Communications with Random Signature Sequences," IEEE Trans. on Communications, Vol. COM-35, pp. 87-98, January 1987.

33. P. K. Enge, D. V. Sawarte, "Spread-Spectrum Multiple-Access Performance of Orthogonal Codes: Linear Receivers," IEEE Trans. on Communications, Vol. COM-35, December 1987.

34. L. F. Chang, S. Ariyavisitakul, "Performance of Power Control Method for CDMA Radio Communication System," IEE Electronics Letters 23rd, Vol. 27, No. 11, May 1991.

35. R. Diaz, R. Agusti, "Analysis of a Fast CDMA Power Control Scheme in an Indoor Environment," Proceedings VTC '92, pp. 67-70.

36. S. Soliman, C. Wheatley, R. Padovani, "CDMA Reverse Link Open Loop Power Control," Proceedings GLOBECOM'93, pp. 69-73.

37. R. Lupas and S. Verdu, "Linear Multiuser Detectors for Synchronous Code-Division Multiple Access Channels," IEEE Trans. on Information Theory, Vol. 35, No. 1, pp. 123-136, January 1989.

38. R. Lupas and S. Verdu, "Near-far Resistance of Multiuser Detectors in Asynchronous Channels," IEEE Trans. on Communications, Vol. 38, No. 4, pp. 496-508, April 1990.

39. M. K. Varanasi and B. Aazhang, "Multistage Detection in Asynchronous Code-Division Multiple Access Communications," IEEE Trans. on Communications, Vol. 38, No. 4, pp. 509-519, April 1990.

40. Y. C. Yoon, R. Kohno, H. Imai, "A Spread-Spectrum Multiaccess System with Cochannel Interference Cancellation for Multipath Fading Channels," IEEE Journal on Selected Areas in Communications, Vol. 11, No. 7, pp. 1067-1075, September 1993.

41. S. Kubota, S. Kato, K. Feher, "Inter-Channel Interference Cancellation Technique for CDMA Mobile/Personal Communication Systems," Proceedings of the IEEE, pp. 112-117, 1992.

42. A. J. Viterbi, "Very Low Rate Convolutional Codes for Maximum Theoretical Performance of Spread-Spectrum Multiple-Access Channels," IEEE Journal on Selected Areas in Communications, Vol. 8, pp. 641-649, 1990.

43. A. Duel-Hallen, "Decorrelating Decision Feedback Multiuser Detector for Synchronous Code-Division Multiple Access Channel," IEEE Trans. on Communications, Vol. COM-41, No. 2, pp. 285-290, February 1993.

44. P. Dent, B. Gudmundson, M. Ewerbring, "CDMA-IC: A Novel Code Division Multiple Access Scheme Based on Interference Cancellation," Proceedings of the IEEE, pp. 98-102, 1992.

45. Z. Xie, R. Short, and C. K. Rushforth, "A Family of Suboptimum Detectors for Coherent Multiuser Communications," IEEE Journal on Selected Areas in Communications, Vol. 8, No. 4, pp. 683-690, May 1990.

46. S. Miller,"An Adaptive Direct-Sequence Code-Division Multiple Access Receiver for Multiuser Interference Rejection," to appear in IEEE Trans. on Communications.

47. R. Kohno, H. Imai, M. Hatori, S. Pasupathy, "An Adaptive Canceller of Cochannel Interference for Spread-Spectrum Multiple-Access Communication Networks in a Power Line," IEEE Journal on Selected Areas in Communications, Vol. 8, No. 4, pp. 691-699, May 1990.

48. M. Varanasi, B. Aazhang, "Optimally Near-Far Resistant Multiuser Detection in Differentially Coherent Synchronous Channels," IEEE Trans. on Information Theory, Vol. 37, No. 4, pp. 1006-1018, July 1991

49. M. Varanasi, "Noncoherent Detection in Asynchronous Multiuser Channels," IEEE Trans. on Information Theory, Vol. 39, No. 1, pp. 157-176, January 1993.

50. U. Fawer, B. Aazhang, "A Coherent Diversity Receiver for Code Division Multiple Access Communications over Multipath Fading Channels," Conference Record of The Communication Theory Mini-Conference (in conjunction with GLOBECOM '92), Orlando, Florida, December 1992, pp. 71-76.

51. S. Vasudevan, M. Varanasi, "Multiuser Detectors for Asynchronous CDMA Communications over Rician Fading Channels," Conference Record of The Communication Theory Mini-Conference (in conjunction with GLOBECOM'92), Orlando, Florida, December 1992, pp. 77-81.

52. Z. Zvonar, D. Brady, "Suboptimum Multiuser Detector for Synchronous CDMA Frequency-Selective Rayleigh Fading Channels," Conference Record of The Communication Theory Mini-Conference (in conjunction with GLOBECOM'92), Orlando, Florida, December 1992, pp. 82-86.

53. R. Prasad, H. S. Misser, A. Kegel, "Performance Analysis of Direct Sequence Spread-Spectrum Multiple Access Communication in an indoor Rician-Fading Channel with DPSK Modulation," Electronics Letters, Vol. 26, pp. 1366-1367, August 1990.

54. S. Wijayasuriya, J. McGeehan, and G. H. Norton, "RAKE Decorrelating Receiver for DS-CDMA Mobile Radio Networks," Electronics Letters, Vol. 29, No. 4, pp. 395-396, February 1993.

55. Z. Zvonar, "Multiuser Detection For Rayleigh Fading Channels," Ph.D. Dissertation, Northeastern University, Boston, Massachusetts, September 1993.

56. S. S. H. Wijayasuriya, J. P. McGeehan, and G. H. Norton, "Sliding Window Decorrelating Algorithm for DS-CDMA Receivers," Electronics Letters, Vol. 28, No. 17, pp. 1596-1597, August 1992.

57. R. Smith, and S. Miller, "Code Timing Estimation in a Near-Far Environment for Direct Sequence Code-Division Multiple Access," to appear in Proceedings of MILCOM'94.

58. R. Iltis,"Joint Estimation of PN Code Delay and Multipath Using the Extended Kalman Filter," IEEE Trans. on Communications, Vol. 38, No. 10, October 1990, pp. 1677-1685.

59. E. Strom, S. Parkvall, and B. Ottersten, "Near-Far Resistant Propagation Delay Estimators for Asynchronous Direct-Sequence Code Division Multiple Access Systems," Proceedings of the 1994 International Zurich Seminar on Digital Communications, Zurich, Switzerland, March 1994.

60. A. Howard, <u>Elementary Linear Algebra</u>, Second edition, New York: John Wiley and Sons, Inc., 1977.

61. R. Lupas, "Near-Far Resistant Linear Multiuser Detection," Ph.D. Dissertation, Princeton University, Princeton, New Jersey, January 1989.

62. T. H. Wallace, "Improving the Computational Efficiency of Subspace Algorithms for Frequency Estimation of Sinusoidal Signals," Ph.D. Dissertation, University of Florida, Gainesville, Florida 1994.

63. R. Price, P. E. Green, Jr., "A Communication Technique for Multipath Channels," Proceedings of IRE, Vol. 46, pp. 555-570, March 1958.
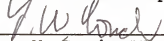
BIOGRAPHICAL SKETCH

Michael Feeney received the Bachelor of Science degree in electrical engineering from the University of Missouri-Rolla in 1988 and the Master of Science degree in electrical engineering from the University of Florida in 1989. From 1990 to 1991 he worked for Motorola Inc. in the Personal Communication Systems Subscriber Division developing hardware for a digital wireless PCS telephone. Since 1991 he has been a participant in the Motorola Distinguished Employee-Student Program while working on his Ph.D. in electrical engineering.

I certify that I have read this study and that in my opinion it conforms to acceptable standards of scholarly presentation and is fully adequate, in scope and quality, as a dissertation for the degree of Doctor of Philosophy.
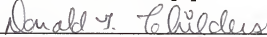
Scott L. Miller, Chair
Associate Professor of
    Electrical Engineering

I certify that I have read this study and that in my opinion it conforms to acceptable standards of scholarly presentation and is fully adequate, in scope and quality, as a dissertation for the degree of Doctor of Philosophy.

Leon W. Couch, II, Cochair
Professor of Electrical
    Engineering

I certify that I have read this study and that in my opinion it conforms to acceptable standards of scholarly presentation and is fully adequate, in scope and quality, as a dissertation for the degree of Doctor of Philosophy.
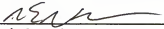
Donald G. Childers
Professor of Electrical
    Engineering

I certify that I have read this study and that in my opinion it conforms to acceptable standards of scholarly presentation and is fully adequate, in scope and quality, as a dissertation for the degree of Doctor of Philosophy.

Haniph A. Latchman
Associate Professor of
    Electrical Engineering

I certify that I have read this study and that in my opinion it conforms to acceptable standards of scholarly presentation and is fully adequate, in scope and quality, as a dissertation for the degree of Doctor of Philosophy.

Richard E. Newman-Wolfe
Assistant Professor of
    Computer and Information
    Sciences

This dissertation was submitted to the Graduate Faculty of the College of Engineering and to the Graduate School and was accepted as partial fulfillment of the requirements for the degree of Doctor of Philosophy.

December, 1994

Winfred M. Phillips
Dean, College of Engineering

Karen A. Holbrook
Dean, Graduate School